

**SPATIALLY EXPLICIT ASSESSMENT OF ENVIRONMENTAL
IMPACTS IN THE ELECTRONICS SECTOR**

by

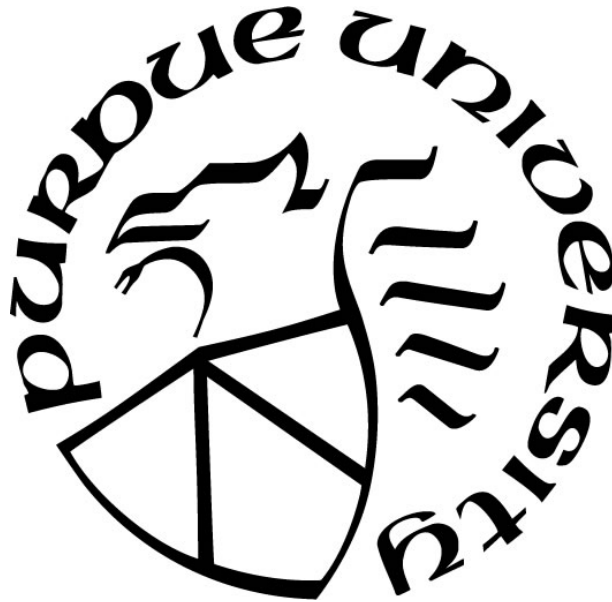
Kali Frost

A Dissertation

Submitted to the Faculty of Purdue University

In Partial Fulfillment of the Requirements for the degree of

Doctor of Philosophy



Division of Environmental and Ecological Engineering

West Lafayette, Indiana

December 2021

THE PURDUE UNIVERSITY GRADUATE SCHOOL
STATEMENT OF COMMITTEE APPROVAL

Dr. Inez Hua, Chair

Lyles School of Civil Engineering

Dr. John Howarter

School of Materials Engineering

Dr. Shweta Singh

School of Agricultural and Biological Engineering

Dr. John W. Sutherland

Division of Environmental and Ecological Engineering

Approved by:

Dr. John W. Sutherland

In memory of my uncle and godfather, Richard C. Lee. Your belief in me and not so subtle prodding that I could achieve more than I thought I was capable of has been a motivational voice in my head these past five years. I hope I made you proud.

And to my husband, Eric, there is no way I could have made it through the past five years without you. Thank you for never having any doubt that I could complete this journey and supporting me every step of the way.

ACKNOWLEDGMENTS

To my advisor, Dr. Inez Hua, thank you for the countless hours of consultation, editing sessions, and advice over the past five years. To Dr. Carol Handwerker, thank you for your mentorship and the amazing learning opportunities provided by the IGERT program. The invaluable experiences we had during the IGERT trips will stay with me for the rest of my life.

TABLE OF CONTENTS

LIST OF TABLES	10
LIST OF FIGURES	11
ABSTRACT	15
1. INTRODUCTION	17
1.1 The Electronics & ICT Sectors	17
1.2 Environmental Impacts of Electronics	18
1.2.1 Critical Materials	19
1.3 ICT Sector Sustainability	19
1.4 Quantifying Environmental Sustainability with Life Cycle Assessment	20
1.4.1 LCA and the Electronics Circular Economy	21
1.4.2 Limitations of LCA	22
1.5 LCA and Planetary Boundaries	22
1.6 Footprinting as a Bridge	25
1.6.1 Freshwater Use	27
1.6.1.1 Industrial Freshwater Use	27
1.6.1.2 Water-Energy Nexus	27
1.6.1.3 Water Scarcity	28
1.6.1.4 Consumption vs Withdrawals	28
1.6.1.5 Water Use in the Semiconductor Industry	29
1.6.2 Toxic Chemical Pollution	30
1.7 Regionalized Footprinting	31
1.8 Problem Statement & Aims	31
1.9 References	33
2. FRESHWATER USE BY THE GLOBAL SEMICONDUCTOR MANUFACTURING INDUSTRY	40
2.1 Background	40
2.1.1 Water Use in Semiconductor Manufacturing	40
2.1.2 Electricity-related Water Withdrawals	42
2.1.3 Industrial Water Use	43

2.1.4	Water Scarcity	44
2.2	Materials and Methods.....	47
2.2.1	Estimating Facility Water Use.....	47
2.2.1.1	Semiconductor Facility Production Data.....	47
2.2.1.2	Geocoding.....	47
2.2.2	Fab Feedwater (FW) Use: Water Use By Technology Type.....	48
2.2.3	Electricity Water Use.....	50
2.2.3.1	U.S. Electricity Water Use	51
2.2.3.2	Chinese Electricity Water Use.....	53
2.2.3.3	Rest of World.....	54
2.2.4	Characterizing Water Use Per Facility	55
2.2.5	Scarcity-weighted Water Use	56
2.2.6	Temporal Variability of Water Scarcity	57
2.3	Results.....	57
2.3.1	Feedwater (FW) Withdrawals.....	57
2.3.2	Scarcity-Weighted Withdrawals.....	60
2.3.3	Temporal Analysis.....	63
2.3.4	Fab Electricity Water Use.....	64
2.3.5	Total Water Withdrawals.....	66
2.4	Discussion and Conclusion.....	67
2.4.1	Discussion.....	67
2.4.2	Limitations.....	68
2.4.3	Conclusions.....	69
2.5	References.....	70
2.6	Appendix. Chapter 2 Supporting Information	76
3.	ENVIRONMENTAL IMPACTS OF A CIRCULAR RECOVERY PROCESS FOR HARD DISK DRIVE RARE EARTH MAGNETS.....	82
3.1	Introduction.....	82
3.1.1	Circular Economy and the ICT Sector.....	82
3.1.2	The HDD Recovery Cascade.....	83
3.1.3	Rare Earth (RE) Magnets LCA.....	85

3.1.4	Piloting of HDD Rare Earth Magnet Assembly (MA) Recovery & Reuse	86
3.2	Methods.....	88
3.2.1	Study Description & Goal	88
3.2.2	Functional Unit & System Boundary	88
3.2.2.1	Business As Usual (BAU) System	89
3.2.2.2	Magnet Assembly Recovery & Reuse (R&R) System.....	89
3.2.3	Life Cycle Inventory.....	92
3.2.3.1	Description of Pilot MA Recovery & Reuse System.....	92
3.2.3.2	Data Collection.....	93
3.2.3.2.1	Electricity Use.....	93
3.2.3.2.1.1	Tools	93
3.2.3.2.1.2	Cleanroom (CR).....	94
3.2.3.2.2	Material Use.....	95
3.2.3.2.3	Transportation	95
3.2.3.2.4	Direct Emissions	96
3.2.3.3	Business As Usual (BAU) Processes	96
3.2.4	Unit Process Data & Impact Assessment Methods	101
3.2.5	Life Cycle Interpretation.....	101
3.2.5.1	Renewable Energy Purchasing	101
3.2.5.2	Automated MA Recovery.....	102
3.2.5.2.1	Electricity & Material Use for Automated MA Recovery Scenario	102
3.2.6	Data Limitations & Uncertainty Analysis	103
3.2.6.1	Scaling Assumptions	103
3.2.6.2	Monte Carlo Uncertainty Analysis.....	103
3.3	Results & Discussion	104
3.3.1	Life Cycle Impact Assessment (LCIA)	104
3.3.1.1	Comparative Analysis: MA Recovery & Reuse vs BAU	104
3.3.1.2	Contribution Analysis: MA Recovery & Reuse (R&R).....	107
3.3.2	Data Center Renewable Energy Purchasing.....	108
3.3.3	Scenario Analysis – Automated MA Recovery	109
3.3.4	Uncertainty Analysis	110

3.4	Conclusions.....	111
3.5	References.....	113
3.6	Appendix. Chapter 3 Supporting Information	119
4.	A REGIONALIZED CHEMICAL FOOTPRINT METHOD FOR HARD DISK DRIVE RARE EARTH MAGNETS	120
4.1	Introduction.....	120
4.1.1	Environmental Impacts of Rare Earth Elements	120
4.1.2	Human and Ecotoxicity of Rare Earth Mining and Processing.....	121
4.1.3	LCA & Chemical Footprint.....	122
4.1.4	Dilution Volume of Receiving Body.....	123
4.1.5	Research Gaps & Aims.....	123
4.2	Methods.....	124
4.2.1	Target and Scope	125
4.2.1.1	System Boundary & Spatiotemporal Scale	126
4.2.2	Quantification of Emissions	126
4.2.2.1	LCA Unit Process Inventory - Step 1.....	126
4.2.2.2	Emissions Inventory – Step 2.....	126
4.2.2.3	Assigning Spatial Unit Processes - Step 3	127
4.2.2.3.1	Manufacturing Materials.....	127
4.2.2.3.1.1	Steel Manufacturing Emissions	127
4.2.2.3.2	Electricity.....	128
4.2.2.3.2.1	Chinese Electricity Emissions.....	128
4.2.2.3.2.2	Other Countries.....	129
4.2.2.3.2.3	Downscaling Grid Emissions to each Power Plant Facility.....	129
4.2.2.4	Summarizing Emissions Per CoC – Step 3 & Step 7	129
4.2.3	Quantifying Fate and Exposure of CoCs - Step 4.....	130
4.2.4	Chemical Pollution Boundary – Step 5	131
4.2.5	Dilution Volume – Step 6.....	132
4.2.5.1	Hydrobasins of Interest.....	132
4.2.5.2	Mapping SUP Emissions to Hydrobasins.....	133
4.2.6	Relating ChF to Local Dilution Capacity – Step 7	134

4.3	Results & Discussion	134
4.3.1	Chemical Footprint	134
4.3.2	Dilution Factor (DF)	135
4.3.3	Chemical Footprint by TENORMs.....	137
4.3.4	Contribution per CoC	137
4.3.5	Predicted vs Sampled Concentrations of CoCs	138
4.4	Conclusions.....	139
4.4.1	Beyond LCA.....	139
4.4.2	Supply Chain Transparency and SUPs	140
4.4.3	Tools to Enable Chemical Footprinting.....	140
4.4.4	Potential of HydroBASINs for Use in Footprinting	141
4.4.5	Linking with Science-Based Targets	141
4.5	References.....	142
4.6	Appendix. Chapter 4 Supporting Information	147
5.	CONCLUSION.....	157
5.1	Reference	159

LIST OF TABLES

Table 2.1. Table of fab FW use and electricity use by technology type and node	49
Table 2.2. Default water use intensity factors for each electricity generation type. All values from Meldrum et al. (2013), except for petroleum and hydroelectric (Macknick et al., 2012).....	55
Table 2.3. Top five global watersheds for semiconductor manufacturing FW withdrawals.	60
Table 2.4. Percent of total wafer production occurring in areas of various water scarcity. Description of water scarcity factors are adapted from Boulay et al. (2017).	61
Table 2.5. Top five global watersheds for scarcity-weighted semiconductor manufacturing FW withdrawals.	63
Table 3.1. The HDD & RE magnet value recovery cascade. The table was summarized from Frost et al (2020). These are listed in order from highest to lowest economic and environmental value.	84
Table 3.2. Summary of distinctive processes and associated data collection for major materials and energy inputs for the R&R and BAU systems. The table follows the process order outlined in the resource flow diagram (Figure 3). Refer to Table S1 and S2 for documentation of all processes used in the study.....	97
Table 4.1. Radiotoxicity and chemotoxicity footprints of three radionuclides associated with RE mining and processing.	137
Table 4.2. Modelled Concentrations vs Selected Monitoring Data from the Yellow River near Baotou, CN Rare Earth Processing Facilities.	139

LIST OF FIGURES

Figure 1.1. Results from a life cycle inventory (LCI) are used to determine an array of mid-point impacts as part of the life cycle impact assessment analysis. Used with permission. © European Union, 2010. ILCD	21
Figure 1.2. Depiction of the planetary boundaries concept. J. Lokrantz/Azote based on Steffen et al (2015). Used with permission.	23
Figure 1.3. The framework from Hauschild et al., (2020) depicts how life cycle engineering relates to PBs and absolute sustainability. Used with permission (CC BY NC ND).....	25
Figure 1.4. Family of footprint indicators and how they relate to planetary boundaries. Used with permission under CC BY 4.0.	26
Figure 2.1. Derived water use intensity factors (in L/kWh) of NERC electricity regions overlaid with the thermoelectric power plants from Diehl and Harris (2014). The boundaries of NERC electricity regions were provided by EIA (2015). FRCC = Florida Reliability Coordinating Council, MRO = Midwest Reliability Organization, NPCC = Northeast Power Coordinating Council, RFC = Reliability First Corporation, SERC = SERC Reliability Corporation, SPP = Southwest Power Pool, TRE = Texas Regional Entity, WECC = Western Electricity Coordinating Council. The white areas of the map are classified by EIA as ‘indeterminate, with various NERC memberships’; thus, a WUI was not calculated for these areas.	52
Figure 2.2. Calculated water withdrawal intensity (in liters per kilowatt hour) of Chinese electricity regions. The boundaries of Chinese electricity regions were adopted from N. Zhang et al. (2017).	54
Figure 2.3. Annual wafer production (in 8-inch [200 mm] wafer equivalents) by countries producing more than one million wafer starts per year.	58
Figure 2.4. Annual fab FW withdrawals by country and technology. Countries producing more than one million wafer starts per year are displayed. The value next to each bar represents the average FW withdrawal intensity (in L/cm ²) for each country’s semiconductor manufacturing facilities, averaged across all technology types.	59
Figure 2.5. Semiconductor manufacturing facility annual wafer starts overlaid on AWaRe scarcity factors, by watershed. *Wafer production normalized to 8-inch [200 mm] wafer.....	59
Figure 2.6. Annual semiconductor manufacturing FW withdrawals summed by AWaRe watershed.	60
Figure 2.7. Scarcity-weighted FW withdrawals by country. The withdrawal is expressed in billions of liter-equivalents to denote the transformation of withdrawal inventory data (in liters) into an impact equivalent (in liter equivalents).....	61
Figure 2.8. Annual scarcity-weighted semiconductor manufacturing FW withdrawals summed by AWaRe watershed. The withdrawal is expressed in billions of liter-equivalents to denote the	

transformation of withdrawal inventory data (in liters) into an impact equivalent (in liter equivalents).	62
Figure 2.9. Difference between maximum monthly scarcity weighted withdrawals and minimum monthly scarcity weighted withdrawals on an annual basis. This represents the difference between a best-case and worst-case scenario for water scarcity in a year, per watershed. The data is divided into deciles to better visualize variation across the dataset.....	64
Figure 2.10. Coefficient of variation (standard deviation of annual scarcity factor normalized by mean annual scarcity) of the AWaRE scarcity factor per watershed. This indicates watersheds that are likely to exhibit the largest percentage change in scarcity over the course of a year.	64
Figure 2.11. Fab ERW withdrawals by country. The value next to each bar represents the average ERW withdrawal intensity (L/cm ²) for each country's semiconductor manufacturing facilities.	65
Figure 2.12. Map of East Asian (i.e. Japan, South Korea, China, Taiwan) fab electricity-related water withdrawals by facility, overlaid on AWaRE scarcity factors. A map of global ERW withdrawals is available in the Appendix (Figure A.1).	66
Figure 2.13. Total water withdrawals (FW + ERW) by the five highest producing countries in the semiconductor manufacturing sector.	67
Figure 3.1. Magnet assembly (MA) within a specialized shipping tray. Image used with permission (photo courtesy of Ikenna Ike).	89
Figure 3.2. Fig (a) is the Business As Usual (BAU) process, depicting MA virgin manufacturing processes and EOL treatments for two sets of MAs. Fig (b) depicts the life cycle diagram for the MA R&R system with one-time reuse of one MA set. Boxes in green represent the new R&R processes and boxes in orange represent virgin manufacturing processes. Boxes shaded in gray represent those processes that are common to both the BAU and R&R systems, which are excluded from our system boundary for the comparative assessment. Boxes in blue depict EoL recycling processes that occur at the end of first life for BAU and second life for R&R. CN=China, JP=Japan, MY=Malaysia, TH=Thailand, OK=Oklahoma, USA.....	90
Figure 3.3. Material and energy inputs, direct emissions, and associated unit process data for the MA recovery process of the MA set from one HDD (Model Number ST16000NM003G). IPA= isopropyl alcohol, PET= polyethylene terephthalate, CNC= computer numerical controlled, methac. = methacrylate, PS= polystyrene, Non-ESD = non-electrostatic discharge, PP = polypropylene. Material and electricity inputs associated with operation of the cleanroom (CR) are highlighted separately in the green boxes.	93
Figure 3.4. Comparison of GHG impacts in kg CO ₂ -eq for one life cycle of an MA set, Business As Usual (dark gray; modeled with Eq. 1), Asia MA Recovery (light gray; modeled with Eq. 4, using sea transportation of an entire HDD to Asia and disassembly for MAs), and U.S. MA Recovery (light green; modeled with Eq. 2, using the US domestic disassembly of an HDD and shipping only MAs to Asia). The net GHG benefits (or the reduced GHG impacts via R&R) are represented by ΔEF	105
Figure 3.5. The difference in environmental impacts between BAU and R&R, with BAU considered the base case.	106

Figure 3.6. Contribution of upstream RE magnet processing impacts and MA manufacturing and transport to the BAU scenario. Nd and Pr Metals, shown here with patterned bars, includes the mining, refining, separation, and transport of RE metals to the magnet manufacturer. This includes yield losses of RE metals inputs during magnet processing. “Other RE Magnet” includes the iron, nickel coating, electricity, and other process chemicals required to manufacture a sintered NdFeB magnet (including yield losses of input materials). MA manufacturing includes raw materials and forming of the steel bracket and the process and materials required to adhere the NdFeB magnet to the bracket. MA transport includes the transport of the MA to the HDD manufacturer and return transport of the MA trays. EoL is not depicted due to its minor contribution to BAU impacts (0.25%)...... 106

Figure 3.7. Summarized unit operation contribution to each of the TRACI impact categories for the R&R system. Tool Electricity includes electricity for dewelding, screw removal, and vacuum sealing during the disassembly and recovery process. CR Electricity includes the CR air handler and lights. Materials includes the PET wipes, isopropyl alcohol, vacuum seal bags, CR gowns, MA packaging, and CO₂ required to clean the MAs. Transport includes the transport from the datacenter to the HDD manufacturer and return transport of the MA trays to the datacenter.... 108

Figure 3.8. Figure (a) depicts the global warming impacts (in kg CO₂-eq) due to electricity supplied from SPP Grid Mix vs the DC grid mix which is comprised of 96% CFE and 4% CBE. Figure (b) displays the overall system impacts of BAU, R&R with SPP grid mix, and R&R with 96/4 mix. 109

Figure 3.9. Global warming demand of DC recovery steps in kg CO₂-eq per set of MAs under manual, semi-automated, and fully automated operating scenarios under two assumptions: 1) an underutilized CR operating an 8-hr shift, 5 days a week (8/5), and (2) a fully utilized CR operating 24 hours a day, 7 days a week (24/7). This *Processes such as screw removal and vacuum seal are not depicted due to minor impact contribution. For the automation scenarios the deweld process is included as part of the category “automation tools”, instead of being considered as a separate process step. 110

Figure 3.10. Boxplots representing the distribution of global warming impacts associated with each of the RE magnet inputs affected by yield loss. In this plot the diamond is the mean, the bar is the median, the lower and upper hinges represent the 25th-75th percentile, and the whiskers extend to the minimum and maximum. *Fe, Fe sludge, and Boron carbide are not depicted separately in the graph due to their relatively small impact contribution but are included in the Total plot..... 111

Figure 4.1. Process flow diagram for HDD RE magnets with locations assumed for this study (Bailey et al, 2020; Frost et al, 2021)...... 121

Figure 4.2. Summary of the major methodological steps used in this study and the data sources and transformations performed. This methodology can be applied to any manufactured product, by adjusting Step 1 to include the product-specific Bill of Materials and supply chain (i.e. geographic scoping). 125

Figure 4.3. Figure a (left) is a map of the Level 4 basins for East Asia available from HydroBASINs with RE manufacturing locations represented as yellow stars. Figure b (right) displays the 15 arc-second resolution river reaches within the Level 4 basin near Bayan Obo (top yellow star) and Baotou (bottom yellow star). 133

Figure 4.4. Chemical footprint in m3 from Scope 1 magnet manufacturing emissions by basin of interest (a) and by each major production unit (b). The labels for each basin represent a general description of the geographic area (city, province or country) where the manufacturing occurs, based on granularity of location data available..... 135

Figure 4.5. Dilution factors of the river reach required to dilute the sum of each of the chemicals of concern to its PNEC for locations associated with RE magnet processing (Scope 1) and process electricity use (Scope 2)..... 136

Figure 4.6. Chemical footprint for each hydrobasin, displaying contribution by chemicals of concern (CoCs). This figure excludes CoCs which contribute less than 0.01% of the total footprint. 138

ABSTRACT

As society rapidly migrates to digitized services, the Information, Communications, and Technology (ICT) sector is projected to sustain a 16% compound annual growth rate (CAGR) over the next five years, surpassing \$1 trillion in revenue by 2024. The hardware infrastructure that supports ICT growth, such as semiconductor chips and hard disk drives (HDDs), is also experiencing parallel growth trajectories. Thus, large technology companies need to understand the environmental implications of growth in these vital components within their supply chains, as they strive to reach ambitious targets for carbon, water, and waste reduction.

Life cycle assessment (LCA) is a powerful tool for measuring environmental impacts along the life cycle of a product and is implemented here to measure emissions and resource use in the semiconductor and HDD manufacturing supply chains, and to quantify the benefits of circularity for HDD components. However, to understand how environmental impacts of a manufacturing process relate to the landscapes (i.e. ecosystems) where manufacturing occurs, one must look to methods beyond LCA.

Footprinting methods are a promising tool for bridging the gap between LCA process data inventories and site-specific impacts on ecosystems. Further, the footprint assesses the total volume of emission over a time period, which is aligned with the concept of absolute sustainability. As such, regionalized footprint methods for freshwater use in the semiconductor industry and toxic chemical pollution for the HDD rare earth magnet supply chain were undertaken. In each case, data from the LCA literature or custom LCAs were used as the basis for the life cycle inventory, but advanced methods including regional databases of water scarcity and toxicity factors were used to quantify and communicate impacts. Further, geographic information systems (GIS) were used to allocate emissions or water use from a manufacturing facility with their associated watershed, which enabled aggregation of data across various geographies (i.e. watershed, region, country).

This work implements multi-disciplinary methods, databases, and tools with the aim to bring water and chemical footprinting methods a step closer towards meaningful assessment of a product's impact on local, regional, and planetary boundaries.

1. INTRODUCTION

1.1 The Electronics & ICT Sectors

The electronics sector is comprised of the computer and electronic product manufacturing entities (U.S. Census Bureau, 2017) that provide the hardware to support the information technology and communication (ICT) sectors. This hardware includes servers and their associated circuit boards, processor chips, and storage devices (e.g. HDDs) which underpin ICT services, such as cloud computing. As society rapidly migrates to more digitized services (Giemzo et al., (2020), industries which provide hardware, software, or internet as a service (i.e. SaaS, HaaS, IaaS) are projected to sustain a 16% compound annual growth rate (CAGR) over the next five years, surpassing \$ 1 trillion in revenue by 2024 (IDC, 2020). The semiconductor industry manufactures key components (i.e. chips) which support IT infrastructure, and enables aviation, automotive, appliance, and other connected IoT devices, as well. The industry is currently valued at \$476 billion (IDC, 2021a) and is projected to have a 5% CAGR over the period from 2019-2024 (IDC, 2021b). Similarly, storage devices such as hard disk drives (HDDs) and solid-state drives (SSDs) are vital to data center and personal computer markets and the storage market is projected to grow 18% between 2019 and 2024, with an estimated doubling of the volume of data stored every 4 years (Reinsel & Rydning, 2020).

Further, the entire digital economy, which is more broadly defined as “goods and services that either were produced using digital technologies or include these technologies,” is estimated to currently represent 15.5% of global GDP and is growing 2.5 times faster than global GDP (Henry-Nickie et al, 2019). Thus, the societal impact of this digital transformation cannot be emphasized enough, and the so-called 4th Industrial Revolution will continue to disrupt and shape the way we live our lives (Schwab, 2016). This transformation has shifted the production and consumption of goods and services, and ultimately will inform how we mitigate technology’s impact on society. Our society must continue to decouple growth from environmental damage (Everett et al., 2010) and the ICT sector has an opportunity to accelerate this process with innovations within the electronics supply chain, by enabling efficiency improvements in other sectors such as transit and

using technology to empower consumers to make low-carbon decisions, among others (Varro & Kamiya, 2021).

1.2 Environmental Impacts of Electronics

Both consumer and enterprise electronics, often referred to as “electrical and electronic equipment (EEE)” are being manufactured and disposed of at an accelerating pace (3-5% growth per year, Shittu et al, 2021). Environmental impacts along the life cycle of electronics are due to extraction and processing of raw materials such as aluminum, gold, copper and palladium, highly complex manufacturing of silicon into advanced microprocessor devices, transport impacts due to the globalized nature of the electronics supply chain, electricity-related impacts during use phase, and a growing volume of toxic waste attributed to a low global recycling rate (17.4%) of consumer electronics (Forti et al, 2020).

“The 1.7 Kilogram Microchip: Energy and Material Use in the Production of Semiconductor Devices” by Williams et al. (2004) was one of the first papers to estimate the life cycle emissions of semiconductor devices and highlighted that one of the most impactful products in the electronics industry comes in a very small package. The authors describe the material and energy inputs required to produce a DRAM (i.e. memory) chip and highlight how the high purity chemicals, water, and electricity required to transform silicon into advanced computing chips are orders of magnitude more intensive than traditional goods. Water and energy use have continued to be areas of concern for this industry (Boyd et al, 2012), especially in arid environments where many of these fabs are located (Klop & Wellington, 2008).

Waste EEE (WEEE) comprises a relatively small portion of the total solid waste stream (<2%) but represents approximately 70% of the contribution of heavy metals (and their associated toxicity) to municipal solid waste landfills (USEPA, 2004). And although the recycling rates of enterprise electronics (i.e. servers in a hyperscale datacenter) are very high, at up to 90%, (Polverini et al, 2018), resource-intensive recycling practices for precious metals (e.g. chemical extraction and smelting of gold) are often required due to low concentrations of the materials within products and the associated difficulty in separating materials. In some cases, there are no viable reuse pathways

for electronic products and components and there is a complete lack of recycling streams for many critical metals (Jin et al, 2020) and low-value plastics.

1.2.1 Critical Materials

The specialized nature of electronic components such as semiconductors and rare earth magnets require an ever-expanding list of rare and precious metals (Graedel et al, 2015), which have unique properties and have enabled Moore’s law scaling over the last two decades. However, many of these substances are considered “critical materials”, because of vulnerability to supply chain disruptions, supply chain restrictions, or low substitutability (Graedel, 2015). Material criticality can be considered a sustainability issue because of the integral role of these materials in the functioning of most electronics products, yet the U.S. is 100% import reliant for 14 critical minerals (Center for Sustainable Systems, 2021). Additionally, many of these materials also typically have intensive environmental impacts in the mining and processing phase, as well as minimal or non-existent recycling streams (Jin et al, 2020).

1.3 ICT Sector Sustainability

The overall picture is of an industry that is among the strongest drivers of growth for the U.S. and global economies, but with increasing environmental concerns within the supply chain and at end-of-life (EoL). Given the urgency of carbon reductions required to meet Paris Agreement targets (UNEP, 2021) and the market competition around sustainability (Unruh, 2010), top technology companies have made aggressive sustainability commitments (Quinson, 2021), promising to grow their revenue and increase their physical footprint, all while reducing their environmental footprint. These commitments are usually focused on the reduction of greenhouse gases (e.g. Microsoft’s pledge to be carbon negative by 2030), but increasingly companies have made pledges related to water positivity, zero waste, and ecosystem health, as well (Microsoft, 2020).

These metrics are often defined, and progress is measured, relative to the greenhouse gas (GHG) accounting standard which classifies an organization’s emissions or resource use into Scope 1, 2 and 3 (GHG Protocol, n.d.). Scope 1 emissions are direct emissions from an organization’s owned or controlled assets, Scope 2 are indirect emissions from purchased electricity, and Scope 3 are all

emissions associated with the supply chain of the organization, both upstream and downstream. While technology companies comprise only a small amount (~1%) of the total global GHG emissions, they have led the shift towards renewable energy, accounting for 3.5% of all global renewable capacity additions (Varro & Kamiya, 2021), and have made impressive progress towards completely offsetting Scope 2 emissions (BBC, 2020). However, Scope 3, or ‘supply chain emissions’, are often difficult to quantify and mitigate, especially for impact categories that are subject to large spatial and temporal variability.

While the focus of most sustainability initiatives has been on lowering greenhouse gas emissions, to date, advances in the quantification and mitigation of freshwater use, emissions of toxic chemicals, and other impacts within the electronics supply chain (Scope 3) must be pursued, in parallel, as these represent real threats to the Earth’s environmental boundaries. (Clift et al., 2017).

1.4 Quantifying Environmental Sustainability with Life Cycle Assessment

One of the most powerful tools available to quantify the environmental impact over the life cycle of a product is life cycle assessment. Life cycle assessment (LCA) is a comprehensive environmental management tool that quantifies the environmental inputs (e.g. water, energy, minerals) and outputs (emissions, co-products) of a product from raw material acquisition to end-of-life. LCA also considers a comprehensive set of impact categories, which convert inventories of emissions and resource use to impacts associated with three main areas of protection: human health, biotic environment, and abiotic environment (ILCD, 2010) (Figure 1). LCA uses a systematic approach, establishing clear boundaries and accounting methods which allow for fair comparisons to be made among products or over product generations. Additionally, LCA has been in active development over the last four decades to support product sustainability assessment, and there are robust methodologies (e.g. ISO standards), professional organizations, generic and sector-specific inventory databases, and a suite of software tools to support modeling of products.

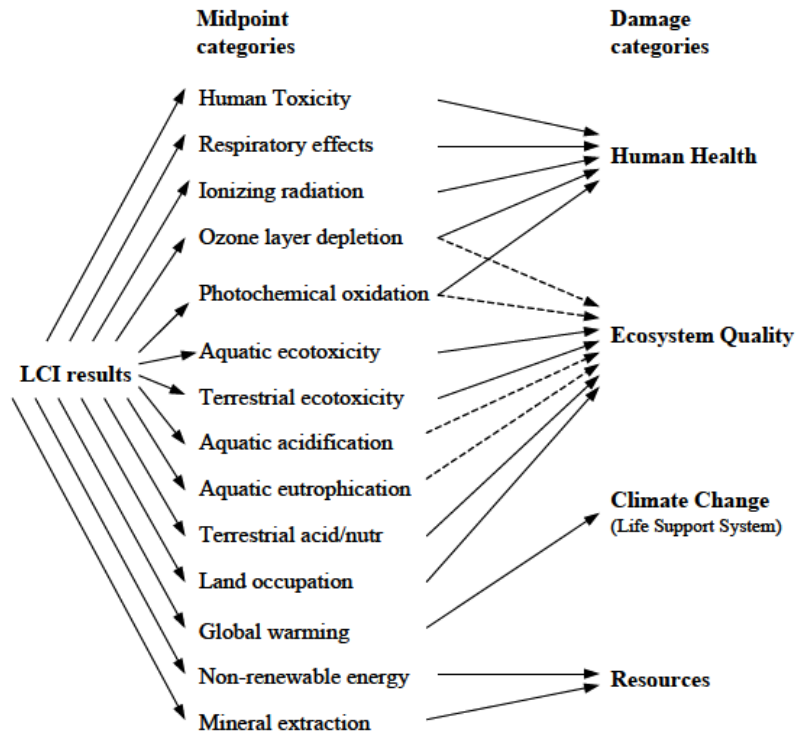


Figure 1.1. Results from a life cycle inventory (LCI) are used to determine an array of mid-point impacts as part of the life cycle impact assessment analysis. Used with permission. © European Union, 2010. ILCD

1.4.1 LCA and the Electronics Circular Economy

The circular economy (CE) is “an industrial system that is restorative or regenerative by intention and design” (Ellen MacArthur Foundation, 2012). As society transitions from a linear “take-make-waste” economy to a circular economy, LCA will continue to be important as a systems-level analysis tool to support decision-making. Organizations are increasingly looking to incorporate principles of circular economy such as design for reuse, remanufacturing, and advanced recycling into their business models (Frost et al, 2020); thus, providing real-world examples of reuse of subassemblies or components is important to demonstrate the feasibility of a circular business model.

Electronic devices are comprised of high value components and critical materials (Buechler et al., 2020). Hard disk drives (HDDs), in particular, are a prime candidate for circularity because of the stable design form and high collection rates from commercial users (i.e. estimates of 90-95% from

hyperscale or enterprise data centers) (Handwerker et al., 2017). It is important to understand the potential environmental impacts and benefits of a new circular business model and be able to compare it to “business as usual” to understand the potential circularity benefits, especially when large, upfront capital investments are required. LCA can help communicate these benefits, as well as describe any burden shifting which may occur when implementing new processes.

1.4.2 Limitations of LCA

There is widespread acknowledgement that LCA is best suited to assess the eco-efficiency of a functional unit of product, i.e. relative improvements in sustainability, but is not optimal for considering macro-level impacts (Williams, 2011) or ‘absolute sustainability’ (Bjorn et al 2015; Kara et al, 2018). The absolute sustainability framework considers sustainability with respect to the “foreseeable growth in market volume that results from increases in population and affluence” (Hauschild et al., 2020).

Additionally, in a typical LCA study, environmental impacts are defined at the midpoint level (e.g. aquatic ecotoxicity) but these potential impacts are not quantified with respect to the ecosystems in which they occur (e.g. the ability of a waterbody to assimilate the toxic pollutant) (Bare, 2006; Hauschild and Potting, 2005). This is especially problematic when considering highly localized impacts such as water use, nutrient pollution, or toxic chemical pollution (Clift et al, 2017). Because environmental systems are dynamic and highly variable, describing impacts without relating them to local conditions may lead to under- or overestimation of impacts and consequently, erroneous decision-making.

1.5 LCA and Planetary Boundaries

This issue can be addressed by combining the rich life cycle process emissions data provided by LCA with consideration of local, regional, or global ecosystems and their associated boundaries. (Bjorn et al., 2015; Kara et al, 2018; Ryberg et al, 2020). The concept of a ‘planetary boundary’ was introduced by Rockström et al. in 2009, and since has garnished wide attention from the research community and beyond (Steffen et al, 2015). Planetary boundaries (PBs) are “... scientifically based levels of human perturbation of the ES [earth system] beyond which ES

functioning may be substantially altered”: nine processes were identified as critical to maintaining the ES (Figure 1.2). Staying within the associated boundary for each process allows the ES to remain within a “safe operating space” for humanity and takes a conservative, precautionary principle approach to boundary setting. (Rockström et al, 2009).

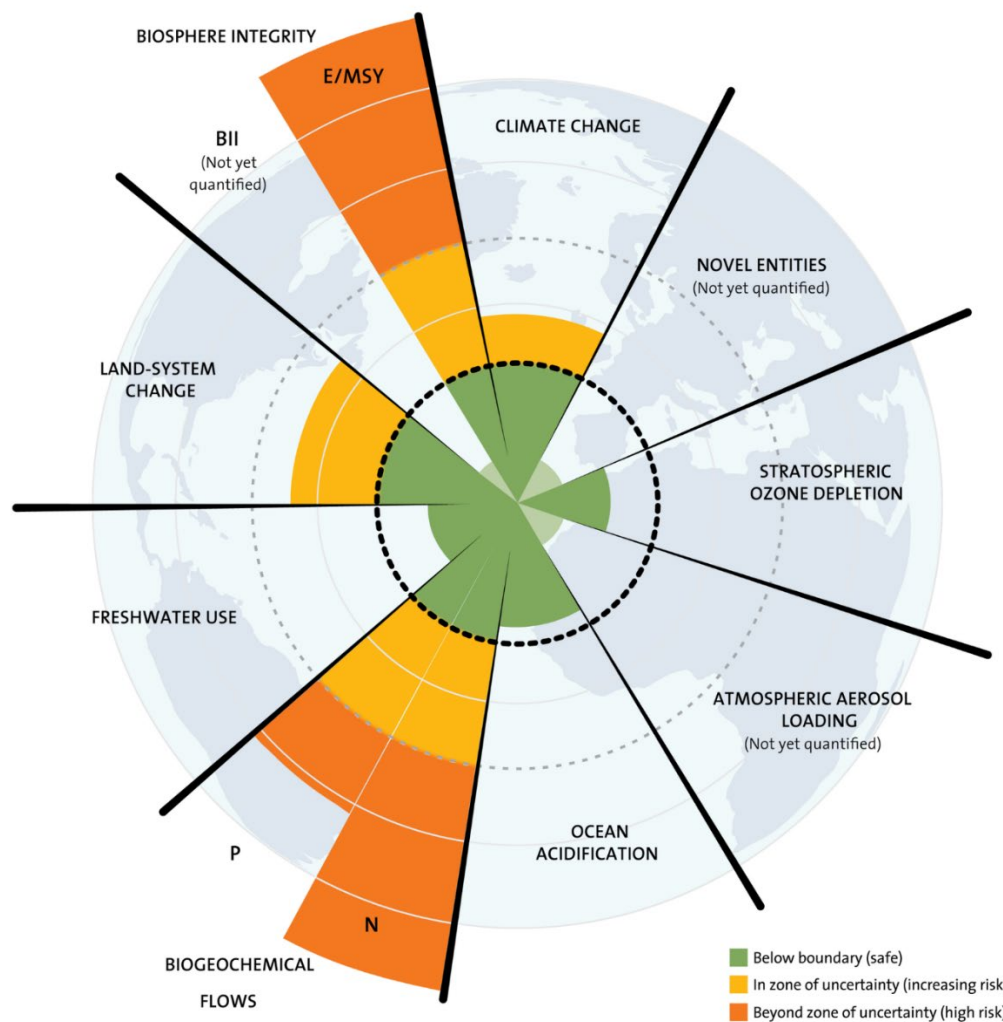


Figure 1.2. Depiction of the planetary boundaries concept. J. Lokrantz/Azote based on Steffen et al (2015). Used with permission.

Since PBs were conceptualized in 2009, many authors have advocated for PBs that account for spatial heterogeneity and researchers have been working towards the development of regional boundaries for impact categories such as freshwater use and biosphere integrity (Steffen et al,

2015). For example, Clift et al (2017), promoted the use of the Available Water Remaining (AWaRe) indicator as a step towards quantifying regional and global PBs for freshwater use. The Science-Based Targets initiative is another example of how a PB for climate change (i.e. 1.5°C of warming) has been operationalized to assign reductions across sectors and within specific timeframes (SBTi, 2021).

However, the other impact categories still do not have an agreed upon regional or planetary boundary. This is especially true for “novel entities” (Rockström et al, 2009) such as chemical pollution due to the inherent complexity in quantifying emissions of thousands of chemicals, the fact that they interact with several PBs (e.g. biosphere integrity, nutrient pollution) (Clift et al, 2017), and lack of agreement or standardization of methods.

Although operationalizing the PBs is still under active development (Bjorn et al, 2020; Ryberg et al, 2016), the PB framework has brought into focus the need to place a product or process-LCA within the context of total environmental impact (Hauschild et al., 2020). The functional unit, a cornerstone of LCA, is key for comparing environmental impacts among products and measuring product or process improvements (i.e. eco-efficiency) (Bjorn et al, 2015). However, only when the impact of a product is considered in terms of absolute sustainability and related to planetary boundaries, can society truly begin to measure progress in reducing global pollution, allocating environmental space to various entities, and ensuring that we maintain a safe operating space for humanity (Bjorn et al, 2015; Hauschild et al., 2020).

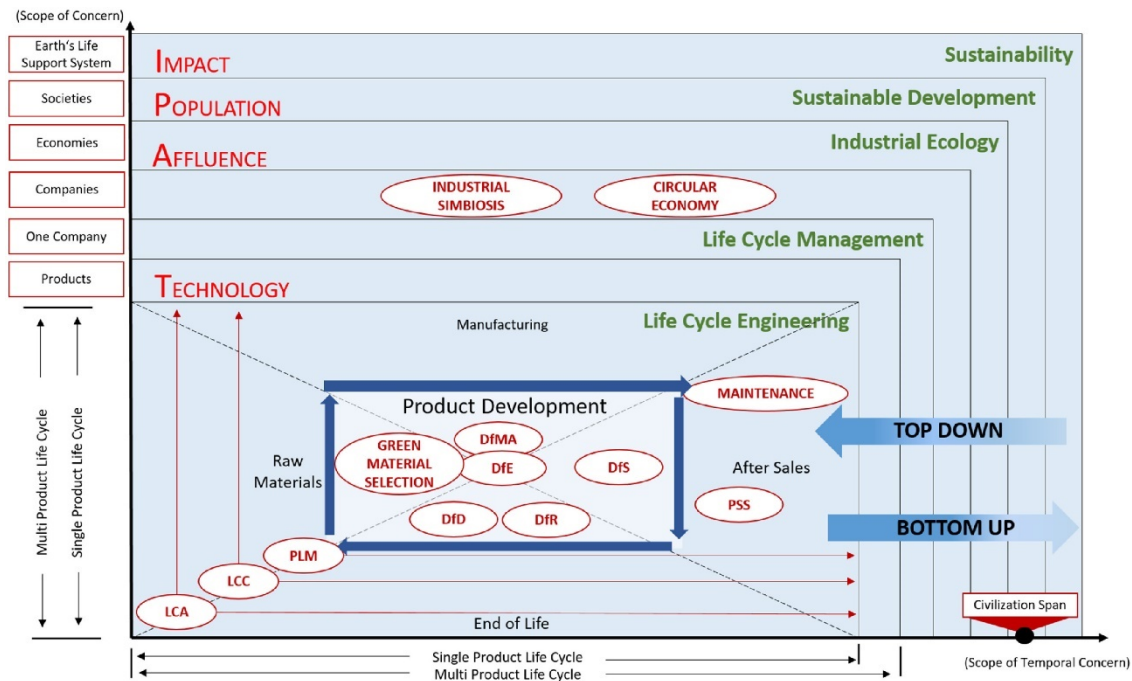


Figure 1.3. The framework from Hauschild et al., (2020) depicts how life cycle engineering relates to PBs and absolute sustainability. Used with permission ([CC BY NC ND](#)).

In practice, this means that the unit of product under consideration (i.e. functional unit) needs to be analyzed with the following questions in mind:

1. What is the total volume of emissions over a time period (i.e. how many products or functional units are being manufactured each year?)
2. Where are the locations of emissions along the life cycle (i.e. where in the supply chain are the emissions actually occurring?)
3. What is the proximity of emissions to the receiving ecosystem (e.g. waterbody)?
4. What is the carrying capacity of that receiving ecosystem?

1.6 Footprinting as a Bridge

Footprint indicators are a promising tool to bridge LCA-derived product emissions and PBs as they are already designed to integrate life cycle emissions data with measures of absolute sustainability (Vanham et al, 2019). Hoekstra defines a footprint as the “quantitative measure describing the appropriation of natural resources by humans” (2011) and environmental footprints

can be implemented at the product, organization, sector, region, or country level. Footprints have arisen within the last decade as a response to a common criticism of LCA impact assessment, namely the difficulty in interpretation of LCA results by a non-technical audience (Ridoutt & Pfister, 2013). The carbon footprint, the most notable of the footprint family, has seen great success because communicating impacts of a single facet of pollution is much easier (Ridoutt & Pfister, 2013) and can be summarized at an organizational level (Fang & Heijungs, 2014). The two footprint categories explored in this work are related to freshwater use and chemical pollution (i.e. chemical footprint) by major stakeholders within the electronics supply chain.

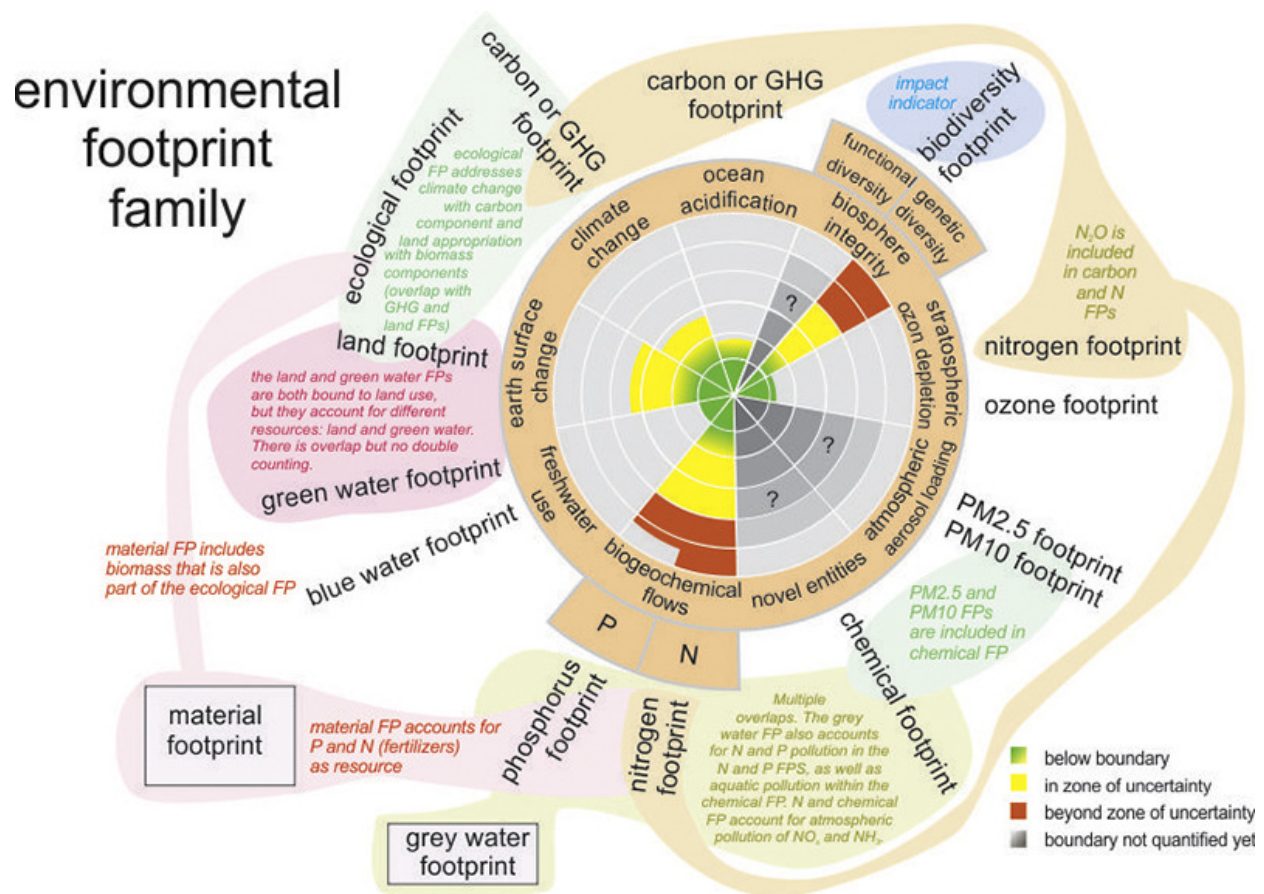


Figure 1.4. Family of footprint indicators and how they relate to planetary boundaries. Used with permission under [CC BY 4.0](https://creativecommons.org/licenses/by/4.0/).

1.6.1 Freshwater Use

1.6.1.1 Industrial Freshwater Use

In most countries, including the U.S., industrial water use is not understood with a high degree of spatial or temporal granularity (Frost and Hua, 2019). McCall et al. (2021) described the pressing need to accurately understand the volume of industrial water use across sectors and at more granular spatial and temporal scales. They argue that in order to ensure there is enough water to meet the demands of all users (industry, people and ecosystems), more comprehensive, transparent, and publicly available databases providing water use per facility, along with its location within a sub-basin, is needed. Without first understanding what the baseline of water use is within an industry, or within a watershed, it is difficult to prioritize process improvements related to water reuse and water efficiency or determine regulatory interventions to influence behavior. It is also difficult to predict risk when considering new manufacturing facilities in a watershed unless co-location of water-using industries within a watershed are accounted for (McCall et al, 2021).

McCall et al. (2021) make recommendations to help address the gaps in water use data that are prevalent within the U.S. and globally due to lack of standardized data collection and disparate governing bodies. Estimates of water use based on process data, or other sources such as economic input-output data should attempt to disaggregate data to the facility-level and be responsive to changes in technology, as well as the hydro-environmental variables within a watershed (i.e existing scarcity) (McCall et al, 2021). Spatial analysis tools such as GIS can be used to spatially aggregate or disaggregate facility-level inventories, allowing this data to be summed over geographies of interest.

1.6.1.2 Water-Energy Nexus

Industry is estimated to use 33% of total energy in the United States (EIA, 2020) and 57% of the world's total delivered energy (IEA, 2021). Accurate estimation of water use from electricity production is vital given the outsized impact of the energy sector on water resources (Macknick et al., 2012), which is often referred to as the 'water-energy' nexus. Water use data have been categorized by electricity generating type (e.g. coal, natural gas, hydroelectric) and associated cooling technologies (i.e. open loop cooling, closed loop cooling, and air cooling) and Meldrum

et al. (2013) summarized and reported both water consumption and withdrawal factors by life cycle phase for use in LCA studies. The impact of electricity use during the manufacturing phase is highly dependent on up-to-date data for the mix of fuels supplying the grid in a given location, and where feasible, technology and location-specific, water use metrics should be used (McCall et al., 2021).

1.6.1.3 Water Scarcity

Many areas of the globe are already reaching the limits of a sustainable supply of freshwater for human and ecosystems demands (UN Water, 2019), i.e. water scarcity. In general, water scarcity describes the relative water demand to total water availability for a given area, or the ‘potential of water deprivation’ for humans or ecosystems (Boulay et al., 2017). Xu and Wu (2017) reviewed several water scarcity indices and methodologies that have been developed over the past thirty years and found that these metrics have converged around two basic approaches: “water crowding” indices which are focused on per capita human water needs and “use-to-resource ratio” indices which are focused on the ratio of water withdrawals or consumption to available resources (Xu & Wu, 2017).

The AWaRe (Available Water Remaining) method is a ‘use-to-resource ratio’ method and has obtained wide consensus among LCA practitioners. This method implements the AWaRe index, which is a watershed-based water scarcity characterization factor developed by the SETAC/UNEP Water Use Life Cycle Assessment Group (WULCA, 2018). The AWaRe index is calculated by assessing water availability minus demand by humans and aquatic ecosystems, per area and by month; thus, taking into account the spatial and temporal variability of freshwater supply. The AWaRe water scarcity factors (Boulay et al., 2017) can be used to assess existing scarcity, acting as a scarcity ‘multiplier’ for water use to indicate potential risk of depriving other users (i.e. humans or aquatic organisms) of freshwater.

1.6.1.4 Consumption vs Withdrawals

Water withdrawals are defined as “water removed from the ground or diverted from a surface-water source for use” (USGS, 2016). Alternatively, consumptive water use refers to water

withdrawn that is incorporated into a product or crop, or evaporated, transpired or consumed by animals or humans. Water that is withdrawn but ultimately returned to the same watershed from which it came does not count as consumptive use (USGS, 2016). The AWaRe method put forth by WULCA is based on a blue water consumption calculation.

Although consumptive water use is the recommended approach by WULCA, industrial water use data is often not reported with respect to consumptive use and withdrawals-to-consumption ratios have not been established for many industries, or are highly aggregated (Bijl et al, 2016). Thus, a withdrawals-based approach is often required, due to data limitations, but can also be considered more aligned with the use of a precautionary principle within the PB framework (Rockström et al, 2009). In this way, withdrawals-based inventories can be used as a screening-level assessment of potential impacts on other users (e.g. aquatic ecosystems), rather than an absolute measurement of volumetric water use.

1.6.1.5 Water Use in the Semiconductor Industry

Although the electronics industry (including the semiconductor industry) is considered a small user of direct water when compared to paper or primary metals, Rao et al. (2017) reported that the electronics sector has the third highest energy-water ratio (after “Machinery” and “Electrical Equipment” sectors, respectively), highlighting the importance of the water-energy nexus for electronics. The semiconductor industry has shown improving trends in water reuse, but semiconductor industry trends (i.e. doubling of transistor density every two years) has led to increases in the need for high purity water and chemicals, and more complex and energy-intensive patterning steps. In addition, increases in wafer size and the associated transition from batch processing to single wafer processing which requires more water per wafer, has also contributed to increased total water demands by the industry (Libman & Neuber, 2008; Sematech, 2013). This indicates that the semiconductor industry constitutes a small, but growing user of direct and energy-related water.

Boyd has provided water use data for semiconductor manufacturing, stratified by semiconductor technology type (e.g. DRAM, NAND flash, CMOS) and technology node (e.g. 32 nm, 57 nm).

This can be applied to a global semiconductor production database (SEMI, 2017) so that facility-level water use with respect to production volume and technology type can be calculated.

1.6.2 Toxic Chemical Pollution

A chemical footprint has been defined by Sala as “a quantitative measure describing the environmental space needed to dilute chemical pollution due to human activities to a level below a specified boundary condition” (2013). Interest in chemical footprinting has been on the rise in response to public health research that indicates chemical pollution is a growing, global problem, and its impacts on human health and ecosystems are often poorly defined (Landrigan et al., 2018). Government regulations related to chemicals management has also increased rapidly over the last couple of decades, led by European initiatives such as REACH (Registration, Evaluation, Authorization and Restriction of Chemicals) and RoHs (Restriction of Hazardous Substances) (ECHA, 2021).

Thus, industry must consider the management of chemicals as part of its operational, regulatory, and reputational risk management strategy. These considerations gave rise to the chemical footprint project (CFP), a program of Clean Production Action, which works towards the goal of “environmentally sound management of chemicals.” (Peele et al., 2018). The CFP uses an annual survey of companies which assesses their chemical inventory and quantifies their chemical footprint. There is wide support for this project across all industrial sectors and signatories include Johnson & Johnson, Kimberly-Clark, Seagate, and Walmart, among others. This effort is centered around the identification of chemicals of high concern (CoHCs) and the strategies that companies have in place to reduce these chemicals not only within their own facilities, but in their supply chain and through end of life.

This type of ‘chemical footprint’ is an excellent first step towards understanding chemical use at an aggregate level and encouraging companies to initiate the intensive process towards full chemicals disclosure. However, there is much to be gained by using tools such as LCA to quantify chemical use throughout the product’s life cycle, use supply chain data to locate the emissions to a geographic area, and then determine the potential impacts of those chemicals in that geography.

An advanced chemical footprint method, as conceptualized by Sala & Goralcyk (2013), combines life cycle methodology with human and ecological risk assessment principles to determine the release of chemicals into air, soil, and water and potential impacts on ecosystems (Sala, 2013; Zijp et al, 2014; Bjorn et al 2014). According to Zijp et al. (2014), the chemical footprint considers 1) exposure assessment and 2) impact assessment (grounded in traditional risk assessment and LCA principles), 3) boundary conditions (i.e. safe thresholds of pollution defined at local, regional or global scale (Steffen et al., 2015), and 4) the dilution volume needed to maintain the boundary condition, which is a concept advanced by the grey water footprint method (Hoekstra, 2011).

1.7 Regionalized Footprinting

Regionalized footprint and LCA methods, and associated regional PBs, are preferred for several categories of environmental impact such as freshwater use, and nutrient and chemical pollution. For freshwater use (i.e. bluewater footprint), these regions have been well-defined and Bjorn et al. (2020) described how to bridge the gap between LCA process data and regional PBs. Regionalization of footprints have also been described for chemical footprints (Makarova, et al., 2018; Wang, 2019), but the method is still under development and is ripe for increased standardization. One of the current major barriers to uptake of a regionalized chemical footprint is method complexity (Clift et al, 2017). There are two main ways to address this: thoughtful geographic and chemical substance scoping (Clift et al, 2017) and the use of state-of-the-art, regionalized datasets for chemical toxicity (Verones et al, 2020) and hydrology (Linke et al, 2019).

1.8 Problem Statement & Aims

A lack of spatially explicit unit process data in LCA may lead to over or under-estimation of impacts. Further, the eco-efficiency approach of LCA does not consider absolute sustainability, which strives to understand the impacts of a product with respect to the total volume of emissions and relate impacts to regional or global planetary boundaries. Research has begun to bridge this gap, but methods must be advanced and standardized to promote wider adoption, with the tenets of the precautionary principle, in mind. And given the importance and growth rate of the ICT sector, more case studies within the electronics industry are needed.

This dissertation aims to assess the spatial variability of impacts of the electronics sector by 1) applying LCA and a water footprint technique to determine the risks to freshwater ecosystems by the semiconductor industry, 2) illustrating how LCA can be used to assess a circular economic business model for HDDs, and 3) advancing methods to bridge the gap between LCA and planetary boundaries, with respect to chemical pollution from HDD component manufacturing. Below is a summary of the chapters addressing these aims:

Chapter 2: The objective of this chapter is to provide the first report of total global water withdrawals for the semiconductor manufacturing industry, a known large user of process water and electricity, using a bottom-up approach and application of derived regional electricity water use coefficients. This project quantified the water withdrawals from fab process water and electricity use that are associated with various chip technologies by using existing LCA data and industry estimates. The water use intensity of electricity (water-energy nexus) was also delineated at a regional level, when possible, to fully explore the variability across geographies. A water scarcity multiplier was applied to water withdrawals to determine scarcity-weighted water use at each individual facility and summed to quantify use by the global semiconductor industry. The results are presented using maps to describe spatial variability, and an assessment considering temporal variability (i.e. seasonal fluctuation in water scarcity) was also presented.

Chapter 3: This chapter describes the environmental impacts of implementing a closed-loop recovery and reuse process for a highly reliable HDD subassembly, known as the voice coil motor assembly (aka “magnet assembly”), using data from an industry pilot study. The pilot project demonstrated a circular business model to disassemble an HDD within a datacenter, remove the rare earth magnet assembly (MA), and send the MA back to the HDD manufacturer for direct reuse in a new HDD and quantified process impacts using LCA. The inventory implemented up to date rare earth (RE) metals and RE magnet unit process data and material and power use measurements of a magnet assembly (MA) recovery process in a hyperscale DC, use of supply chain specific shipping/logistics data, inclusion of packaging configurations based on a commercially scaled process, and updated RE magnet data from an enterprise helium drive which is expected to serve as a flagship technology in DCs for the next decade. Further, this study presented several scenarios

for MA recovery including the effect of purchasing renewable energy and the effect of automation of recovery processes on environmental impacts.

Chapter 4: Among other impacts, the LCA in Chapter 3 identified aquatic ecotoxicity concerns with respect to HDD RE magnet mining and processing. Because the RE magnet manufacturing supply chain is concentrated in just a few locations, spatial unit processes were determined, and a spatially explicit chemical footprint was undertaken to understand the impact of HDD RE magnet manufacturing on local ecosystems. Specifically, this method uses a typical LCA inventory process to determine chemical emissions to air, soil and water, but implements regionalized fate and exposure data from USETox, a chemical regulatory boundary concept, and the use of a standardized, hydrobasin dataset to determine the capacity of the receiving ecosystem to assimilate pollution.

1.9 References

Bailey, G., Joyce, P. J., Schrijvers, D., Schulze, R., Sylvestre, A. M., Sprecher, B., ... & Van Acker, K. (2020). Review and new life cycle assessment for rare earth production from bastnäsite, ion adsorption clays and lateritic monazite. *Resources, Conservation and Recycling*, 155, 104675.

Bare, J. C. (2006). Risk assessment and life-cycle impact assessment (LCIA) for human health cancerous and noncancerous emissions: integrated and complementary with consistency within the USEPA. *Human and ecological risk assessment*, 12(3), 493-509.

BBC (2020, September 14). *Google says its carbon footprint is now zero*. BBC News. Available at <https://www.bbc.com/news/technology-54141899> (accessed 7 November 2021).

Bijl, D. L., Bogaart, P. W., Kram, T., de Vries, B. J., & van Vuuren, D. P. (2016). Long-term water demand for electricity, industry and households. *Environmental Science & Policy*, 55, 75-86. DOI: <https://doi.org/10.1016/j.envsci.2015.09.005>

Bjørn, A. Diamond, M., Birkved, M. and Hauschild, M.Z. (2014). Chemical footprint method for improved communication of freshwater ecotoxicity impacts in the context of ecological limits *ES&T*. 48 (22) 13523-13262. DOI: <https://doi.org/10.1021/es503797d>.

Bjørn, A. Diamond, Owsianiak, M., Verzat, B. and Hauschild, M.Z. (2015). Strengthening the Link between Life Cycle Assessment and Indicators for Absolute Sustainability To Support Development within Planetary Boundaries. *ES&T*. 49 (11) 6370-6371. DOI: <https://doi.org/10.1021/acs.est.5b02106>.

Bjørn, A., Sim, S., King, H., Patouillard, L., Margni, M., Hauschild, M. Z., & Ryberg, M. (2020). Life cycle assessment applying planetary and regional boundaries to the process level: a model case study. *The International Journal of Life Cycle Assessment*, 25(11), 2241-2254.

Boulay, A.-M., Bare, J., Benini, L., Berger, M., Lathuillière, M. J., Manzardo, A., . . . Pfister, S. (2017). The WULCA consensus characterization model for water scarcity footprints: assessing impacts of water consumption based on available water remaining (AWARE). *The International Journal of Life Cycle Assessment*. doi: <https://doi.org/10.1007/s11367-017-1333-8>

Buechler, D. T., Zyaykina, N. N., Spencer, C. A., Lawson, E., Ploss, N. M., & Hua, I. (2020). Comprehensive elemental analysis of consumer electronic devices: Rare earth, precious, and critical elements. *Waste Management*, 103, 67-75. DOI: <https://doi.org/10.1016/j.wasman.2019.12.014>

Center for Sustainable Systems, University of Michigan. (2021). *Critical Materials Factsheet*. Pub. No. CSS14-15. Available at <https://css.umich.edu/factsheets/critical-materials-factsheet> (accessed 7 November 2021)

Clift, R., Sim, S., King, H., Chenoweth, J. L., Christie, I., Clavreul, J., ... & Murphy, R. (2017). The challenges of applying planetary boundaries as a basis for strategic decision-making in companies with global supply chains. *Sustainability*, 9(2), 279. DOI: <https://doi.org/10.3390/su9020279>

EIA. (2019). Monthly Energy Review: Annual Total Energy. Data for 2019. Retrieved 11-7-2021, from U.S. Energy Information Administration. Available at <https://www.eia.gov/totalenergy/data/browser/index.php?tbl=T02.01#/?f=A&start=200001>

Ellen MacArthur Foundation. (2012). Towards the Circular Economy: Economic and Business Rationale for an Accelerated Transition. Available at <https://www.ellenmacarthurfoundation.org/assets/downloads/publications/Ellen-MacArthur-Foundation-Towards-the-Circular-Economy-vol.1.pdf>

Everett, T., Ishwaran, M., Ansaloni, G.P. and Rubin, A. (2010). Economic Growth and the Environment. Defra Evidence and Analysis Series: Paper 2. March 2010. Available at https://assets.publishing.service.gov.uk/government/uploads/system/uploads/attachment_data/file/69195/pb13390-economic-growth-100305.pdf

Fang, K., & Heijungs, R. (2014). There Is Still Room for a Footprint Family without a Life Cycle Approach—Comment on “Towards an Integrated Family of Footprint Indicators”. *Journal of Industrial Ecology*, 18(1), 71-72.

Forti, V., Balde C.P., Kuehr, R. and Bel, G. (2020). The Global E-waste Monitor 2020: Quantities, flows and the circular economy potential. Available at <http://ewastemonitor.info/>

Frost, K., & Hua, I. (2019). Quantifying spatiotemporal impacts of the interaction of water scarcity and water use by the global semiconductor manufacturing industry. *Water Resources and Industry*, 22, 100115.

Frost, K., Jin, H., Olson, W., Schaffer, M., Spencer, G., & Handwerker, C. (2020). The use of decision support tools to accelerate the development of circular economic business models for hard disk drives and rare-earth magnets. *MRS Energy & Sustainability*, 7. DOI: <https://doi.org/10.1557/mre.2020.21>

Frost, K., Sousa, I., Larson, J., Jin, H., & Hua, I. (2021). Environmental impacts of a circular recovery process for hard disk drive rare earth magnets. *Resources, Conservation and Recycling*, 173, 105694.

Giemzo, J., Gu, M., Kaplan, J. and Vinter, L. (2020). How CIOs and CTOs can accelerate digital transformations through cloud platforms. (15 September 2020). McKinsey Digital. Available at <https://www.mckinsey.com/business-functions/mckinsey-digital/our-insights/how-cios-and-ctos-can-accelerate-digital-transformations-through-cloud-platforms> (accessed 2 November 2021).

Graedel, T.E., Harper, E.M., Nassar, N.T. Nuss, P. and Reck, B.K. Criticality of metals and metalloids. *PNAS*, 112 (14), 4257-4262. DOI: <https://doi.org/10.1073/pnas.1500415112>

Greenhouse Gas Protocol. (n.d.) Frequently Asked Questions. Available at https://ghgprotocol.org/sites/default/files/standards_supporting/FAQ.pdf (accessed 6 November 2021)

Handwerker C.A., Olson W., and Rifer W. (February, 2017). Value Recovery from Used Electronics. iNEMI Final Project Report – Phase 1. Available at: https://community.inemi.org/value_recovery.

Hauschild, M.Z, Kara, S. and Ropke, I. (2020) Absolute sustainability: Challenges to life cycle engineering. *CIRP Annals*. 69 (2), 533-553. DOI: <https://doi.org/10.1016/j.cirp.2020.05.004>

Hauschild, M., & Potting, J. (2005). Spatial differentiation in Life Cycle impact assessment-The EDIP2003 methodology. *Environmental news*, 80, 1-195.

Henry-Nickie, M. Friimpong, K. and Sun, H. (2019, March 19). Trends in the Information Technology Sector. The Brookings Institute. Available at <https://www.brookings.edu/research/trends-in-the-information-technology-sector/> (accessed November 5 2021).

Hoekstra, A. Y., Chapagain, A. K., Aldaya, M. M., & Mekonnen, M. M. (2011). *The Water Footprint Assessment Manual: Setting the Global Standard*. Washington D.C.: earthscan.

IDC (2020, October 15). Cloud Adoption and Opportunities Will Continue to Expand Leading to a \$1 Trillion Market in 2024, According to IDC. International Data Corporation. Available at <https://www.idc.com/getdoc.jsp?containerId=prUS46934120> (accessed 5 November 2021).

IDC. (2021a, February 2). Worldwide Semiconductor Revenue Grew 5.4% in 2020 Despite COVID-19 and Further Growth Is Forecast in 2021, According to IDC. International Data Corporation. Available at <https://www.idc.com/getdoc.jsp?containerId=prUS47424221> (accessed 5 November 2021).

IDC. (2021b, September 19). Semiconductor Market to Grow By 17.3% in 2021 and Reach Potential Overcapacity by 2023, IDC Reports. International Data Corporation. Available at <https://www.idc.com/getdoc.jsp?containerId=prAP48247621> (accessed 3 November 2021)

IEA. (2019). World electricity final consumption by sector, 1974-2019. Available at <https://www.iea.org/data-and-statistics/charts/world-electricity-final-consumption-by-sector-1974-2019> (accessed 7 November 2021).

ILCD. (2010). *ILCD Handbook: Analysis of existing Environmental Impact Assessment methodologies for use in Life Cycle Assessment*. European Commission Institute for Environment and Sustainability. Available at <https://eplca.jrc.ec.europa.eu/uploads/ILCD-Handbook-General-guide-for-LCA-DETAILED-GUIDANCE-12March2010-ISBN-fin-v1.0-EN.pdf>

Jin H., Frost K., Sousa I., Ghaderi H., Bevan A., Zakotnik M., and Handwerker C. (2020). Life cycle assessment of emerging technologies on value recovery from hard disk drives. *Resour. Conserv. Recycl.* 157, 104781 DOI: <https://doi.org/10.1016/j.resconrec.2020.104781>.

Kara, S., Hauschild, M. Z., & Herrmann, C. (2018). Target-driven life cycle engineering: Staying within the planetary boundaries. *Procedia CIRP*, 69, 3-10.

Klop, P & Wellington, F. (2008). Watching Water: A Guide to Evaluating Corporate Risks in a Thirsty World. Pgs 6-19. JP Morgan Global Equity Research. Retrieved at https://files.wri.org/d8/s3fs-public/pdf/jpmorgan_watching_water.pdf

Landrigan, P. J., Fuller, R., Acosta, N. J., Adeyi, O., Arnold, R., Baldé, A. B., ... & Chiles, T. (2018). The Lancet Commission on pollution and health. *The Lancet*, 391(10119), 462-512.
Libman, V., & Neuber, A. (2008). Water Reuse Trends in the Electronics Industry. *Water Practice*, 2(3), 1-12. doi: <https://doi.org/10.2175/193317708X314193>

Linke, S., Lehner, B., Ouellet Dallaire, C., Ariwi, J., Grill, G., Anand, M., Beames, P., Burchard-Levine, V., Maxwell, S., Moidu, H., Tan, F., Thieme, M. (2019). Global hydro-environmental sub-basin and river reach characteristics at high spatial resolution. *Scientific Data* 6: 283. DOI: 10.1038/s41597-019-0300-6.

Macknick, J., Newmark, R., Heath, G., & Hallett, K. C. (2012). Operational water consumption and withdrawal factors for electricity generating technologies: a review of existing literature. *Environmental Research Letters*, 7(4). doi: <https://doi.org/10.1088/1748-9326/7/4/045802>

McCall, J., Rao, P., Gonzalez, S. G., Nimbalkar, S., Das, S., Supekar, S., & Cresko, J. (2021). US Manufacturing Water Use Data and Estimates: Current State, Limitations, and Future Needs for Supporting Manufacturing Research and Development. *ACS ES&T Water*, 1(10), 2186-2196.

- Meldrum, J., Nettles-Anderson, S., Heath, G., & Macknick, J. (2013). Life cycle water use for electricity generation: a review and harmonization of literature estimates. *Environmental Research Letters*, 8(1). doi: <https://doi.org/10.1088/1748-9326/8/1/015031>
- Makarova, A., Shlyakhov, P., & Tarasova, N. (2018). Estimating Chemical Footprint on High-resolution Geospatial Grid. *Procedia CIRP*, 69(1), 469-474.
- Microsoft. (2020). *2020 Environmental Sustainability Report: A Year of Action*. Microsoft. Available at <https://query.prod.cms.rt.microsoft.com/cms/api/am/binary/RWyG1q> (accessed 4 November 2021).
- Peele, C., Rossi, M. & Edwards, S. (2018). Chemical Footprint Project: *2018 Annual Report*. Clean Production Action, Somerville, MA. 20 pages. Retrieved from: <https://www.chemicalfootprint.org/assets/downloads/2018ChemicalFootprintProjectReport.pdf>
- Polverini, D. Ardente, F. Sanchez, I., Mathieux, F. Tecchio, P, and Beslay, L. (2018). Resource efficiency, privacy and security by design: A first experience on enterprise servers and data storage products triggered by a policy process. *Computers & Security*, 76, 295-310. DOI: <https://doi.org/10.1016/j.cose.2017.12.001>.
- Quinson, T. (2021). Tech Companies Are Setting the Most Ambitious Net-Zero Goals. (7 April 2021). Bloomberg Green. Available at <https://www.bloomberg.com/news/articles/2021-04-07/tech-firms-are-setting-the-most-ambitious-net-zero-goals-green-insight> (accessed 6 November 2021).
- Reinsel D. and Rydning, J. (2020). Worldwide Global StorageSphere Forecast, 2020–2024: Continuing to Store More in the Core. (May 2020). Abstract available at <https://www.idc.com/getdoc.jsp?containerId=US46224920> (accessed 4 November 2021).
- Ridoutt, B. G., and Pfister, S. (2013). Towards an integrated family of footprint indicators. *Journal of Industrial Ecology*, 17(3), 337-339.
- Rockström, J., W. Steffen, W. Noone, K. Persson, Å,...& Foley, J. 2009. Planetary boundaries: exploring the safe operating space for humanity. *Ecology and Society*, 14(2): 32. Available at <http://www.ecologyandsociety.org/vol14/iss2/art32/>.
- Ryberg, M. W., Owsianiak, M., Richardson, K., & Hauschild, M. Z. (2016). Challenges in implementing a planetary boundaries based life-cycle impact assessment methodology. *Journal of Cleaner Production*, 139, 450-459. DOI: <https://doi.org/10.1016/j.jclepro.2016.08.074>.
- Ryberg, M. W., Andersen, M. M., Owsianiak, M., & Hauschild, M. Z. (2020). Downscaling the Planetary Boundaries in absolute environmental sustainability assessments—a review. *Journal of Cleaner Production*, 276, 123287. DOI: <https://doi.org/10.1016/j.jclepro.2020.123287>.

Sala, S. and Goralcyk, M. 2013. Chemical Footprint: A Methodological Framework for Bridging Life Cycle Assessment and Planetary Boundaries for Chemical Pollution. *Integrated Environmental Assessment and Management*. <https://setac.onlinelibrary.wiley.com/doi/pdf/10.1002/ieam.1471>

SBTi. (2021). Science Based Targets – How it works. Available at <https://sciencebasedtargets.org/> (accessed 7 November 2021)

Schwab, K. (2016). The Fourth Industrial Revolution: what it means, how to respond. World Economic Forum (14 January 2016). Available at <https://www.weforum.org/agenda/2016/01/the-fourth-industrial-revolution-what-it-means-and-how-to-respond/> (accessed 5 November 2021).

Sematech. (2013). *Environment, Safety and Health Chapter [Table]*. Retrieved from https://www.dropbox.com/sh/qz9gg6uu4kl04vj/AADD7ykFdJ2ZpCR1LAB2XEjla?dl=0&preview=ESH_2013Tables.xlsx (accessed 7 November 2021)

[dataset] SEMI. (2017). *SEMI Fab Database*. [XLS]. <http://www1.semi.org/eu/MarketInfo/FabDatabase>

Shittu, O.S., Williams, I.D. and Shaw, Peter J. (2021). Global E-waste management: Can WEEE make a difference? A review of e-waste trends, legislation, contemporary issues and future challenges. *Waste Management*. 120, 549-563. DOI: <https://doi.org/10.1016/j.wasman.2020.10.016>

Steffen, W., Richardson, K., Rockström, J., Cornell, S. E., Fetzer, I., Bennett, E. M., ... & Folke, C. (2015). Planetary boundaries: Guiding human development on a changing planet. *Science*, 347(6223), 1259855.

United Nations Environment Programme (2021). Emissions Gap Report 2021: The Heat Is On – A World of Climate Promises Not Yet Delivered. Nairobi. Available at <https://www.unep.org/emissions-gap-report-2021>.

Unruh, G. (2010). Can You Compete on Sustainability? (22 March 2010). Harvard Business Review. Available at <https://hbr.org/2010/03/can-you-compete-on-sustainability> (accessed 5 November 2021).

UN Water. (2019). Water Scarcity. United Nations. Retrieved from <http://www.unwater.org/water-facts/scarcity/>

US Census Bureau. 2017. North American Industry Classification System: Computer and Electronic Product Manufacturing. Available at <https://www.census.gov/naics/?input=334&year=2017&details=334> (accessed 3 November 2021).

USEPA. (2004). *Multiple Actions Taken to Address Electronic Waste, But EPA Needs to Provide Clear National Direction*. (Report No 2004-P-00028). USEPA. <https://www.epa.gov/office-inspector-general/report-multiple-actions-taken-address-electronic-waste-epa-needs-provide>.

USGS. (2016). Water Use Terminology. Retrieved from <https://water.usgs.gov/watuse/wuglossary.html>

Vanham, D., Leip, A., Galli, A., Kastner, T., Bruckner, M., Uwizeye, A., ... & Hoekstra, A. Y. (2019). Environmental footprint family to address local to planetary sustainability and deliver on the SDGs. *Science of the Total Environment*, 693, 133642.

Varro, L. and Kamiya, G. (2021, March 25). 5 ways Big Tech could have big impacts on clean energy transitions. International Energy Agency. Available at <https://www.iea.org/commentaries/5-ways-big-tech-could-have-big-impacts-on-clean-energy-transitions> (accessed 4 November 2021).

Verones, F., Hellweg, S., Antón, A., Azevedo, L. B., Chaudhary, A., Cosme, N., ... & Huijbregts, M. A. (2020). LC-IMPACT: A regionalized life cycle damage assessment method. *Journal of Industrial Ecology*, 24(6), 1201-1219.

Wang, L.L. (2019). *Methodology for Accounting for the Chemical Footprint of Products Based on Regional Toxic Stress Indices, China*, (Zhejiang, CN CN201811009866.3). Hangzhou Huiliang Intellectual Property Agency Co., Ltd. 33259. Available online: <http://d.wanfangdata.com.cn/patent/CN201811009866.3> (accessed on 12 August 2021).

Williams, E.D., Ayres, R.U., and Heller, M. (2002). The 1.7 Kilogram Microchip: Energy and Material Use in the Production of Semiconductor Devices. *Environmental Science & Technology*, 36 (24), 5504-5510.

Williams, E. (2011). Environmental effects of information and communications technologies. *Nature*, 479, 354–358. DOI: <https://doi.org/10.1038/nature10682>.

WULCA. (2018). WULCA: Mission and Goals. Retrieved from <http://www.wulca-waterlca.org/mission.html>

Xu, H., & Wu, M. M. (2017). *Water Availability Indices—A Literature Review* (No. ANL/ESD-17/5). Argonne National Lab.(ANL), Argonne, IL (United States). doi: <https://doi.org/10.2172/1348938>.

Zijp, M.C., Posthuma, L. and van de Meent, D. (2014). Definition and Applications of a Versatile Chemical Pollution Footprint Methodology. *Environmental Science & Technology*, 48 (18), 10588–10597. <https://pubs.acs.org/doi/abs/10.1021/es500629f>

2. FRESHWATER USE BY THE GLOBAL SEMICONDUCTOR MANUFACTURING INDUSTRY

Reprinted under CC BY-NC-ND from Frost, K., & Hua, I. (2019). Quantifying spatiotemporal impacts of the interaction of water scarcity and water use by the global semiconductor manufacturing industry. *Water Resources and Industry*, 22, 100115. <https://doi.org/10.1016/j.wri.2019.100115>

2.1 Background

The high-tech semiconductor manufacturing sector is integral to the international electronics industry and was valued at over \$400 billion USD in 2017 (Manoca, 2018). Semiconductors are the silicon microchips utilized in electronics to control the flow of electrical signals. The complex transistor circuitry required to transmit these signals is layered onto silicon wafers at semiconductor fabrication plants ('fabs').

Semiconductor fabs are largely concentrated in the United States, Taiwan, China, South Korea, and Japan. These areas currently account for 83% of fab manufacturing capacity and the rapid evolution of the technology sector means that new fab facilities are being constructed at a high rate. As such, China and Taiwan are outpacing the growth rates of other industry leaders (Semiconductor Industry Association, 2016; Boyd, 2012), which will result in a spatial shift in resource demands by the industry.

2.1.1 Water Use in Semiconductor Manufacturing

Semiconductor fabrication is a water intensive process and efforts have been made by individual companies to assess the water-related risks posed by supply chain (raw materials, transportation and electricity), operations, use, and end-of-life (Quantis International, 2012). Industry has focused on reducing water use in their operations and correspondingly, relative water use efficiency has improved over the years (Sematech, 2013). However, growth in absolute water use is predicted due to year-to-year increases in chip sales (2%-24% from 2016-2018) and associated production capacity, including a 41% increase in capacity for multi-layer flash memory (Liu, 2018). And despite overall improving trends in water reuse efficiency, industry pursuit of Moore's Law (i.e.

doubling of transistor density every two years) has led to increases in the use of higher purity water and chemicals and more complex processing steps. In addition, increases in wafer size (i.e. moving from predominantly 200 mm to 300 mm, and now 450 mm), and the associated transition from batch processing to single wafer processing which requires more water per wafer, has also contributed to increased water demands by the industry (Libman & Neuber, 2008; Sematech, 2013).

Boyd (2012) and Cooper et al. (2011) indicated that the use phase (i.e. use of the chips within the electronic devices) and manufacturing phase are the two most water intense stages in the life cycle of a semiconductor chip (2012). Electricity-related water from the use phase is the primary water user for most chip types and the manufacturing phase is the second largest user of water (Boyd, 2012). Within the chip manufacturing process, water used in the production of electricity to power the semiconductor fabs (i.e. indirect water use) is the single largest user of water; while fab feedwater (i.e. direct water use) represents another major user (Boyd 2012, Cooper et al., 2011). Fab manufacturing water, or ‘feedwater’, serves three major functions in chip manufacturing: process cooling water, production of ultrapure water to rinse the wafer between processes, and cooling water to maintain cleanroom heating, ventilation and cooling (HVAC) systems.

The focus of this assessment is on fab feedwater (FW) and electricity-related water (ERW) withdrawals for the following reasons: i) as mentioned, these two elements represent the two largest water use categories in chip manufacturing (Cooper et al, 2011), ii) there is precedent for manufacturing (i.e. direct or ‘Scope 1’) and electricity-related (i.e. indirect or ‘Scope 2’) resource use as the boundary for analysis within the carbon footprinting literature (Matthews, Hendrickson, & Weber, 2008), iii) both FW and ERW withdrawals associated with a fab are likely to be spatially related and impacts may occur within the same watershed, and iv) water uses related to other processes in the life cycle of a semiconductor chip (e.g. silicon ingot processing, infrastructure/transportation) are comparatively smaller withdrawals (total just 6%, according to estimates from Cooper et al. [2011]). Another important consideration is that feedwater and electricity use are managed by the manufacturer, as opposed to embedded within the supply chain; thus, quantification of withdrawals and associated decisions related to water reduction efforts can be more easily managed within this scope (Mueller et al, 2015). Manufacturing process data from the life cycle assessment literature (Boyd, 2012) and industry reports (Sematech, 2013) provide

estimates of water and energy use intensity, reported at the single microchip or wafer (i.e. hundreds of chips) level.

2.1.2 Electricity-related Water Withdrawals

Estimates of water use from electricity production has been examined over the last decade (Cai, Zhang, Bi, & Zhang, 2014; Jiang & Ramaswami, 2015; Liao, Hall, & Eyre, 2016; Macknick, Newmark, Heath, & Hallett, 2012; Maupin et al., 2014; Spang, Moomaw, Gallagher, Kirshen, & Marks, 2014; Tidwell & Moreland, 2016; Vassolo & Döll, 2005) as understanding of the large impact of the energy sector on water use (the water-energy nexus) has emerged. Water use data have been categorized by electricity generating type (e.g. coal, natural gas, hydroelectric) and associated cooling technologies (i.e. open loop cooling, closed loop cooling, and air cooling). Meldrum, Nettles-Anderson, Heath, and Macknick (2013) summarized and reported withdrawal factors by life cycle phase for ease of use in life cycle assessment (LCA) studies.

A closer examination of the application of electricity water withdrawal metrics is appropriate (Pfister, Saner & Koehler, 2011; Lee, Han, Elgowainy, & Wang, 2018) and addressed here by calculating regionalized electricity water use intensity factors for two of the world's major semiconductor producing countries: the U.S. and China. In the U.S., electricity generation by fuel type for each of the country's eight major electricity trading regions (collectively known as the North American Electric Reliability Corporation or NERC) are provided by the U.S. EPA EGRID program (USEPA, 2014), and Diehl and Harris (2014) provide water use estimates for many of the country's largest electricity generating facilities. In China, provincial electricity data is supplied by the National Bureau of Statistics of China and summarized by Cai et al., 2014; Jiang and Ramaswami, 2015; Liao et al., 2016; Zhang et al., 2016 for China's six regional energy grids. For all countries except the U.S. and China, country averaged estimates of electricity mixes are provided by the International Energy Agency (IEA, 2015). It should be noted that power plants commonly use freshwater resources for cooling. For example, in the U.S., it is estimated that power plants account for 40% of the nation's freshwater withdrawals (Averyt et al., 2011).

2.1.3 Industrial Water Use

Water withdrawals are defined as “water removed from the ground or diverted from a surface-water source for use” (USGS, 2016). Alternatively, consumptive water use refers to water withdrawn that is incorporated into a product or crop, or evaporated, transpired or consumed by animals or humans. Water that is withdrawn but ultimately returned to the same watershed from which it came does not count as consumptive use (USGS, 2016). This study is an extension of our previous work (Frost and Hua, 2017) and assesses water withdrawals for manufacturing and electricity from fab facilities (Note: the terms water use and water withdrawals are used interchangeably in this text). Thus, this assessment does not consider a facility’s efforts to recycle or return water to the watershed. And although individual companies have invested considerable effort into lowering their consumptive water use rates, reuse rates across the industry are highly variable, thus difficult to quantify on an industry-wide basis. Libman and Neuber (2008) reported a benchmarking study in which only 2 out of 7 companies met the water consumption targets set by the International Technology Roadmap for Semiconductors (ITRS) with exceedances ranging from 10-50% of the target.

Water withdrawn is a good measure of potential water use impacts because water used in manufacturing would rarely be returned to the same water body without some loss in water quality). The appropriation of water resources due to degradation in water quality, known as ‘grey water’ (Hoekstra et al., 2011), is often quantified separately from consumptive water use (i.e. ‘blue water’) (Scherer & Pfister, 2016); however, as this study does not separately address water quality issues associated with semiconductor manufacturing (and the associated freshwater required to assimilate pollution), water withdrawals serve as a proxy for both consumptive and degradative uses of water (Bonamente et al., 2017). However, water withdrawn may not be a good measure of actual physical scarcity of water (Boulay et al., 2017) and could overestimate impacts from manufacturing water demands in a watershed. Therefore, withdrawals-based water use inventories represent a conservative approach to estimating water use impacts and should be used as a screening-level assessment of potential impacts, rather than an absolute measurement of volumetric water use.

In most countries, including the U.S., industrial water use is not understood with a high degree of spatial or temporal granularity (Frost and Hua, 2017; Mueller et al, 2015). As mentioned, the water-energy nexus is vital to capture since industry is estimated to use 22% of total energy in the United States (EIA, 2016) and 54% of the world's total delivered energy. Although Rao, Sholes, Morrow, and Cresko (2017) reported that the electronics sector is currently considered a smaller user of water when compared to the major users (i.e. paper, primary metals, and chemical manufacturing sectors), they report that the electronics sector has the third highest energy-water ratio, further enumerating the importance of the water-energy nexus for electronics. According to the U.S. Energy Information Agency, the semiconductor subsector comprises 1.2% of U.S. manufacturing net demand for electricity (2013). This indicates that the semiconductor industry constitutes a small, but growing demand for direct water use and energy-related water use.

2.1.4 Water Scarcity

Many areas of the globe are already reaching the limits of a sustainable supply of freshwater for human and ecosystem demands (UN Water, 2019). Brown and Matlock (2011) and later, Xu and Wu (2017) reviewed several water scarcity indices and methodologies that have been developed over the past thirty years to quantify vulnerability of water resources. These metrics have converged around two basic approaches, as defined by Xu and Wu (2017): “water crowding” indices which are focused on per capita human water needs and “use-to-resource ratio” indices which are focused on the ratio of water withdrawals or consumption to available resources. Although there is considerable debate as to which metric, (of the almost two dozen available) is appropriate to quantify sustainable water use (Hoekstra, 2016; Pfister et al., 2017; Xu & Wu, 2017), this study incorporates the AWaRe (Available Water Remaining) indicator.

The AWaRe indicator is the result of a consensus-based process from the United Nations Environment Program/Society of Environmental Toxicology and Chemistry (UNEP/SETAC) Water Use Life Cycle Assessment (WULCA) group, comprised of industry, academic, government, and consulting experts, which was charged with creating a standardized water footprinting method that could be implemented in life cycle-based assessments of products, services and economies (WULCA, 2018). The AWaRe index utilizes data from the WaterGAP3 model which implements a global hydrology model (Muller Schmied et al., 2014) and a study

simulating global industrial and domestic water use (Florke et al., 2013). The available water remaining (aka ‘AWaRe’) in a watershed is calculated by assessing freshwater availability (surface + renewable groundwater) minus demand (AMD) by humans (i.e. domestic, industrial, agricultural, livestock and energy sectors) and by freshwater aquatic ecosystems, per area and by month. The AWaRe method is described by Boulay et al. (2017) and represented by the following equation, expressed in terms of volume of water remaining per month (m³/month) within a watershed area (m²):

$$AMD_i = \frac{Avail_{surf+renew-grdwater} - Human\ Water\ Cons_{surf+grdwater} - Env.\ Water\ Req'_{s_{surf}} * (m^3)}{Watershed\ Area\ (m^2) * month} \quad (2.1)$$

The inverse of AMD_i , or 1/AMD_i, is used to represent the ‘potential for water deprivation’ in a watershed i. This potential for deprivation is then used to create a scarcity characterization factor (CF_{AWaRe}) for a watershed. To calculate the CF, 1/AMD_i is first normalized to the world average (m³_i/m³_{world-avg}) and a dimensionless index is created by ranking each watershed against the normalized values calculated for all of the other watersheds in the world on a scale from .01 to 100, where 1 represents the world average and 100 represents areas that have 100 times less water available than the world average (Boulay et al., 2017).

The AWaRe method and its associated scarcity CF was selected as the scarcity indicator for this work because it is i) a consensus indicator and associated with an ISO standard (Boulay et al, 2017), ii) the metric is ‘ecocentric’ as it considers ecosystem water requirements (EWR) (Xu and Wu, 2017), iii) it is relatively simple to apply and communicate, consisting of a single characterization (weighting) factor to measure potential to deprive another user (human or ecosystem) of water (Xu & Wu, 2017; Boulay et al., 2017) and iv) it has been integrated as a midpoint impact characterization factor in the major LCA software tools (e.g. GaBi and Simapro), and is thus, gaining wider use in LCA and water footprinting communities.

However, the AWaRe indicator only addresses physical water scarcity and does not take into account socio-economic water scarcity (e.g. Aqueduct) and its associated risk factors. Another point of debate regarding the use of a scarcity characterization factor, such as those employed by

the AWaRe method, is that multiplying a water use inventory by a scarcity CF lacks ‘physical meaning’ (Hoekstra, 2016). However, Pfister et al. (2017) argued that the process of transforming inventory flows and their associated potential impacts into a common unit, represented here as H₂O equivalents, is common in both LCA and footprinting methods (e.g. carbon equivalents, toxicity equivalents). Thus, in our study, the goal of the water scarcity-weighted characterization step is to transform the water use inventory (i.e. H₂O in liters) to an impact equivalent that relates the pressure exerted on the resource to the resource in question (i.e. H₂O in liter equivalents) (Pfister et al, 2017). Maps displaying the water scarcity impact data will help locate regions of potential concern and will be utilized to identify current locales with the highest potential water use impacts from semiconductor production.

This study represents the first report of total global water withdrawals for the semiconductor manufacturing industry and improves upon our prior water withdrawal estimates (Frost & Hua, 2017) using a bottom-up approach and application of derived regional electricity water use intensity coefficients. This study also presents facility-level estimates of FW and ERW withdrawals, addressing the need for highly granular data due to the local and regional issues surrounding water use and water scarcity. We report watershed-specific impacts by presenting scarcity-weighted withdrawals (quantified in liters of H₂O equivalents) for semiconductor fab feedwater to better understand the potential for manufacturers in a watershed to deprive other users (both ecosystems and humans) of water.

Semiconductor manufacturing and other industrial water use estimates within the literature have either been limited geographically (Rushforth and Ruddell, 2018), not technology specific (based on sector wide input-output assessment), use only national averages for electricity-related water use (Cooper et al., 2011), and often do not address spatial variation in impacts (Blackhurst, Hendrickson, & Sels i Vidal, 2010). Reporting of water withdrawals by semiconductor manufacturers, typically through their Corporate Social Responsibility (CSR) reports, is often limited in its usefulness because withdrawals are reported at a company-wide level, instead of individual facilities (where impacts are felt), and the metrics for reporting may not be easily compared with other companies due to a lack of metrics standardization within the industry (Den,

Chen, and Luo, 2018). Further, with the exception of a few, companies rarely report their Scope 2 indirect water withdrawals (i.e. ERW withdrawals).

2.2 Materials and Methods

2.2.1 Estimating Facility Water Use

2.2.1.1 Semiconductor Facility Production Data

SEMI is an industry association which tracks global semiconductor fabrication (fab) manufacturing facilities for both current and planned operations (SEMI, 2017). The SEMI database consists of 1129 facilities and its characteristics are described in detail in our previous work (Frost and Hua, 2017). Most notably, the database contains information about location, integrated circuit (IC) technology node produced at the plant (e.g. 250 nm, 32 nm), wafer size (e.g. 8 inch [200 mm]), and fab production capacity, reported in wafer starts per month. In the past, a ‘technology node’ referred to the transistor gate length, which approximately scaled with transistor density in a microchip. Improvements in chip technology allowed for smaller gate lengths and thus, tighter packing of transistors over time (e.g. a 350 nm logic chip was state-of-the-art in 1995, compared to 45 nm in 2007). However, as the industry has reached the physical limits of size scaling, the term technology node has become uncoupled with gate length and now generally refers to a specific generation of microchip and its associated processes and design parameters. Production capacity was used as a proxy for actual production, as many of these facilities would be expected to operate at full or near full capacity, although this assumption may lead to overestimates of water withdrawals in some locations operating below capacity. The database was used to estimate total chip production (by product and per technology node) at each facility using the aforementioned parameters. Only production lines with valid wafer production data from the fourth quarter of 2016 were used (N=1021).

2.2.1.2 Geocoding

For each production line, addresses provided by SEMI were geocoded using two software services to obtain geographic coordinates for input into a Geographic Information System (GIS). The Environmental Systems Research Institute’s World Geocoder, accessed via ArcGIS Pro (ESRI, 2017), and the GoogleMaps API, accessed through the R ‘ggmap’ library (Kahle & Wickham,

2013) geocoding services, were used to obtain the latitude and longitude in decimal degrees for each geocoded address. The geocoding software returns information about the estimated precision of each geocode. For each geocoded address that returned a rooftop centroid (indicating a high level of precision) we utilized the data as provided by either software (N=594). If neither geocoding service provided a rooftop geocode (N=427), corrections to the data were made using a manual geocoding process which included use of aerial imagery from GoogleMaps or Bing, and if needed, confirmation of the correct address by investigation of the company's website. Manual correction of geocoded data is vital to ensure accurate locations (McDonald, Schwind, Goldberg, Lampley, & Wheeler, 2017; Swift, Goldberg, & Wilson, 2008) of fab facilities which are used to estimate localized water use impacts. If manual correction of an address was not feasible, less precise location data provided by the geocoding software was used (N=12). Only one facility was unable to be located and was excluded from the analysis; thus, water use analysis was conducted for 1020 fab production lines.

2.2.2 Fab Feedwater (FW) Use: Water Use By Technology Type

As previously described (Frost and Hua, 2017), the SEMI database is categorized by the product type and technology node for each production line. This includes major categories such as 'logic', 'memory', 'foundry', and 'discrete' which represent various types of semiconductor products such as CMOS (complementary metal-oxide semiconductor), DRAM (dynamic random-access memory), NAND (logic gate that stands for negative-AND), and ASICS (application-specific integrated circuits). Foundry facilities comprise a growing portion of the semiconductor manufacturing sector (SIA, 2016) and may produce multiple technologies; however, specific production lines will often produce one dominant product type. The use of general product categories provided by the SEMI database was determined to be adequate for purposes of water withdrawal estimation but would need to be refined with facility level data for a detailed, local assessment.

Estimates of fab FW are drawn from the LCA work of Boyd (2009; 2012) and semiconductor industry reports (Sematech, 2001-2013). Boyd reports comprehensive estimates of FW and electricity use for CMOS, DRAM and NAND products for technology nodes during the period 1995-2013 (350 nm to 22 nm) at the chip level for a typical U.S. semiconductor facility. Feedwater

estimates for other technology types (e.g. MEMS) and newer technology nodes (i.e. 2013-2016) were estimated using ITRS reports from 2001-2013 (Sematech). These industry targets were used when specific values from Boyd were not available and may represent an optimistic estimate of feedwater withdrawals. Other estimates of semiconductor chip water use from the life cycle literature were difficult to interpret due to aggregated reporting of results. Further difficulties arise from trying to pinpoint the exact kind of chip made from a foundry facility as it may manufacture a mix of technology types and nodes, so assumptions about the primary technology produced at these facilities were made by using text analysis from the SEMI database.

Table 2.1. Table of fab FW use and electricity use by technology type and node

Approximate Technology Year	Technology Node (nanometers) - oldest to newest	Fab Feedwater Use (liters per cm² of wafer)	Fab Electricity Use (kWh per cm² of wafer)
Logic (e.g. CMOS, Bipolar, MEMs) ^a			
1995 & older	350-1000000	25.32	3.31
1996-1997	250-350	25.32	3.31
1998-1999	180-250	5.12	3.06
2000	130-180	11.27	1.33
2001-2004	90-130	21.85	1.53
2005-2006	65-90	20.63	1.49
2007	45-65	15.72	1.75
2008-2009	32-45	6.55	2.07
2010	32	7.21	2.12
2012 & newer	5-22	7.8 ^b	2.12
Memory (e.g. RAM, DRAM, MRAM) ^a			
1998 & older	250-1000	0.16	0.14
1999	180-250	0.16	0.14
2000-2001	130-180	0.07	0.45
2002-2003	90-130	0.93	1.04
2004-2005	70-90	2.12	0.76
2006-2007	57-70	1.18	0.10
2008-2011	40-57	5.24	8.73
2012-2015	25-40	10.48	17.47
2016 & newer	10-22	20.96	34.93
Flash (CMOS, NAND) ^a			

Table 2.1 continued

2000 & older	150-400	48.55	2.07
2000-2001	120-150	48.55	2.07
2002-2003	90-120	21.24	3.03
2004-2005	65-90	12.14	2.53
2006-2008	45-65	12.73	4.24
2009-2016	14-40	7.8 ^b	6.60
<hr/>			
Other (e.g. GaAs, Sapphire, MEMs, Indium) ^b			
2000 & older	130-20000	7.0	1.4
2001-2004	90-130	7.0	1.4
2005-2007	65-90	9.0	1.4
2008-2010	40-65	8.1	1.5
2011-2015	22-40	7.0	1.0
2016 & newer	5-22	7.8	1.0

*a Boyd (2012)**b Sematech (2001-2013)*

2.2.3 Electricity Water Use

Electricity use by each fab was calculated using technology-specific values from Boyd and where these values were not available, industry targets reported by ITRS were used. Electricity use values from Boyd, reported in kWh per chip, were normalized to kWh per cm² of wafer. Semiconductor fabs typically use electricity purchased from the grid, so determining the grid mix (the fuel mix and/or power sources for electricity generation in each area) of a region or country is vital to determining the water use associated with electricity consumption.

Typically, water use intensity values from electricity are based on LCA estimates of the impacts of 1 kWh of net electricity from a standard national grid mix of electricity. Because electricity use is such a large determinant of water use in a Scope 2 assessment, and often dominates water use values for technology (Boyd, 2012), this study includes refined electricity values, estimated for China and the U.S. Regional electricity factors were calculated for the U.S. and China because of the large geographic variation in grid mixes across these two countries.

2.2.3.1 U.S. Electricity Water Use

Water withdrawal data from Diehl and Harris (2014), Macknick et al. (2012), and Meldrum et al. (2013) were used to characterize water use intensity (water withdrawal per kWh of production) for each electricity generation type. Diehl and Harris calculated detailed water withdrawal estimates in MGal/day for 1290 thermoelectric power plants in the U.S., covering a variety of fuels and cooling technologies. They also provided net generation values for each plant in megawatt hours (MWh) and these values were used to calculate water use intensity (in liters per kWh) for each thermoelectric facility. Figure 1 depicts the locations of each thermoelectric facility in the U.S. (EIA, 2015) that were estimated by Diehl and Harris. An average of water use intensities (WUI) weighted by annual net generation of electricity for each facility was used to calculate an average thermoelectric WUI over the electricity trading regions in which the facilities were located. This approach is preferred over national or regional grid mixes from the LCA literature because it incorporates a large and representative amount of detailed facility level water use data. The North American Electric Reliability Corporation (NERC) is the entity responsible for coordinating and supplying electricity to various regions of the U.S. A NERC region operates as a trading region and electricity supply is mixed and redistributed within this region; thus, this is the appropriate level of spatial aggregation to calculate electricity water use intensity.

For non-thermoelectric power plants in the U.S. (i.e. hydroelectric, solar photovoltaic, and wind), estimates of water withdrawal from Meldrum et al. (2013) were used and production-weighted water use intensities were calculated by averaging known production levels of thermoelectric and non-thermoelectric power within each NERC region (USEPA, 2014) using the following equation:

$$WUI_{regional} = \sum TEWU_i * \left(\frac{PC_i}{RPC} \right) + (WUI_{solar} * RSP) + (WUI_{wind} * RWP) + (WUI_{hydro} * RHP) \quad (2.2)$$

where:

$WUI_{regional}$: U.S. NERC electricity region water use intensity (Liters/kwh);

$TEWU_i$: Annual thermoelectric water use per facility (liters);

PC_i : annual production capacity per thermoelectric facility (kWh); RPC : total annual thermoelectric regional production capacity (kWh);

WUI_{solar} : water use intensity of solar photovoltaic power (L/kWh); RSP: regional solar electricity production as percentage of total production (%);

WUI_{wind} : water use intensity of wind power (L/kWh); RWP: regional wind production as percentage of total production (%);

WUI_{hydro} : water use intensity of hydroelectricity production (L/kWh); RHP: regional hydro production as percentage of total regional electricity production (%)

Each fab facility in the U.S. was then assigned an ERW withdrawal intensity associated with its derived NERC region water use intensity ($WUI_{regional}$) factor. This assignment was determined by overlaying fab locations with a map of electricity regions provided by the U.S. Electricity Information Agency (EIA). Detailed information about the production mix and net generation of each region are provided in Appendix A, Table A.1.

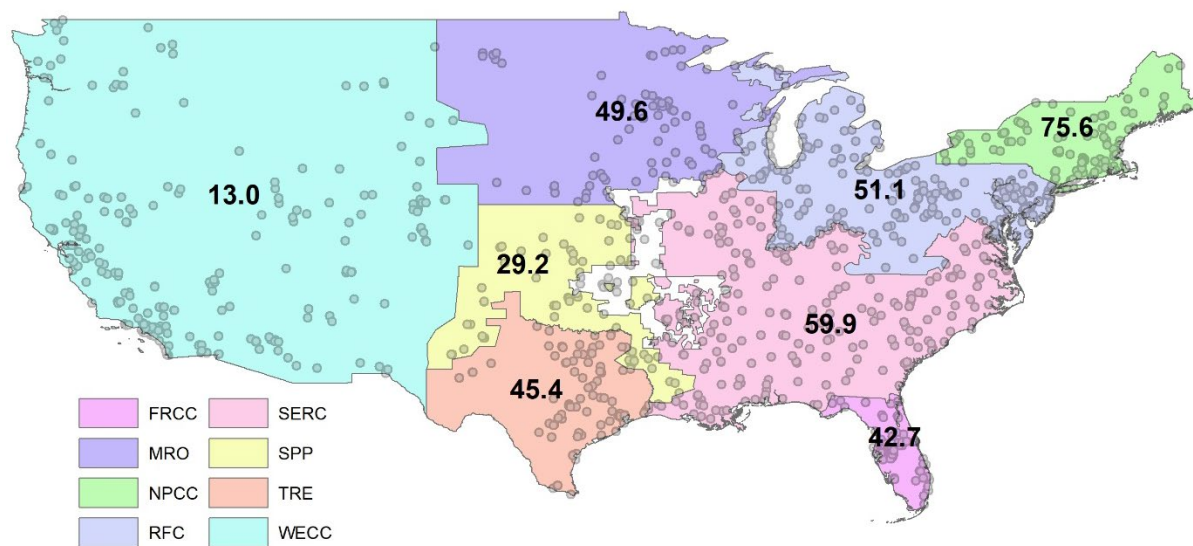


Figure 2.1. Derived water use intensity factors (in L/kWh) of NERC electricity regions overlaid with the thermoelectric power plants from Diehl and Harris (2014). The boundaries of NERC electricity regions were provided by EIA (2015). FRCC = Florida Reliability Coordinating Council, MRO = Midwest Reliability Organization, NPCC = Northeast Power Coordinating Council, RFC = Reliability First Corporation, SERC = SERC Reliability Corporation, SPP = Southwest Power Pool, TRE = Texas Regional Entity, WECC = Western Electricity Coordinating Council. The white areas of the map are classified by EIA as ‘indeterminate, with various NERC memberships’; thus, a WUI was not calculated for these areas.

2.2.3.2 Chinese Electricity Water Use

C. Zhang, Zhong, Fu, Wang, and Wu (2016) reported water withdrawals by the various thermoelectric cooling technologies (i.e. recirculating, once-through cooling, dry cooling, and seawater cooling) used across China. By understanding province-level electricity production mixes and cooling types, water use intensities by province were calculated for China using equation 2 below. Province-level water use intensities, production and cooling type data (Table A.2), and sample calculations are available in Appendix A.

$$\begin{aligned} WUI_{prov} = & \sum PCPC((RC_{coal} * WUI_{recirc}) + (OTC_{coal} * WUI_{otc}) + (DC_{coal} * WUI_{dry})) + PNGPC((RC_{ng} * \\ & WUI_{recirc}) + (OTC_{ng} * WUI_{otc})) + (PNPC * WUI_{nuclear}) + (PBP * WUI_{biomass}) + (PSP * WUI_{solar}) + \\ & (PWP * WUI_{wind}) + (PHP * WUI_{hydro}) \end{aligned} \quad (2.3)$$

where:

WUI_{prov} : Chinese provincial water use intensity (liters/kWh); PCPC: Provincial coal-power capacity (kWh); RC: electricity production from recirculating cooling as percentage of total thermoelectric production in province (%);

WUI_{recirc} : water use intensity of recirculating cooling operations in China; OTC: electricity production from once through cooling as percentage of total thermoelectric production in province (%);

WUI_{otc} : water use intensity of once through cooling operations in China; SC: electricity production from seawater cooling as percentage of total thermoelectric production in province (%); PNGPC: Provincial natural gas power capacity (kWh); NPC: Provincial nuclear power capacity (kWh);

$WUI_{nuclear}$: water use intensity of nuclear power (L/kWh);

WUI_{solar} : water use intensity of solar photovoltaic power (L/kWh); PBP: biomass electricity production as percentage of total provincial electricity production (%); PSP: solar electricity production as percentage of total provincial electricity production (%);

WUI_{wind} : water use intensity of wind power (L/kWh); PWP: wind production as percentage of total provincial electricity production (%);

WUI_{hydro} : water use intensity of hydroelectricity production (L/kWh); PHP: hydro production as percentage of total provincial electricity production (%)

Like the U.S., China has electricity producing regions in which electricity is mixed and redistributed; however, electricity grid mixes by region were not directly accessible. Thus, a weighted average of production capacity for each province within the electricity region was used to calculate a production capacity weighted average for the region. A map of electricity regions was adopted from N. Zhang, Hu, Shen, He, and Zheng (2017) and using spatial overlays, each fab within that electricity region was assigned a water use intensity associated with its regional mix of electricity production (Figure 2.2). This may result in error if a fab does not purchase electricity from the grid of the electricity region in which it is located.

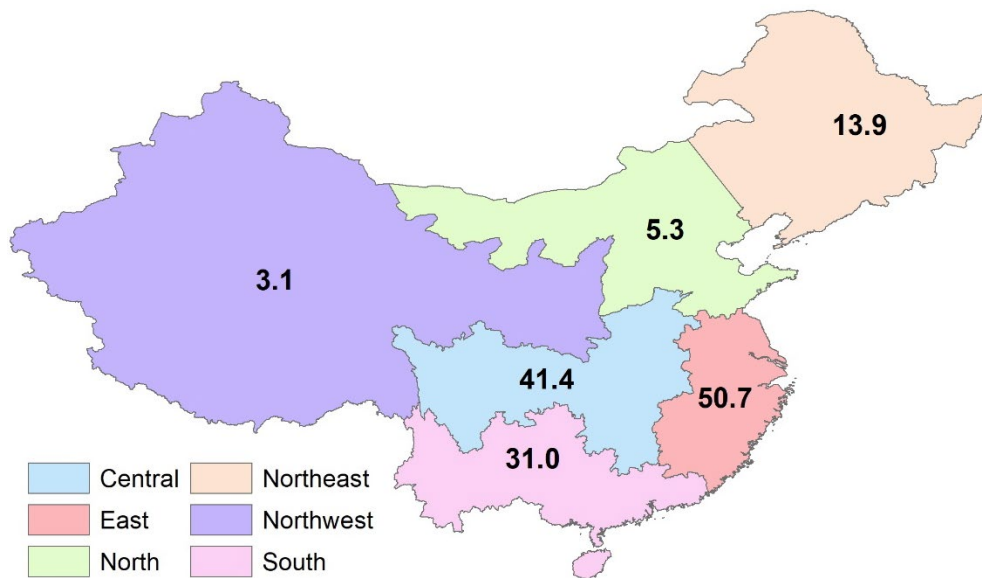


Figure 2.2. Calculated water withdrawal intensity (in liters per kilowatt hour) of Chinese electricity regions. The boundaries of Chinese electricity regions were adopted from N. Zhang et al. (2017).

2.2.3.3 *Rest of World*

For all other countries in which fab production takes place, country specific average grid mixes from the IEA were utilized. Average water use intensity factors (Macknick et al., 2012; Meldrum et al., 2013) were applied per generation type to electricity production within these countries. Table 2.2 summarizes the water use factors associated with each generating type and Table A.4 displays the water use intensities calculated for each country based on their grid mix and factors' from Table 2.2.

Table 2.2. Default water use intensity factors for each electricity generation type. All values from Meldrum et al. (2013), except for petroleum and hydroelectric (Macknick et al., 2012).

Electricity Generation Type	Water use intensity (liters per kWh)
Coal	2.5
Natural gas	9.5×10^{-1}
Petroleum	3.9×10^{-1}
Nuclear	1.8×10^2
Biomass	1.7×10^{-2}
Geothermal	1.2
Solar thermal	2.9×10^{-1}
Hydroelectric	1.1×10^1
Solar	2.3×10^{-2}
Photovoltaic	
Wind	5.7×10^{-3}

2.2.4 Characterizing Water Use Per Facility

As developed in detail in our previous work, an estimate of global water use by the semiconductor industry can be calculated using the following basic equation (Frost & Hua, 2017):

$$SMGWU = \sum_{i=1}^n (FWW_i + EWW_i) * MWS_i \quad (2.4)$$

$$FWW = WUI_{tech} * SA_{wafer} \quad (2.5)$$

$$EWW = EI_{tech} * WUI_{elec} * SA_{wafer} \quad (2.6)$$

where:

SMGWU: semiconductor monthly global water use; n: the number of semiconductor facilities in Q4 of 2016 with valid production data;

FWW: fab feedwater per wafer;

WUI_{tech} : water use intensity of semiconductor technology at facility i (Liters/cm²);

SA_{wafer} : surface area of wafer (cm²);

EWW: electricity water per wafer;

EI_{tech} : electricity intensity of semiconductor technology (kWh/cm²);

WUI_{elec} : water use intensity of electricity mix (Liters/kWh); and

MWS: monthly wafer starts per facility in Q4 2016 (SEMI, 2017). This monthly figure was annualized to calculate total annual consumption.

2.2.5 Scarcity-weighted Water Use

The AWaRe characterization factors (CFs) described in Section 2.1.4 have been developed for 11,050 watersheds, with the largest 34 watersheds divided into subwatersheds. These are available for download from the WULCA website as a kmz file and are provided both on a monthly basis and as an annual average (WULCA, 2017). By utilizing location specific information about semiconductor production, water use at various spatial extents (e.g. watershed, country, globally) could be aggregated. This data was summed at the watershed level and was weighted by the AWaRe CFs available for each watershed. This analysis resulted in 202 scarcity-weighted watersheds associated with the 1020 fab facilities. Due to the difficulty and potential error associated with allocating water withdrawn for electricity from the grid mix to a specific watershed, only fab FW withdrawals (which can be associated with an exact location or area) was considered as part of the scarcity-weighted assessment. For the purposes of this assessment, it was assumed that facilities were withdrawing water from within their own watershed to meet their manufacturing needs. All of the fab facility water withdrawals within a watershed were summed across the watershed using spatial libraries in R (R Core Team, 2017) and visualized using ArcMap 10.5.1 (ESRI, 2018). This work modified our previously developed equation to summarize the scarcity-weighted withdrawals for each of the watersheds that contain semiconductor facilities, and was expanded to include many more facilities and watersheds (Frost and Hua, 2017):

$$SWWU = \sum_{i=1}^m AFW_n * WSF_{(avg)} \quad (2.7)$$

$$AFW_n = FWW_n * MWS_n * 12 \text{ (months)} \quad (2.8)$$

where:

SWWU: Scarcity Weighted Water Use (Liter equivalents);

m: the number of facilities in a given watershed;

AFW_n: annual feedwater withdrawals per facility;

FWW_n: Feedwater withdrawals per wafer (see equation 2.5);

MWS: monthly wafer starts and

WSF_(avg): the average annual water scarcity factor for that watershed.

2.2.6 Temporal Variability of Water Scarcity

Due to the seasonal nature of water scarcity, monthly AWaRe scarcity indicators were also considered. For each of the 202 watersheds associated with fab production, the minimum annual scarcity values, as well as maximum annual scarcity values for each watershed in a year were mapped to represent best and worst-case scenarios of water scarcity. These maps identified seasonal “hotspots”: locations characterized by seasonally high water scarcity and water withdrawals by semiconductor fabrication.

2.3 Results

The following results describe the facility level production data and associated FW and ERW withdrawals for the 1020 semiconductor fab production lines available for analysis. Scarcity-weighted withdrawals were calculated using AWaRe scarcity characterization factors applied to each of the 1020 facilities located in 202 watersheds across the globe and are summarized and presented here. The raw data used to produce each of these graphs and maps are available along with an interactive web map (Frost & Hua, 2019).

2.3.1 Feedwater (FW) Withdrawals

The annual FW withdrawals by semiconductor facilities were summarized over various spatial extents. Total annual semiconductor wafer production and total annual water withdrawals per country for the top global producers is presented in Figures 2.3 and 2.4. The top five producers are Japan, Taiwan, South Korea, China and the United States, respectively. Japan has the largest FW withdrawals for any single semiconductor producing country, which aligns with its large wafer production numbers. Taiwan is the second largest semiconductor producer, despite having the third largest water withdrawals after South Korea and Japan. This is likely due to the type of chips

being produced in Taiwan, compared to South Korea, which are dominated by newer, more water intensive chip production.

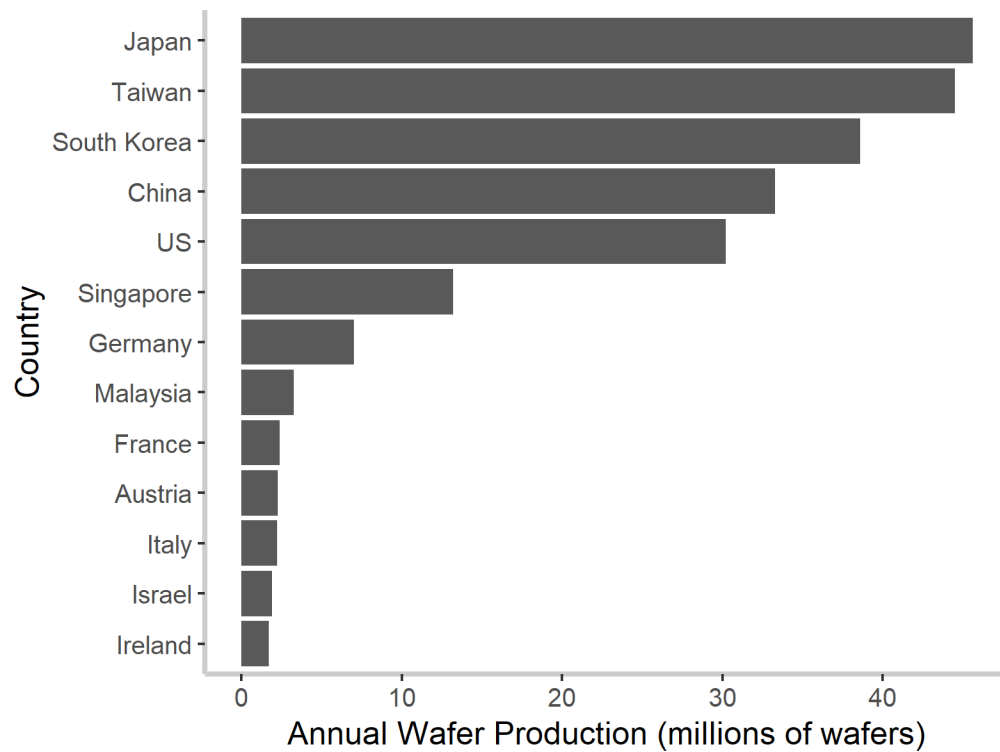


Figure 2.3. Annual wafer production (in 8-inch [200 mm] wafer equivalents) by countries producing more than one million wafer starts per year.

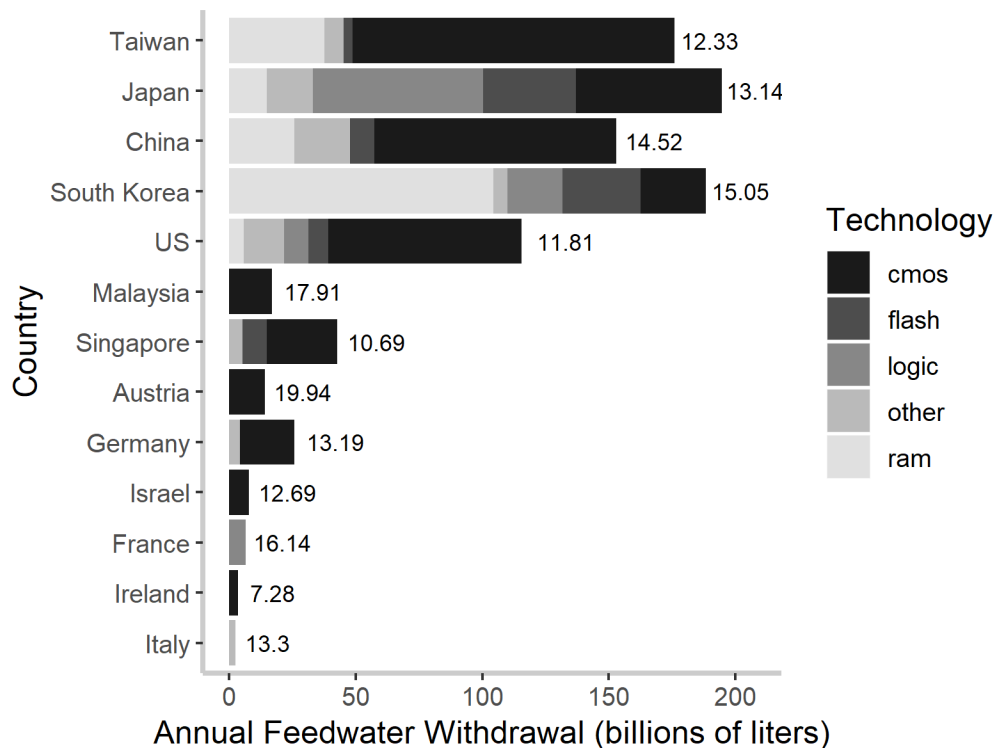


Figure 2.4. Annual fab FW withdrawals by country and technology. Countries producing more than one million wafer starts per year are displayed. The value next to each bar represents the average FW withdrawal intensity (in L/cm²) for each country's semiconductor manufacturing facilities, averaged across all technology types.

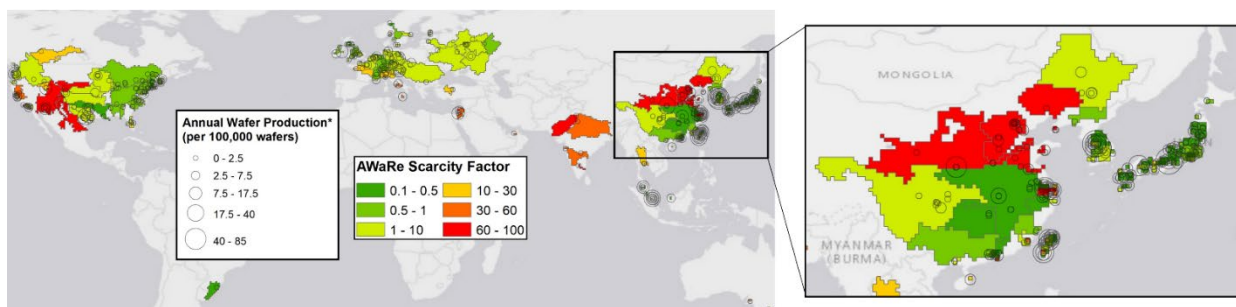


Figure 2.5. Semiconductor manufacturing facility annual wafer starts overlaid on AWaRe scarcity factors, by watershed. *Wafer production normalized to 8-inch [200 mm] wafer.

Figure 2.6 is a map of fab annual FW withdrawals summed at the AWaRe watershed level. Table 2.3 indicates that watersheds located in South Korea, Taiwan, Malaysia, and China display the highest levels of fab FW withdrawals. Summarizing by watershed reveals potentially high impact areas that may not be apparent when delineated at the state/province or country level.

Manufacturing facilities in these watersheds have the potential to cause physical shortages of water resources; however, this must be further investigated with consideration of existing watershed scarcity-related factors such as climate, ecosystem water needs, and human water use patterns.

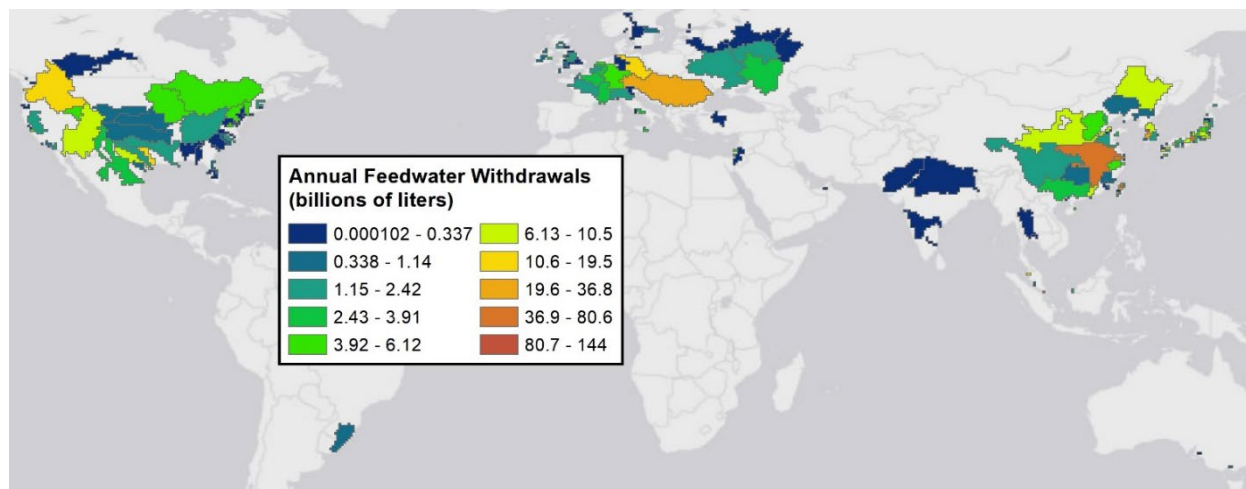


Figure 2.6. Annual semiconductor manufacturing FW withdrawals summed by AWARe watershed.

Table 2.3. Top five global watersheds for semiconductor manufacturing FW withdrawals.

AWaRe Watershed ID	Country	# of Fab Facilities in Watershed	Unweighted Feedwater Withdrawals (billions of liters)	AWaRe Scarcity Factor (.01-100)
6339	South Korea	27	143.99	8.20
7282	Taiwan	47	80.60	0.52
8837	Malaysia	24	45.78	0.79
6895	China	26	45.28	67.58
6848	China	37	45.20	0.22

2.3.2 Scarcity-Weighted Withdrawals

Wafer production and watershed scarcity data can be combined to gain a general understanding of how much semiconductor production is located in areas with high potential water use impacts. Table 2.4 summarizes the amount of total wafer production in areas considered to be water scarce by the AWARe index, indicating that almost 13% of production occurs in very water scarce areas (60-100 times less water than the global average), and nearly half (~47%) of all semiconductor manufacturing occurs in locales exhibiting more scarcity than the global average (scarcity factor >1).

Table 2.4. Percent of total wafer production occurring in areas of various water scarcity.
Description of water scarcity factors are adapted from Boulay et al. (2017).

AWaRe Scarcity Characterization Factor	Description of Scarcity	% of Global Wafer Production
0.01-0.5	values <1 for regions with less problems of scarcity than the world average	21.97
0.5-1	values <1 for regions with less problems of scarcity than the world average	33.29
1-10	a value of 10, for example, representing a region where there is 10 times less water remaining per area within a certain period of time than the world average,	21.99
10-30	10 – 30 times less water remaining per area within a certain period of time than the world average,	5.06
30-60	30-60 times less water remaining per area within a certain period of time than the world average,	4.80
60-100	The upper cutoff of 100 affects regions where demand is higher than availability	12.89

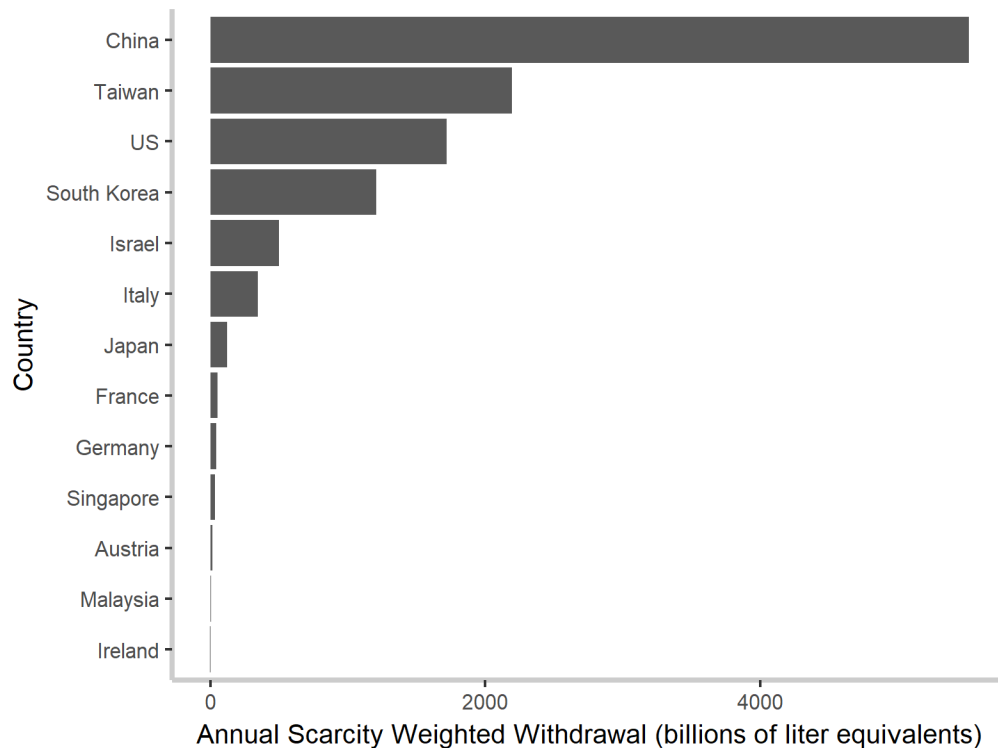


Figure 2.7. Scarcity-weighted FW withdrawals by country. The withdrawal is expressed in billions of liter-equivalents to denote the transformation of withdrawal inventory data (in liters) into an impact equivalent (in liter equivalents).

While four of the top five countries are the same as for unweighted FW withdrawals, the order of the countries changes somewhat. The greatest volume of weighted FW withdrawals from semiconductor manufacturing occurs in China, despite having lower wafer production numbers than Japan, Taiwan and South Korea. Scarcity-weighted withdrawals indicate potential areas of concern with relation to existing water availability for humans and ecosystems. Regional water issues in China are attributed to heavy water demands from agriculture, energy, and dense manufacturing, especially in the heavily populated and industrialized eastern provinces which comprise 47% of China's total industrial output (China Water Risk, 2018).

Figure 2.8 maps the interaction of existing water scarcity and semiconductor FW withdrawals across the globe at the watershed level by summing and displaying scarcity-weighted withdrawals for each watershed. By comparing Figures 2.8 and 2.6, one can see the spatial shift in impacts when scarcity is considered.

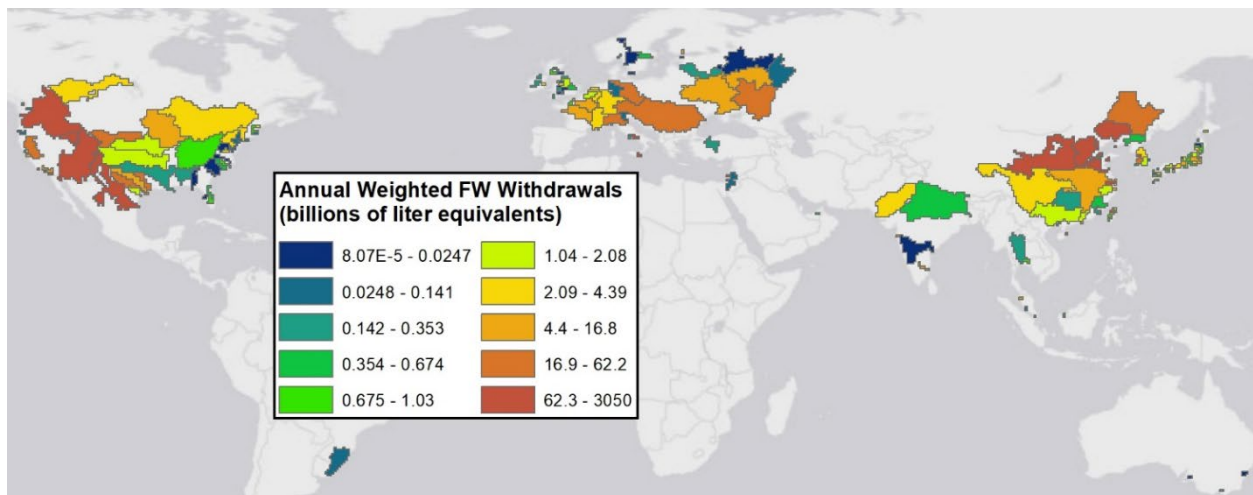


Figure 2.8. Annual scarcity-weighted semiconductor manufacturing FW withdrawals summed by AWaRe watershed. The withdrawal is expressed in billions of liter-equivalents to denote the transformation of withdrawal inventory data (in liters) into an impact equivalent (in liter equivalents).

Table 2.5. Top five global watersheds for scarcity-weighted semiconductor manufacturing FW withdrawals.

AWaRe Watershed ID	Country	# of Facilities in Watershed	Weighted Feedwater Withdrawal (billions of liter equivalents)	AWaRe Avg Scarcity Factor (.01-100)
6895	China	26	3046	67.30
7405	Taiwan	19	1562	42.50
6339	South Korea	27	1181	8.20
6269	China	15	806	82.10
6825	U.S.	8	657	100

2.3.3 Temporal Analysis

The AWARe factors provided by WULCA are comprised of annual average scarcity factors and monthly scarcity factors, with the latter representing the temporal variation in water scarcity throughout the year. The figure below represents the difference in withdrawals when using a best case (minimum annual scarcity value) versus worst case (maximum annual scarcity value) scenario. In Figure 2.9, the dark orange areas highlight the top 10% of watersheds that are of the most concern with regard to seasonal scarcity, representing the largest annual variation (in absolute terms) with respect to scarcity-weighted withdrawals. Figure 2.10 represents the coefficient of variation (standard deviation of each watershed's annual scarcity factor normalized by mean annual scarcity). This shows areas that may display a large swing in annual scarcity, but which may not appear problematic with respect to total withdrawals.

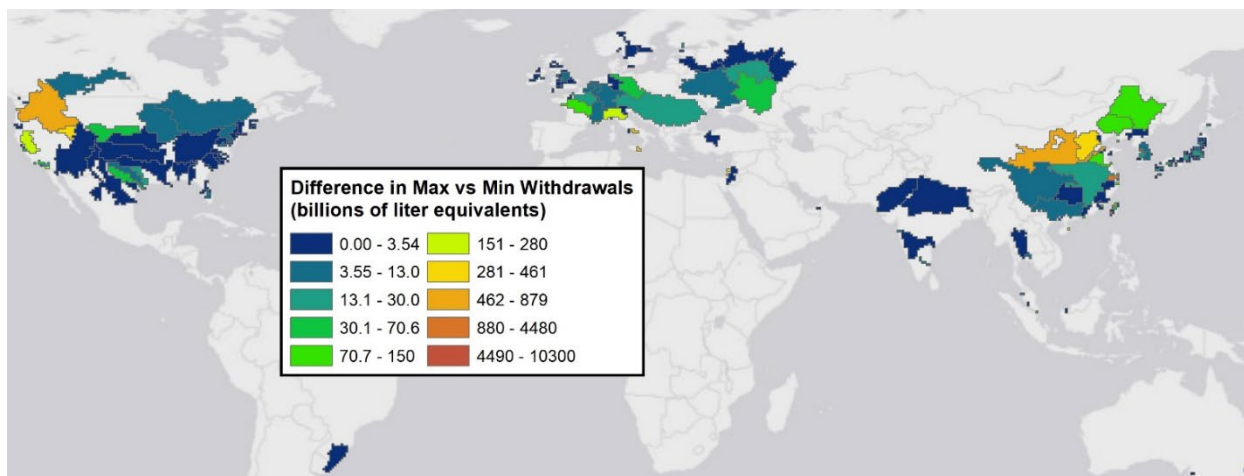


Figure 2.9. Difference between maximum monthly scarcity weighted withdrawals and minimum monthly scarcity weighted withdrawals on an annual basis. This represents the difference between a best-case and worst-case scenario for water scarcity in a year, per watershed. The data is divided into deciles to better visualize variation across the dataset.

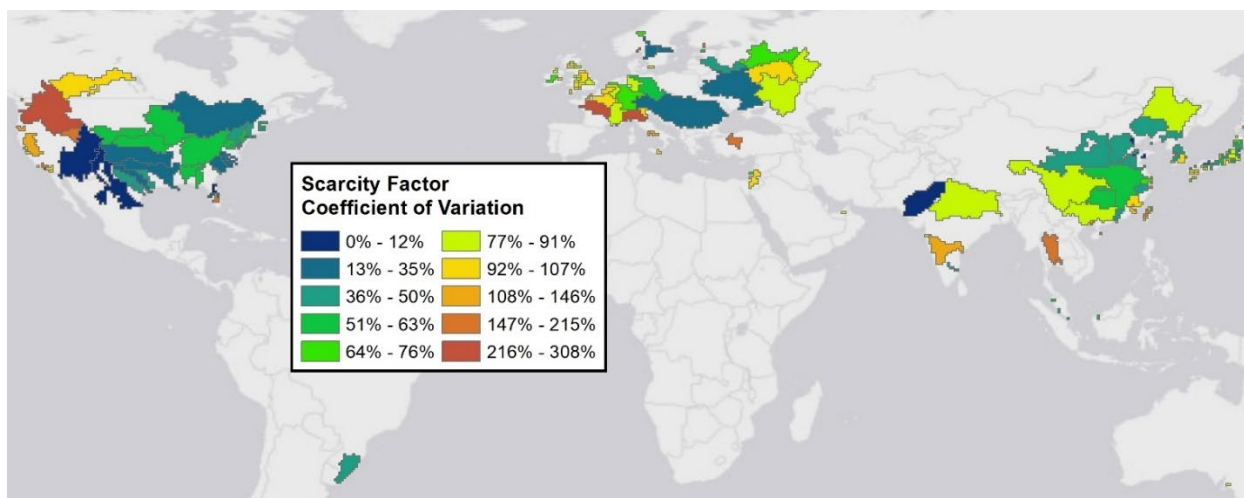


Figure 2.10. Coefficient of variation (standard deviation of annual scarcity factor normalized by mean annual scarcity) of the AWaRE scarcity factor per watershed. This indicates watersheds that are likely to exhibit the largest percentage change in scarcity over the course of a year.

2.3.4 Fab Electricity Water Use

The annual electricity-related water withdrawals by semiconductor facilities were summarized over various spatial extents. Water withdrawals for electricity consumption are not weighted since they are not accurately attributable to a specific watershed. A country-level summary of fab ERW withdrawals for the top global producers is presented in Figure 2.11. This analysis indicates that

South Korea has the largest ERW withdrawals for any single semiconductor producing country and China is the second largest user of ERW. China and South Korea's higher water withdrawals is due to water intensive electricity production such as coal and hydroelectric, and coal and nuclear, respectively. See the Appendix for breakdown of electricity demand by generating type for each country.

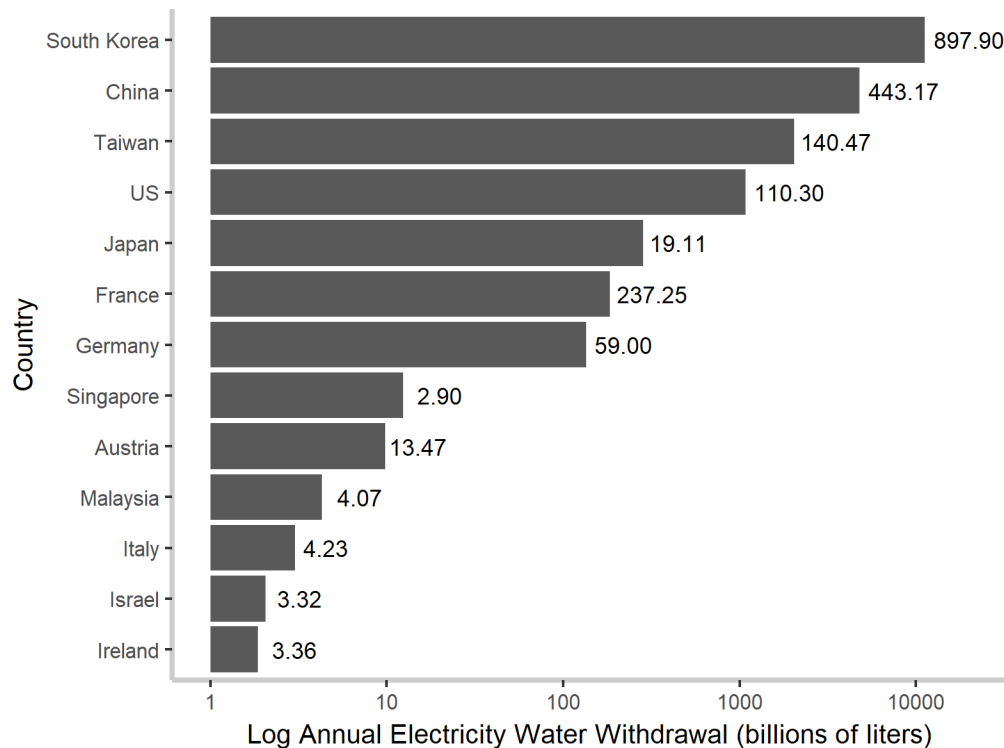


Figure 2.11. Fab ERW withdrawals by country. The value next to each bar represents the average ERW withdrawal intensity (L/cm²) for each country's semiconductor manufacturing facilities.

Although it is difficult to directly associate electricity use from the grid with impacts on a specific watershed, in Figure 2.12 we overlay fab electricity use with water scarce areas in East Asia to draw a general picture of the relationship between water scarcity and fab ERW withdrawals in this important semiconductor manufacturing region.

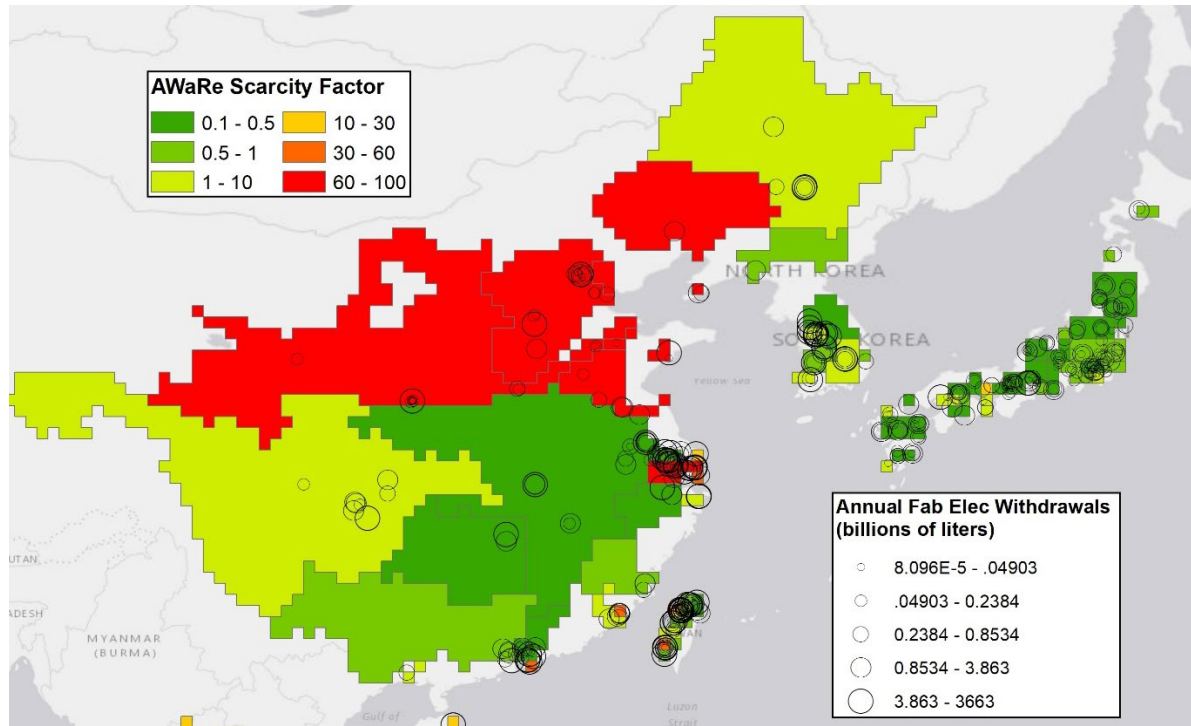


Figure 2.12. Map of East Asian (i.e. Japan, South Korea, China, Taiwan) fab electricity-related water withdrawals by facility, overlaid on AWARe scarcity factors. A map of global ERW withdrawals is available in the Appendix (Figure A.1).

2.3.5 Total Water Withdrawals

The total water withdrawal for each fab is the sum of withdrawals for the fab FW and the ERW withdrawals. This metric is not scarcity weighted. The annual, total global, Scope 2 water withdrawal for semiconductor manufacturing is 2.096×10^{13} liters per year, or approximately 21 trillion liters (2.1 billion m^3) per year. As seen in Figure 2.13, electricity water withdrawals dominate water use for fabs; thus, South Korea's fabs are the largest total water users. Given the relative dominance of ERW withdrawals (10-50 times more than FW withdrawals, in some cases), it is expected that South Korea and China have the largest total withdrawals.

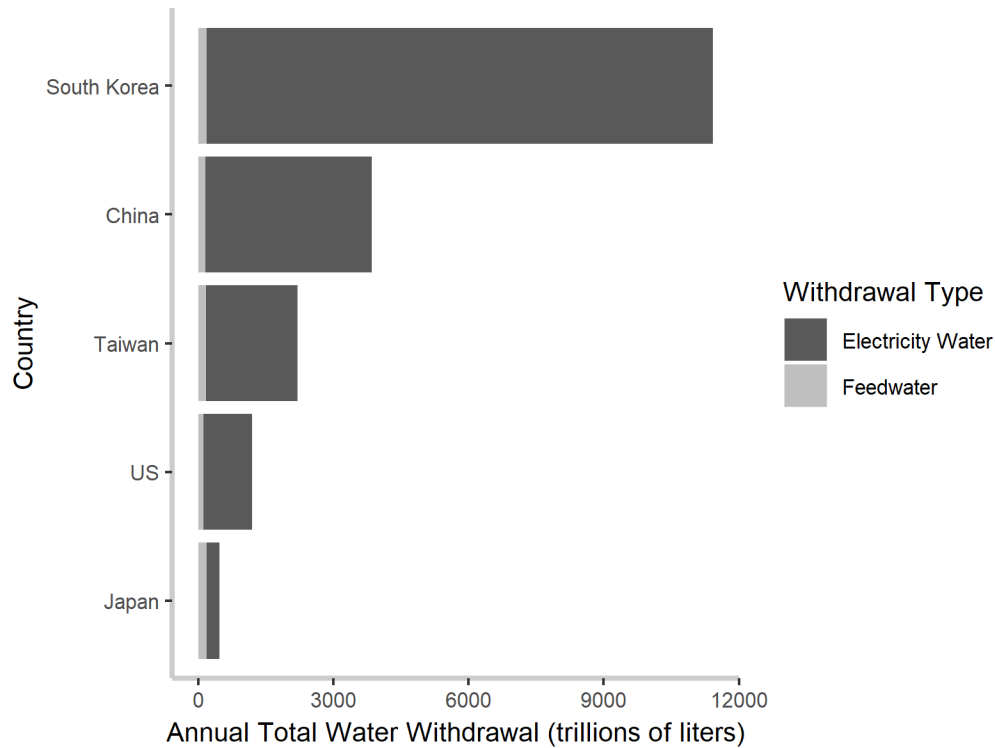


Figure 2.13. Total water withdrawals (FW + ERW) by the five highest producing countries in the semiconductor manufacturing sector.

2.4 Discussion and Conclusion

2.4.1 Discussion

Current understanding of global water use emphasizes agricultural and thermoelectric demand, and less data is available about industrial water uses. Many of the industrial water use studies analyze a single facility or industry, or consider the water use of an entire industry without being spatially explicit. Thus, the methodologies are not easily applied across industries or spatial scales. The present study reports total global water use by an important and growing sector, semiconductor manufacturing, and provides a methodology that could be applied to many other manufacturing sectors.

The increasing production of electronics will likely represent a growing share of the global water demand by the semiconductor industry. Thus, this study enhances the current understanding of water use by semiconductor manufacturing operations around the globe. We report annual water use for nearly 100% of semiconductor manufacturing capacity in Q4 2016 and identify Scope 2

(electricity-related) water withdrawals as more significant than Scope 1. Production data indicates a high level of water use in South Korean, Chinese, Japanese, U.S. and Taiwanese electronics manufacturing sectors. However, we have also segmented semiconductor manufacturing capacity with respect to water scarce locations, using watershed-level scarcity characterization factors provided by the AWaRe index. This analysis indicated that almost 13% of production occurs in very water scarce areas, and nearly half (~47%) of all semiconductor manufacturing occurs in locales exhibiting more scarcity than the global average. This study also examined areas that undergo seasonal scarcity, which is not captured by annual average scarcity values that are often reported. Manufacturers should consider the variability in water use impacts on ecosystems and humans that may occur seasonally.

This study presents a method for applying regional electricity water withdrawals and LCA/industry water use coefficients to calculate industry-wide, global, scarcity-weighted withdrawals. The granularity of the present analysis allows for summary of data at various spatial extents. The regional electricity water use factors calculated for the US (using plant specific data) and China (using provincial production data) provide more accurate withdrawal data for large countries that may exhibit regionally variable electricity production and water scarcity. The derived regional electricity water use factors used in this study can be applied to other industrial sectors.

2.4.2 Limitations

This work does not provide a complete picture of water use by all users (industrial, commercial and residential) within a watershed area; thus additional studies of global water withdrawals by other industrial sectors, at the same spatial granularity as this one, are vital to a better understanding of water use and potential impacts. Withdrawals-based estimates were used here as a conservative estimate of water use, given that degradative consumption (water used to dilute pollutants to an acceptable level) was not included in the analysis.

This study also does not provide a complete water footprint for the semiconductor industry, as it focuses on manufacturing water use and excludes the significant ERW withdrawals attributed to the use phase of these semiconductor chips. Additionally, while some basic benchmarking was

conducted against limited available data, more complete benchmarking of facility level data against these LCA based estimates should be completed.

Scarcity-weighted water withdrawals (quantified in liters of H₂O equivalents) are not a direct measurement of physical water scarcity, thus estimates provided here serve as a screening level indicator of the potential of this industry to deprive other users (ecosystems or humans) of clean water, resulting in regulatory or reputational risk. This study does not explicitly address the operational risks to the manufacturer associated with the withdrawal of feedwater in a water scarce area.

2.4.3 Conclusions

This study may serve as a benchmark for global withdrawals by the semiconductor industry and could be used by industry or regulatory bodies to set withdrawals-based standards. Additionally, the spatially explicit water withdrawal data for the semiconductor sector can be used to improve existing databases of national and regional water use coefficients that are often applied in LCA input-output studies. (Blackhurst et al., 2010; Boero & Pasqualini, 2017)

Industry leaders such as Intel and Taiwan Semiconductor Manufacturing Company (TSMC) have shown that large reductions in fab water use can be achieved with the appropriate investments in water-saving technologies. And although these water savings are vital for reducing localized water impacts, this study indicates that in the case of semiconductor manufacturing, the most efficient way to reduce overall manufacturing water withdrawals (and associated regional watershed impacts) is through reduction in fab electricity use. Reductions in electricity water use can also be achieved by using less water intensive sources of electricity, such as solar PV and wind, which is especially important during seasons of higher water scarcity.

Large electronics OEMs can use this location-specific data to determine water use impacts of operations from this energy and water intensive component within their supply chain. Specifically, the rise in semiconductor manufacturing growth in certain regions in China may enhance water scarcity in areas that are already water stressed, due to existing demands by industry, agriculture and domestic users. Supply chain decisions, such as sourcing semiconductor chips from less water

stressed areas, may be a potential approach to reducing the overall water footprint of electronic products and managing the associated regulatory or reputational risk.

2.5 References

- Averyt, K., J. Fisher, A. Huber-Lee, A. Lewis, J. Macknick, N. Madden, J. Rogers, & Tellinghuisen, S. (2011). *Freshwater use by U.S. power plants: Electricity's thirst for a precious resource. A report of the Energy and Water in a Warming World initiative*. Cambridge, MA: Union of Concerned Scientists. November. Retrieved from https://www.ucsusa.org/clean_energy/our-energy-choices/energy-and-water-use/freshwater-use-by-us-power-plants.html
- Blackhurst, M., Hendrickson, C & Sels i Vidal, J. (2010). Direct and Indirect Water Withdrawals for US Industrial Sectors. *Environmental Science & Technology*, 44, 2126-30. doi: <https://doi.org/10.1021/es903147k>.
- Boero, R. & Pasqualini, D. (2017). Regional water coefficients for U.S. industrial sectors, *Water Resources and Industry*, 18, 60-70. doi: <https://doi.org/10.1016/j.wri.2017.09.001>.
- Bonamente, E., Rinaldi, S., Nicolini, A. and Cotana, F. (2017). National Water Footprint: Toward a Comprehensive Approach for the Evaluation of the Sustainability of Water Use in Italy. *Sustainability*, 9, 1341. doi: <https://doi.org/10.3390/su9081341>
- Boulay, A.-M., Bare, J., Benini, L., Berger, M., Lathuillière, M. J., Manzardo, A., . . . Pfister, S. (2017). The WULCA consensus characterization model for water scarcity footprints: assessing impacts of water consumption based on available water remaining (AWARE). *The International Journal of Life Cycle Assessment*. doi: <https://doi.org/10.1007/s11367-017-1333-8>
- Boyd, S. (2009). *Life-cycle Assessment of Semiconductors*. (Doctor of Philosophy), University of California, Berkeley, Berkely, California. Retrieved from http://digitalassets.lib.berkeley.edu/etd/ucb/text/Boyd_berkeley_0028E_10192.pdf
- Boyd, S. (2012). *Life-Cycle Assessment of Semiconductors*. Springer Science & Business Media. doi: <https://doi.org/10.1007/978-1-4419-9988-7>.
- Brown, A., & Matlock, M. D. (2011). *A Review of Water Scarcity Indices and Methodologies*. Retrieved from <https://www.sustainabilityconsortium.org/downloads/a-review-of-water-scarcity-indices-and-methodologies/>.
- Cai, B. M., Zhang, B., Bi, J., & Zhang, W. J. (2014). Energy's Thirst for Water in China. *Environmental Science & Technology*, 48(20), 11760-11768. doi: <https://doi.org/10.1021/es502655m>
- China Water Risk. (2018). CWR Big Picture: Who's Running Dry – Provinces, autonomous regions and municipalities. Retrieved from <http://www.chinawaterrisk.org/the-big-picture/whos-running-dry/>

Cooper, T., Fallender, S., Pafumi, J., Dettling, J., Humbert, S., Lessard, L., & Ieee. (2011). A Semiconductor Company's Examination of its Water Footprint Approach. *2011 Ieee International Symposium on Sustainable Systems and Technology (Issst)*, 6. <https://doi.org/10.1109/ISSST.2011.5936865>.

Diehl, T. H., & Harris, M. A. (2014). *Withdrawal and Consumption of Water by Thermoelectric Power Plants in the United States, 2010 [Appendix 1]* (2328-0328). Retrieved from <https://pubs.usgs.gov/sir/2014/5184/>

EIA. (2013). *2010 Manufacturing Energy Consumption Survey: Total Consumption of Electricity*. U.S. Energy Information Administration Retrieved from https://www.eia.gov/consumption/manufacturing/data/2010/pdf/Table11_1.pdf.

[dataset] EIA. (2015). *Annual Electric Generator Data [Plant Data]* [XLS]. Retrieved from: <https://www.eia.gov/electricity/data/eia860/>

EIA. (2016). Monthly Energy Review: Annual Total Energy. Retrieved 7-5-2017, from U.S. Energy Information Administration <https://www.eia.gov/totalenergy/data/browser/?tbl=T02.01#/?f=A&start=1949&end=2016&charted=3-6-9-12>

ESRI. (2017). ArcGIS Online World Geocoder. Retrieved from <https://www.arcgis.com/home/item.html?id=305f2e55e67f4389bef269669fc2e284>

ESRI. (2018). ArcGIS Desktop: ArcMap 10.5.1. Redlands, CA: Environmental Systems Research Institute.

Florke, M., Kynast, E., Barlund, I., Eisner, S., Wimmer, F. & Alcamo, J. (2013). Domestic and industrial water uses of the past 60 years as a mirror of socio-economic development: A global simulation study. *Global Environmental Change-Human and Policy Dimensions*, 23, 144-156. doi: <https://doi.org/10.1016/j.gloenvcha.2012.10.018>.

Frost, K., & Hua, I. (2017, 12-14 Nov.). *A spatially explicit assessment of water use by the global semiconductor industry*. Paper presented at the 2017 IEEE Conference on Technologies for Sustainability (SusTech). doi: <https://doi.org/10.1109/SusTech.2017.8333525>

[dataset] Frost, K. & Hua, I. (2019). *Global Semiconductor Manufacturing Water Withdrawals* [Web Application, XLS]. doi: <https://doi.org/10.4231/NYGF-BH18>.

Gleeson, T., Befus, K. M., Jasechko, S., Luijendijk, E., & Cardenas, M. B. (2015). The global volume and distribution of modern groundwater. *Nature Geoscience*, 9, 161. doi: <https://doi.org/10.1038/ngeo2590>

Hoekstra, A. Y. (2016). A critique on the water-scarcity weighted water footprint in LCA. *Ecological Indicators*, 66, 564-573. doi:<http://dx.doi.org/10.1016/j.ecolind.2016.02.026>

- Hoekstra, A. Y., Chapagain, A. K., Aldaya, M. M., & Mekonnen, M. M. (2011). *The Water Footprinting Assessment Manual: Setting the Global Standard*. Washington D.C.: earthscan. doi: <https://doi.org/10.1080/0969160X.2011.593864>
- IEA. (2015). Electricity and Heat Production for 2015 [Table]. Retrieved from <https://www.iea.org/statistics/statisticssearch/>
- Jiang, D. Q., & Ramaswami, A. (2015). The 'thirsty' water-electricity nexus: field data on the scale and seasonality of thermoelectric power generation's water intensity in China. *Environmental Research Letters*, 10(2). doi: <https://doi.org/10.1088/1748-9326/10/2/024015>
- Kahle, D., & Wickham, H. (2013). ggmap: Spatial Visualization with ggplot2. *The R Journal*, 5(1), 144-161. doi: <https://doi.org/10.32614/RJ-2013-014>
- Lee, U. Han, J. Elgowainy, A. & Wang, M. (2018). Regional water consumption for hydro and thermal electricity generation in the United States, *Applied Energy*, 210, 661-672. doi: <https://doi.org/10.1016/j.apenergy.2017.05.025>.
- Liao, X., Hall, J. W., & Eyre, N. (2016). Water use in China's thermoelectric power sector. *Global Environmental Change*, 41, 142-152. doi:<http://dx.doi.org/10.1016/j.gloenvcha.2016.09.007>
- Libman, V., & Neuber, A. (2008). Water Reuse Trends in the Electronics Industry. *Water Practice*, 2(3), 1-12. doi: <https://doi.org/10.2175/193317708X314193>
- Liu, E. (2018). "Global Semiconductor Revenue Forecast Revised Upward to 15 Percent from 7.5 Percent for 2018, SEMI Reports." Semiconductor Industry Association. Retrieved from <https://www.semiconductors.org/global-semiconductor-sales-increase-12-7-percent-year-to-year-in-october-double-digit-annual-growth-projected-for-2018/>
- Macknick, J., Newmark, R., Heath, G., & Hallett, K. C. (2012). Operational water consumption and withdrawal factors for electricity generating technologies: a review of existing literature. *Environmental Research Letters*, 7(4). doi: <https://doi.org/10.1088/1748-9326/7/4/045802>
- Manoca, A. (2018). "The Rebirth of the Semiconductor Industry." Semiconductor Industry Association. Retrieved from <http://blog.semi.org/technology-trends/the-rebirth-of-the-semiconductor-industry>
- Matthews, H. S., Hendrickson, C. T., & Weber, C. L. (2008). The Importance of Carbon Footprint Estimation Boundaries. *Environmental Science & Technology*, 42(16), 5839-5842. doi: <https://doi.org/10.1021/es703112w>
- Maupin, M. A., Kenny, J. F., Hutson, S. S., Lovelace, J. K., Barber, N. L., & Linsey, K. S. (2014). *Estimated Use of Water in the United States in 2010*. Reston, V.A.: U.S. Geological Survey. doi: <http://dx.doi.org/10.3133/cir1405>

- McDonald, Y. J., Schwind, M., Goldberg, D. W., Lampley, A., & Wheeler, C. M. (2017). An Analysis of the Process and Results of Manual Geocode Correction. *Geospatial Health*, 12(526), 84-89. doi: <https://doi.org/10.4081/gh.2017.526>
- Meldrum, J., Nettles-Anderson, S., Heath, G., & Macknick, J. (2013). Life cycle water use for electricity generation: a review and harmonization of literature estimates. *Environmental Research Letters*, 8(1). doi: <https://doi.org/10.1088/1748-9326/8/1/015031>
- Mueller, S. A., Carlile, A., Bras, B., Niemann, T. A., Rokosz, S. M., McKenzie, H. L., ... & Wallington, T. J. (2015). Requirements for water assessment tools: an automotive industry perspective. *Water Resources and Industry*, 9, 30-44. doi: <https://doi.org/10.1016/j.wri.2014.12.001>
- Müller Schmied, H., Eisner, S., Franz, D., Wattenbach, M., Portmann, F. T., Flörke, M., & Döll, P. (2014). Sensitivity of simulated global-scale freshwater fluxes and storages to input data, hydrological model structure, human water use and calibration, *Hydrol. Earth Syst. Sci.*, 18, 3511-3538. <https://doi.org/10.5194/hess-18-3511-2014>.
- Pfister, S., Saner, D. & Koehler, A. (2011). The environmental relevance of freshwater consumption in global power production. *The International Journal of Life Cycle Assessment*. 16, 580-591. doi: <https://doi.org/10.1007/s11367-011-0284-8>.
- Pfister, S., Boulay, A.-M., Berger, M., Hadjikakou, M., Motoshita, M., Hess, T., . . . Henderson, A. (2017). Understanding the LCA and ISO water footprint: A response to Hoekstra (2016) “A critique on the water-scarcity weighted water footprint in LCA”. *Ecological Indicators*, 72, 352-359. doi: <https://doi.org/10.1016/j.ecolind.2016.07.051>
- Quantis International. (2012). *Water and carbon footprint and preliminary risk assessment of ST company*. Retrieved from <https://quantis-intl.com/about/our-work/case-studies/>
- Rao, P., Sholes, D., Morrow, W. R., & Cresko, J. (2017). *Estimating U.S. Manufacturing Water Use*. Paper presented at the 2017 ACEEE Summer Study on Energy Efficiency in Industry, Denver, CO.
- R Core Team. (2017). R: A Language and Environment for Statistical Computing (Version Version 3.4.3 (2017-11-30)). Vienna, Austria. Retrieved from <https://www.R-project.org/>
- Rushforth, R. R. and Ruddell, B. L. (2018). A spatially detailed blue water footprint of the United States economy. *Hydrol. Earth Syst. Sci.*, 22, 3007-3032, doi: <https://doi.org/10.5194/hess-22-3007-2018>.
- Scherer, L., & Pfister, S. (2016). Dealing with uncertainty in water scarcity footprints. *Environmental Research Letters*, 11(5), 054008, doi: <https://doi.org/10.1088/1748-9326/11/5/054008>.

Sematech. (2001). *Environment, Safety and Health Chapter*. Retrieved from <https://www.dropbox.com/sh/vxigcu48nfe4t81/AACuMvZEh1peQ6G8miYFCSEJa?dl=0&preview=ESH.pdf>

Sematech. (2003). *Environment, Safety and Health Chapter*. Retrieved from <https://www.dropbox.com/sh/0ce36nq4118wiag/AACZ1MVxbt8GBSP1la7-FoMda?dl=0&preview=ESH2003.pdf>

Sematech. (2005). *Environment, Safety and Health Chapter*. Retrieved from <https://www.dropbox.com/sh/2urwqghq1gzk511/AADuZE5F68lz2DYGpA3TspSna?dl=0&preview=ESH.pdf>

Sematech. (2007). *Environment, Safety and Health Chapter*. Retrieved from <https://www.dropbox.com/sh/floxh3swiynur47/AAAwTAwf1RUzyNu8qv-PMfiUa?dl=0&preview=ESH.pdf>

Sematech. (2009). *Environment, Safety and Health Chapter*. Retrieved from <https://www.dropbox.com/sh/ialjkem3v708hx1/AAB1fo1HrYIKCIJNk0dB7YrCa?dl=0&preview=ESH.pdf>

Sematech. (2011). *Environment, Safety and Health Chapter [Table]*. Retrieved from https://www.dropbox.com/sh/r51qrus06k6ehrc/AAA956U4Cq1kYZbVXSQP64xya/2011Tables?dl=0&preview=ESH_2011Tables.xlsx

Sematech. (2013). *Environment, Safety and Health Chapter [Table]*. Retrieved from https://www.dropbox.com/sh/qz9gg6uu4k104vj/AADD7ykFdJ2ZpCR1LAB2XEjIa?dl=0&preview=ESH_2013Tables.xlsx

[dataset] SEMI. (2017). *SEMI Fab Database. [XLS]*. <http://www1.semi.org/eu/MarketInfo/FabDatabase>

Semiconductor Industry Association. (2016). *2016 SIA Factbook*. Retrieved from <http://go.semiconductors.org/2016-sia-factbook-0-0>

Spang, E. S., Moomaw, W. R., Gallagher, K. S., Kirshen, P. H., & Marks, D. H. (2014). Multiple metrics for quantifying the intensity of water consumption of energy production. *Environmental Research Letters*, 9(10). doi: <https://doi.org/10.1088/1748-9326/9/10/105003>

Swift, J. N., Goldberg, D. W., & Wilson, J. P. (2008). *Geocoding Best Practices: Review of Eight Commonly Used Geocoding Systems*. Retrieved from Los Angeles, CA:

Tidwell, V., & Moreland, B. (2016). Mapping water consumption for energy production around the Pacific Rim. *Environmental Research Letters*, 11(9). doi: <https://doi.org/10.1088/1748-9326/11/9/094008>

UN Water. (2019). Water Scarcity. United Nations. Retrieved from <http://www.unwater.org/water-facts/scarcity/>

[dataset] USEPA. (2014). *Emissions & Generation Resource Integrated Database (eGRID) Summary Tables: NERC Region Resource Mix (Table 8)* [XLSX]. Retrieved from <https://www.epa.gov/energy/emissions-generation-resource-integrated-database-egrid>

USGS. (2016). Water Use Terminology. Retrieved from <https://water.usgs.gov/watuse/wuglossary.html>

Vassolo, S., & Döll, P. (2005). Global-scale gridded estimates of thermoelectric power and manufacturing water use. *Water Resources Research*, 41(4). doi: <https://doi.org/10.1029/2004WR003360>

[dataset] WULCA. (2017). *AWaRe (Available Water Remaining) Factors* [KMZ]. Retrieved from: <http://www.wulca-waterlca.org/aware.html>

WULCA. (2018). WULCA: Mission and Goals. Retrieved from <http://www.wulca-waterlca.org/mission.html>

Xu, H., & Wu, M. M. (2017). *Water Availability Indices—A Literature Review* (No. ANL/ESD-17/5). Argonne National Lab.(ANL), Argonne, IL (United States). doi: <https://doi.org/10.2172/1348938>.

Zhang, C., Zhong, L. J., Fu, X. T., Wang, J., & Wu, Z. X. (2016). Revealing Water Stress by the Thermal Power Industry in China Based on a High Spatial Resolution Water Withdrawal and Consumption Inventory. *Environmental Science & Technology*, 50(4), 1642-1652. doi: <https://doi.org/10.1021/acs.est.5b05374>

Zhang, N., Hu, Z., Shen, B., He, G., & Zheng, Y. (2017). An integrated source-grid-load planning model at the macro level: Case study for China's power sector. *Energy*, 126, 231-246. doi: <https://doi.org/10.1016/j.energy.2017.03.026>

2.6 Appendix. Chapter 2 Supporting Information

Table A.1. Net generation, fuel mix, and water use intensity for U.S. NERC electricity regions.

NERC Region	Net generation (TWh)	% of Region's Electricity Provided By Fuel Type (EPA, 2014)									Water use intensity (L/kWh)
		Thermoelectric						Non-thermoelectric			
		Coal	Oil	Gas	Nuclear	Biomass	Geo-thermal	Hydro	Wind	Solar PV	
Florida Reliability Coordinating Council (FRCC)	220	21.6	0.8	61.4	12.7	2.0	0.0	0.1	0.0	0.1	42.67
Midwest Reliability Organization (MRO)	227	60.2	0.3	3.9	11.9	1.7	0.0	5.5	16.3	0.0	49.57
Northeast Power Coordinating Council (NPCC)	244	3.9	1.7	41.2	32.3	4.0	0.0	13.2	2.4	0.2	75.55
Reliability First Corporation (RFC)	947	50.3	0.6	15.7	28.6	1.0	0.0	0.7	2.3	0.1	51.10
SERC Reliability Corporation (SERC)	1090	42.2	0.5	25.4	26.1	2.0	0.0	3.0	0.4	0.1	59.88
Southwest Power Pool (SPP)	226	53.5	1.6	26.0	3.8	1.1	0.0	1.5	12.3	0.0	29.23
Texas Regional Entity (TRE)	368	33.4	0.1	44.9	10.7	0.3	0.0	0.1	9.9	0.1	45.41
Western Electricity Coordinating Council (WECC)	741	27.5	0.1	30.1	7.9	1.5	2.1	21.9	6.4	2.0	12.97

Table A.2. Chinese provincial electricity production capacity, fuel mix, and water use intensities. Weighted averages based on production capacity were used to create regional averages.

Province	Chinese Elec. Region	Province Product Capacity (TWh)	% of Provincial Production Capacity for Each Energy Type (Cai et al., 2014)							% of Thermoelectric Production Using Various Cooling Types (C. Zhang et al, 2016)				Provincial Average Water Use Intensity	Capacity Weighted Regional Average WUI (L/kWh)
			Coal	Natural gas	Biomass	Nuclear	Hydro	Wind	Solar	Recirculating Cooling	Once-through Cooling	Dry Cooling	Sea-water Cooling		
Chongqing	Central	109.78	76.7%	0.0%	1.1%	0.0%	21.9%	0.4%	0.0%	66.6%	33.4%	0.0%	0.0%	46.89	51.33
Henan	Central	303.14	94.2%	0.0%	1.3%	0.0%	3.1%	1.4%	0.0%	96.0%	4.0%	0.0%	0.0%	7.71	
Hubei	Central	272.93	37.2%	0.0%	0.4%	12.8%	49.5%	0.1%	0.0%	40.6%	59.4%	0.0%	0.0%	105.69	
Hunan	Central	205.68	52.0%	0.0%	0.9%	17.0%	30.1%	0.0%	0.0%	35.8%	64.2%	0.0%	0.0%	117.27	
Sichuan	Central	364.37	22.4%	0.0%	1.2%	0.0%	75.9%	0.4%	0.1%	98.5%	1.5%	0.0%	0.0%	11.01	
Anhui	East	288.7	95.3%	0.0%	2.1%	0.0%	1.6%	1.0%	0.1%	75.7%	24.3%	0.0%	0.0%	33.39	77.69
Fujian	East	215.21	46.0%	7.0%	1.1%	22.8%	21.1%	2.0%	0.0%	9.1%	13.3%	0.0%	77.6%	120.51	
Jiangsu	East	448.52	71.2%	17.7%	1.3%	7.3%	0.1%	2.2%	0.2%	42.2%	49.3%	0.0%	8.6%	83.85	
Jiangxi	East	118.88	53.2%	2.1%	3.0%	29.4%	10.4%	1.7%	0.2%	63.5%	36.5%	0.0%	0.0%	101.71	
Shanghai	East	149.84	75.2%	22.6%	1.1%	0.0%	0.0%	1.0%	0.1%	7.7%	75.9%	0.0%	16.4%	117.79	
Zhejiang	East	385.59	61.3%	16.0%	1.3%	13.8%	7.0%	0.5%	0.1%	23.9%	7.2%	0.0%	68.9%	56.78	8.31
Beijing	North	48.72	56.4%	37.6%	2.5%	0.0%	1.0%	1.9%	0.5%	90.7%	9.3%	0.0%	0.0%	14.28	
Hebei	North	301.93	93.3%	1.4%	1.4%	0.0%	0.2%	3.6%	0.2%	65.2%	4.0%	12.3%	18.5%	8.59	
Shandong	North	479.07	92.9%	0.0%	1.9%	3.9%	0.1%	1.2%	0.0%	80.7%	1.2%	0.5%	17.6%	11.08	
Shanxi	North	380.12	98.2%	0.0%	0.5%	0.0%	1.1%	0.3%	0.0%	35.9%	3.4%	60.8%	0.0%	7.27	
Tianjin	North	126.24	77.2%	21.5%	1.2%	0.0%	0.0%	0.1%	0.0%	65.1%	0.2%	0.0%	34.6%	2.90	
W. Inner Mong.	North	227.37	87.0%	0.0%	0.3%	0.0%	0.8%	11.8%	0.1%	46.0%	2.6%	51.4%	0.0%	5.57	19.37
E. Inner Mongolia	NE	227.37	87.0%	0.0%	0.3%	0.0%	0.8%	11.8%	0.1%	46.0%	2.6%	51.4%	0.0%	5.57	

Heilongjiang	NE	138.78	88.4%	0.0%	2.1%	0.0%	2.4%	6.9%	0.3%	78.2%	21.8%	0.0%	0.0%	30.14	
Jilin	NE	100.25	63.3%	0.0%	5.6%	0.0%	9.1%	21.8%	0.2%	81.5%	11.5%	7.0%	0.0%	17.51	
Liaoning	NE	183.66	74.7%	0.0%	2.2%	15.2%	2.7%	5.0%	0.2%	62.6%	0.1%	1.9%	35.4%	29.32	
Gansu	NW	121.4	54.5%	0.0%	1.5%	0.0%	22.2%	21.0%	0.8%	55.5%	0.0%	44.5%	0.0%	3.37	3.15
Ningxia	NW	141.67	91.9%	0.0%	0.4%	0.0%	1.3%	5.7%	0.7%	42.3%	0.0%	57.7%	0.0%	1.26	
Qinghai	NW	90	46.9%	0.0%	0.0%	0.0%	48.8%	1.3%	3.0%	100.0%	0.0%	0.0%	0.0%	6.60	
Shaanxi	NW	274.98	92.4%	0.0%	1.1%	0.0%	4.5%	1.5%	0.5%	45.8%	0.0%	54.2%	0.0%	1.69	
Xinjiang	NW	272.03	88.1%	0.0%	0.0%	0.0%	6.6%	5.3%	0.0%	82.8%	1.2%	16.0%	0.0%	4.12	
Xizang	NW	9.91	3.8%	0.0%	0.0%	0.0%	94.6%	0.0%	1.6%	100.0%	0.0%	0.0%	0.0%	10.72	55.63
Guangdong	South	469.69	55.1%	15.0%	0.4%	19.5%	9.1%	0.9%	0.0%	21.0%	12.2%	0.0%	66.8%	84.48	
Guangxi	South	198.14	63.4%	1.6%	1.5%	7.1%	25.7%	0.8%	0.0%	17.9%	48.0%	0.0%	34.0%	110.23	
Guizhou	South	215.65	79.3%	0.0%	2.9%	0.0%	16.4%	1.4%	0.0%	98.5%	1.5%	0.0%	0.0%	5.61	
Hainan	South	20.56	82.5%	0.0%	5.8%	0.0%	7.3%	3.4%	1.0%	11.4%	0.0%	0.0%	88.6%	2.78	
Yunnan	South	264.07	31.0%	0.0%	1.2%	0.0%	67.2%	0.4%	0.1%	100.0%	0.0%	0.0%	0.0%	8.30	

Sample calculation for provincial electricity WUI:

$$\sum PCPC((\%RC_{coal} * WUI_{recirc}) + (\%OTC_{coal} * WUI_{otc}) + (\%DC_{coal} * WUI_{dry})) + PNGPC((\%RC_{ng} * WUI_{recirc}) + (\%OTC_{ng} * WUI_{otc})) + (PNPC * WUI_{nuclear}) + (Biomass * WUI_{biomass}) + (PSP * WUI_{solar}) + (PWP * WUI_{wind}) + (PHP * WUI_{hydro})$$

For Shanghai Province, the calculation would be as follows:

$$\text{Shanghai Province WUI} = 0.752*((.077*2.37) + (.759*95.5) + (0*0.334)) + 0.226((.077/(.077+.759))*2.75) + ((.0759/(.077+.759)*34.07)) + (0*178) + (0.011*0.0172) + (0.01*0.0227) + (0.001*.0057) + (0*11.245)$$

Sample calculation for regionally averaged WUI, weighted by the production capacity of each province in the electricity trading region.

Table A.3. Weighted production capacity of each province in the ‘East’ electricity trading region.

Province	Electricity Region	Provincial Production Capacity (TWh)	Prov Weighting Factor (Prov Capacity/Total Regional Capacity)
Anhui	East	288.7	0.18
Fujian	East	215.21	0.13
Jiangsu	East	448.52	0.28
Jiangxi	East	118.88	0.07
Shanghai	East	149.84	0.09
Zhejiang	East	385.59	0.24
	Total Regional Capacity	1606.74	1.0

East Region WUI = (Anhui_{WUI}*Anhui_{WeightFactor}) + (Fujian_{WUI}*Fujian_{WeightFactor}) + (Jiangsu_{WUI}*Jiangsu_{WeightFactor}) + (Jiangxi_{WUI}*Jiangxi_{WeightFactor}) + (Shanghai_{WUI}*Shanghai_{WeightFactor}) + (Zhejiang_{WUI}*Zhejiang_{WeightFactor})

East Region WUI = (33.39 *0.18) + (120.51*0.13) + (83.85* 0.28) + (101.71*0.07) + (117.79*0.09) + (56.78*0.24)

East Region WUI = 77.69 L/kWh

Table A.4. Electricity grid mix, total production capacity (IEA, 2015) and water use intensities for each semiconductor producing country (except China and U.S.).

Country	Coal	Oil	Gas	Biofuels	Waste	Nuclear	Hydro	Geo-thermal	Solar PV	Solar Thermal	Wind	Tide	Other	Total Elec Prod (GWh)	WUI (L/kWh)
Australia	62.9%	2.7%	20.8%	1.4%	0.0%	0.0%	5.3%	0.0%	2.4%	0.0%	4.5%	0.0%	0.0%	252360	2.378
Austria	7.8%	1.3%	11.9%	6.3%	1.6%	0.0%	62.2%	0.0%	1.4%	0.0%	7.4%	0.0%	0.0%	65299	7.304
Belarus	0.1%	1.1%	97.9%	0.4%	0.1%	0.0%	0.3%	0.0%	0.0%	0.0%	0.1%	0.0%	0.0%	34082	0.969
Belgium	6.0%	0.3%	32.3%	6.6%	3.0%	36.9%	2.0%	0.0%	4.3%	0.0%	7.9%	0.0%	0.6%	70648	66.421
Brazil	4.7%	5.0%	13.7%	8.4%	0.0%	2.5%	61.8%	0.0%	0.0%	0.0%	3.7%	0.0%	0.1%	581652	11.731
Bulgaria	45.8%	0.4%	3.8%	0.6%	0.0%	31.2%	12.5%	0.0%	2.8%	0.0%	2.9%	0.0%	0.0%	49228	58.181
Canada	9.8%	1.2%	10.0%	1.9%	0.0%	15.1%	56.8%	0.0%	0.4%	0.0%	3.9%	0.0%	0.8%	670851	33.626
Czech Republic	52.3%	0.1%	2.7%	5.6%	0.2%	32.0%	3.7%	0.0%	2.7%	0.0%	0.7%	0.0%	0.1%	83892	58.668
Denmark	24.5%	1.1%	6.3%	11.4%	5.8%	0.0%	0.1%	0.0%	2.1%	0.0%	48.8%	0.0%	0.0%	28947	0.689
England	22.6%	0.6%	29.5%	7.8%	1.9%	20.7%	2.7%	0.0%	2.2%	0.0%	11.9%	0.0%	0.0%	339095	38.057
Finland	12.8%	0.3%	7.6%	16.0%	1.2%	33.9%	24.4%	0.0%	0.0%	0.0%	3.4%	0.0%	0.4%	68598	63.433
France	2.1%	0.4%	3.5%	0.7%	0.7%	77.0%	10.4%	0.0%	1.3%	0.0%	3.7%	0.1%	0.1%	568454	138.169
Germany	43.9%	1.0%	9.7%	6.9%	2.0%	14.2%	3.8%	0.0%	6.0%	0.0%	12.2%	0.0%	0.3%	646888	26.872
India	75.3%	1.7%	4.9%	1.8%	0.1%	2.7%	10.0%	0.0%	0.4%	0.0%	3.1%	0.0%	0.0%	1383004	7.871
Ireland	26.0%	1.4%	43.6%	1.4%	0.5%	0.0%	3.9%	0.0%	0.0%	0.0%	23.2%	0.0%	0.0%	28387	1.504
Israel	45.8%	0.7%	51.6%	0.1%	0.0%	0.0%	0.0%	0.0%	1.7%	0.0%	0.0%	0.0%	0.0%	64226	1.641
Italy	16.0%	4.7%	39.2%	6.0%	1.7%	0.0%	16.6%	2.2%	8.1%	0.0%	5.2%	0.0%	0.2%	282994	2.686
Japan	33.0%	9.8%	39.4%	3.3%	0.7%	0.9%	8.8%	0.2%	3.4%	0.0%	0.5%	0.0%	0.0%	1041343	3.837
Korea	42.8%	2.3%	22.2%	0.4%	0.1%	29.8%	1.0%	0.0%	0.7%	0.0%	0.2%	0.1%	0.3%	552876	54.427
Latvia	0.0%	0.0%	49.8%	13.9%	0.0%	0.0%	33.6%	0.0%	0.0%	0.0%	2.7%	0.0%	0.0%	5533	4.254
Malaysia	42.3%	1.2%	46.6%	0.5%	0.0%	0.0%	9.3%	0.0%	0.2%	0.0%	0.0%	0.0%	0.0%	150123	2.545
Netherlands	38.7%	1.3%	42.3%	2.7%	3.3%	3.7%	0.1%	0.0%	1.0%	0.0%	6.9%	0.0%	0.1%	110070	7.971
Norway	0.1%	0.0%	1.8%	0.0%	0.3%	0.0%	95.9%	0.0%	0.0%	0.0%	1.7%	0.0%	0.2%	145021	10.799
Russia	14.9%	0.9%	49.6%	0.0%	0.3%	18.3%	15.9%	0.0%	0.0%	0.0%	0.0%	0.0%	0.0%	1067544	35.211
Scotland	22.6%	0.6%	29.5%	7.8%	1.9%	20.7%	2.7%	0.0%	2.2%	0.0%	11.9%	0.0%	0.0%	339095	38.057
Singapore	1.2%	0.7%	95.0%	0.4%	2.5%	0.0%	0.0%	0.0%	0.1%	0.0%	0.0%	0.0%	0.0%	50415	0.932

Slovakia	12.4%	1.4%	6.0%	6.1%	0.2%	56.3%	15.4%	0.0%	1.9%	0.0%	0.0%	0.0%	0.4%	26903	102.265
Slovenia	29.0%	0.1%	2.7%	1.8%	0.1%	37.4%	27.1%	0.0%	1.8%	0.0%	0.0%	0.0%	0.0%	15100	70.346
Sweden	0.8%	0.2%	0.3%	5.6%	1.8%	34.8%	46.6%	0.0%	0.1%	0.0%	10.0%	0.0%	0.0%	162058	67.120
Switzerland	0.0%	0.1%	1.0%	0.8%	3.4%	34.1%	58.9%	0.0%	1.7%	0.0%	0.2%	0.0%	0.0%	67720	67.292
Taiwan	45.4%	4.2%	32.4%	0.1%	1.2%	12.0%	3.7%	0.0%	0.4%	0.0%	0.6%	0.0%	0.0%	264114	23.206
Thailand	19.5%	0.6%	71.4%	4.1%	0.3%	0.0%	2.7%	0.0%	1.3%	0.0%	0.2%	0.0%	0.0%	177760	1.465
Turkey	29.1%	0.8%	37.9%	0.5%	0.0%	0.0%	25.6%	1.3%	0.1%	0.0%	4.5%	0.0%	0.2%	261783	3.989
United Arab Emirates	0.0%	1.2%	98.5%	0.0%	0.0%	0.0%	0.0%	0.0%	0.0%	0.2%	0.0%	0.0%	0.0%	127366	0.938
Wales	22.6%	0.6%	29.5%	7.8%	1.9%	20.7%	2.7%	0.0%	2.2%	0.0%	11.9%	0.0%	0.0%	339095	38.057

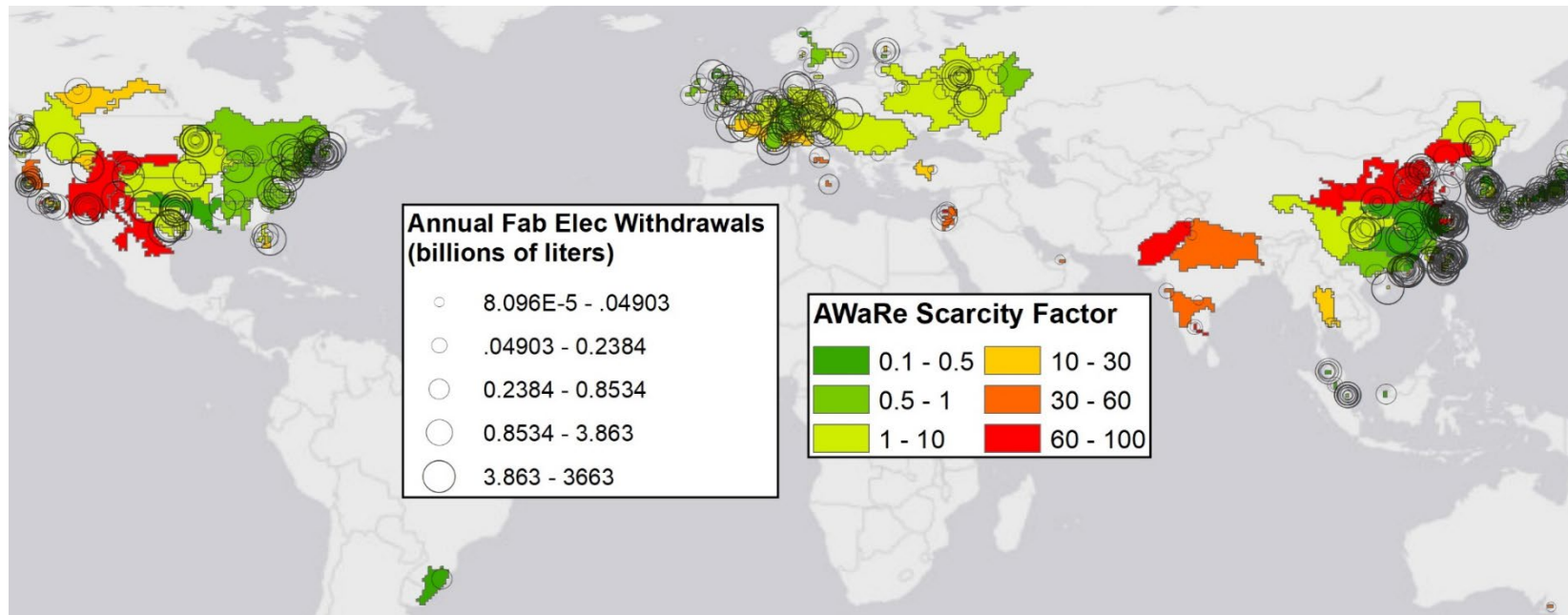


Figure A.1. Map of global fab ERW withdrawals by facility, overlaid on AWaRe scarcity factors.

3. ENVIRONMENTAL IMPACTS OF A CIRCULAR RECOVERY PROCESS FOR HARD DISK DRIVE RARE EARTH MAGNETS

Reprinted with permission from Frost, K., Sousa, I., Larson, J. Jin, H. & Hua, I. (2021). Environmental Impacts of a Circular Recovery Process for Hard Disk Drive Rare Earth Magnets. *Resources, Conservation and Recycling*. 173 105694 <https://doi.org/10.1016/j.resconrec.2021.105694>. Copyright 2021 Elsevier B.V.

3.1 Introduction

3.1.1 Circular Economy and the ICT Sector

Industry, government, and non-profit organizations are developing and promoting innovative business models that are built upon the principles of circular economy (i.e. minimize material input and maintain materials at their highest quality use for as long as possible [WEF, 2014]). However, for these material and waste reduction goals to be viable, circular business models must also align with aggressive carbon reduction targets (UNFCCC, n.d.), all while remaining economically and logistically viable.

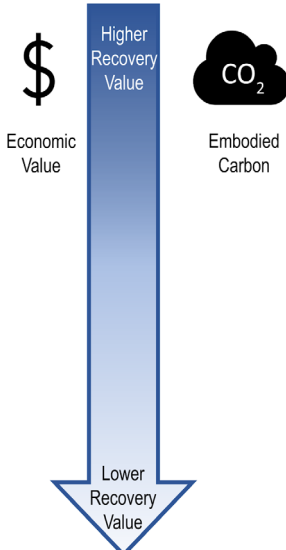
The Information and Communications Technology (ICT) sector, including the electronics devices which support ICT services, are prioritized by many stakeholders for implementation of circular economy (CE) initiatives (EC, 2020; EMF, 2018; Handwerker & Olson, 2019; US CoC 2015) because these products are comprised of many high value components and critical materials (Buechler et al., 2020; Peiro et al., 2020). Hard disk drives (HDDs) and their constituent components are an ideal ICT product for applying CE approaches because of the stable design form (i.e., 2.5” and 3.5”), high collection rates from large commercial users (i.e. estimates of 90-95% from hyperscale or enterprise data centers (DCs) [Nguyen et al., 2017]), and the large economic potential. Additionally, HDDs contain notable amounts of critical materials, such as the rare earth elements (REEs) neodymium and praseodymium, that have major importance to both technology and clean energy but entail high supply risks due to limited availability, low substitution and recycling rates, competing materials demands, and socio-political factors (Balde et al., 2017; Gibbs, 2019; U.S. DOE, 2011; Schulz et al., 2017). Many studies have demonstrated the feasibility of mining critical materials from alternative sources such as waste electronics

(Isildar et al., 2018), mine tailings (Tunsu et al., 2019), and landfills (Blengini et al., 2019); however, HDDs provide a large pool of high quality, concentrated REEs (>10,000 ppm), and have been targeted for various critical material recovery strategies (King, 2017).

3.1.2 The HDD Recovery Cascade

Frost et al. (2020) described the ideal recovery cascade for an HDD & rare earth (RE) magnet circular economy beginning with whole HDD reuse, then subassembly and component reuse, RE magnet recycling, rare earth oxide (REO) recycling, shred & base metals recovery, and finally, energy recovery. Whole HDD reuse is well-established, and several other pathways in the recovery cascade have been successfully demonstrated at various scales by industry, government, and academia (Handwerker and Olson, 2019). For example, Dell recently piloted a project to recover and recycle RE magnets from HDDs wherein the RE magnets from end-of-life (EoL) HDDs were recovered, RE oxides were chemically extracted, and then processed into new RE magnets (RBA, 2019). This is a promising EoL pathway for RE magnets because it does not require a specific HDD design for placement of the reformed magnet; however, reprocessing the magnets is not optimal from an environmental impact perspective when compared to whole HDD or HDD component reuse (Jin et al., 2020). A portfolio of recovery options should be utilized by HDD stakeholders and is often dictated by end user data security policies, the functionality of the EoL HDD, logistics & supply chain constraints, and available recovery technologies (Table 3.1).

Table 3.1. The HDD & RE magnet value recovery cascade. The table was summarized from Frost et al (2020). These are listed in order from highest to lowest economic and environmental value.

	Value Recovery Option	Description of Technology/Process	Barriers/Opportunities for Circular Business Model
	HDD reuse	Secure data wiping and internal company reuse or sell to secondary markets	Highest value recovery option and most environmentally beneficial. A common practice of shredding HDDs for data security reasons precludes other downstream uses.
	HDD component reuse (e.g. magnet assembly)	Disassemble, recover and reuse or remanufacture HDD components	Requires active collaboration among end users (or ITADs) and HDD manufacturers. Currently limited by placement within similar drive model
	Intact magnet recovery for non-HDD Use	Magnets are punched out of HDD and reused as intact magnets for axial gap motors	Technology is theoretically viable*, but motors must be designed with reusing HDD magnets in mind.
	Magnet-to-magnet recycling*	Process HDD RE magnets into new sintered magnets with magnetic properties similar to HDD magnets	Magnets need to be certified in HDDs to close the loop, locked in linear supply chains for RE magnets. Need sufficient volumes of HDD RE magnets
	Making RE Oxides from HDD magnets and other precious metals recycling	HDD magnets can be processed into high purity RE oxides* for open or closed loop recycling	Process needs to be scaled beyond pilots, traceability of RE oxides is difficult; locked in linear supply chains

*See Handwerker and Olson (2019) for detailed technology description.

Within this portfolio, recovery and reuse of intact HDD subassemblies or components (when HDD reuse is not feasible) has potential as a high-value recovery option (Handwerker & Olson, 2019), but current examples are very limited. Component recovery and remanufacturing/reuse is currently challenged by the widespread practice of HDD shredding due to data security concerns, lack of

qualified disassembly and recovery processes, and the existing supply chain structure which could negate the environmental benefits of reuse. In particular, reverse logistics are key: the electronics supply chain is focused in Asia, yet many of the largest DC users and investment in sustainable recovery initiatives are concentrated in Europe and North America (Synergy Research Group, 2020; iNEMI; 2019, CEDaCI, 2020). Thus, careful scrutiny of recovery processes and reverse logistics is key for ensuring sustainability and discovering hotspots that may be associated with introducing these recovery initiatives (Barba-Gutiérrez et al., 2008; Jin et al, 2020).

To mitigate risk of introducing environmental hotspots through implementation of a new CE approach, it is imperative to quantify the potential environmental benefits of the proposed business model to devise the best implementation strategy for full-scale operations. And although important strides are being made to incorporate sustainability into CE performance metrics (Woolven, 2021), these tools are still under development, and current metrics focus on dematerialization or material cycling rates. It is, therefore, necessary to couple CE strategies with mature evaluation tools such as LCA to gain a full understanding of the environmental sustainability of the proposed CE business model (Beaulieu, 2015; Elia et al, 2017; Haupt & Hellweg, 2019; Walker et al., 2018).

Rehberger et al. (2020) reviewed the use of LCA to assess cascading product systems across 100 studies, which featured a wide variety of product types and methodological choices. However, to date, only a handful of studies have addressed the cascades of high-tech products and/or those containing critical materials, which focused largely on electric vehicle lithium-ion battery packs (Ahmadi et al., 2014; Bobba et al., 2018; Riccha et al., 2017), photovoltaic modules (Perez-Gallardo (2017), and more recently HDDs (Jin et al, 2020). Studies show that reuse could save up to~69% of global warming impact compared to the business-as-usual but stressed the importance of a “life cycle centric” approach for analyzing environmental trade-offs among an array of technical and methodological parameters (Richa et al., 2017).

3.1.3 Rare Earth (RE) Magnets LCA

High-quality LCA data for the BAU scenario is vital for a fair comparison to the proposed R&R process. In particular, up-to-date unit process data for the RE metals and RE magnet processing steps is essential because RE magnets contribute almost 80% of the GHG impacts associated with

manufacturing an MA and 8% of the total HDD materials and manufacturing impacts (Jin et al., 2020; Seagate, 2016). Given the growing importance of RE magnets to products such as industrial motors, electric vehicles, wind turbines, and HDDs, extensive work has been done recently to characterize the environmental impacts of RE metal mining and processing, and transformation into high-tech magnets.

The rare earth elements considered in this study are two light rare earth elements (LREEs): neodymium and praseodymium, based on the bill of materials of the HDD MA under investigation. The global supply of LREEs is largely concentrated in the bastnasite/monazite deposits from the Bayan Obo region of China, thus the Bayan Obo mining and production route (Bailey et al., 2020; Arshi et al., 2018) was assumed for this study. Bailey et al. (2020) provided a comprehensive summary of the REE LCA work, to date, and classified rare earth oxide (REO) processing into 5 major stages: mining, beneficiation, acid roasting, leaching, and solvent extraction. REO solvent extraction and separation into individual REOs represents 65% of the GHG impacts and nearly 100% of the human and ecotoxicity impacts from RE processing, when considering the Bayan Obo production route (Bailey et al., 2020). Sprecher et al. (2014) conducted one of the first studies that estimated impacts from extraction and processing of bastnasite and monazite deposits of RE elements and estimated unit process (UP) impacts of both RE metals and subsequent RE magnet production. Vahidi et al. (2016), and Arshi et al. (2018) used Chinese production data to update UP data for RE oxides and RE metals and magnets production from bastnasite, monazite, and ion adsorption clays, which are the three major types of geological deposits of REs in China. Jin et al. (2018) partnered with a US RE magnet recycler to quantify the environmental benefits of RE magnet recycling in comparison with new production. Finally, Jin et al. (2020) assessed reuse of the entire RE magnet assembly (RE magnet + steel bracket) in an enterprise HDD and found 3.8 kg CO₂-eq benefit per MA using assumptions for a small, demonstration recovery process.

3.1.4 Piloting of HDD Rare Earth Magnet Assembly (MA) Recovery & Reuse

Soderman and Andre (2019) point out that case studies of real circular business models are in “short supply”; thus, providing real-world examples of reuse of subassemblies or components, is vital to demonstrating a viable circular business model. The focus of this work is on the closed-loop recovery and reuse of a *highly reliable* subassembly, known as the voice coil motor assembly

(aka “magnet assembly”). An assembly or subassembly is a distinctive part of a product which typically consists of several components. In this case, the upper and lower magnet assembly (MA) consists of two powerful, sintered NdFeB magnets (aka “RE magnets”) each epoxied onto a steel bracket which actuate the head stack assembly, enabling hard drive read-write functionality. Here, highly reliable indicates that the recovery process yield is expected to be very high (~100%), and there is no degradation of functionality between a virgin and reused MA. The reliability of the MA, as demonstrated by internal engineering reliability data by the HDD manufacturer, is due to the properties of the magnets themselves (i.e. ‘permanent magnets’ which have high Curie temperatures, the temperature required to de-magnetize, of ~380°C depending on magnet composition [Jin et al, 2020]) and the fact that the magnet assembly, as a whole, is not subject to the same issues of wear as other components within the HDD.

In 2018, a small demonstration project (n= 6 HDDs) was conducted to investigate the potential of a process for MA recovery and reuse, and to assess environmental impacts using LCA (Handwerker and Olson 2019; Jin et al, 2020). This demonstration project brought together key stakeholders in the HDD recovery supply chain and served as a low-risk opportunity to build trust amongst key actors while exploring a viable circular business model. (Frost et al, 2020). The present work represents the next step towards an HDD MA circular business model and describes a collaborative, large-scale pilot project (n=6100 HDDs) between two major HDD stakeholders to assess the feasibility of a long-term process for recovery of HDD components within a DC and placement into new HDDs at the manufacturer. For highly secure data types, in-house shredding of entire HDDs followed by base and precious metals recovery is the preferred EoL option for many end-users which are subject to strict physical destruction policies and represents a significant barrier to HDD subassembly or component recovery (Handwerker & Olson, 2019). Recovering and diverting components of value before they leave the DC is a novel recovery approach which complies with data security policies and abides by restrictions on the transboundary movement of e-waste (EC, 2019)

Project stakeholders envisioned a process wherein the MAs of HDDs destined for the shredder are recovered within a DC (e.g., U.S.) and shipped back to the HDD manufacturer in Thailand for cleaning and placement into a new HDD. This MA recovery system was piloted over several

months in fall of 2019, during which time data on electricity, materials use, and transport logistics were collected.

3.2 Methods

3.2.1 Study Description & Goal

This LCA study assesses a new recovery process wherein the magnet assemblies within an HDD destined for the shredder are recovered within a datacenter (e.g., U.S.) and shipped back to the HDD manufacturer in Thailand for cleaning and placement into a new HDD. This recovery system was piloted over several months in fall of 2019, during which time data on electricity, materials use, and transport logistics were collected.

The study was carried out for the MA recovery and reuse (R&R) pilot with the following purposes: 1) quantify the environmental impacts of a circular MA recovery option as compared to the current business practice (shred and base metals recovery) and 2) identify environmental hotspots in the MA recovery process and evaluate alternative scenarios. The LCA study is attributional. The results are intended to be used for decision support in the final design and scale-up of a MA recovery process and to document environmental impacts of components that contain critical materials which are important for the electronics industry.

3.2.2 Functional Unit & System Boundary

The functional unit for this product system is a set of rare earth MAs, consisting of an upper and a lower MA (weighing 57.86 g and 46.36 g, respectively), within a Seagate Evans 16 TB SATA, Model Number ST16000NM003G (an enterprise helium drive with 16 TB capacity weighing 670 g). In the R&R system, the MAs are subsequently recovered for reuse in the second life cycle. System expansion was used to include the avoided production of a second magnet; thus, the functional unit for the business as usual (BAU) system is equivalent to two corresponding sets of MAs that are not recovered at EOL, providing a similar function to the R&R system (virgin MA + 1-time reuse). See Figure 1 for an image of the MA and constituent NdFeB magnet.

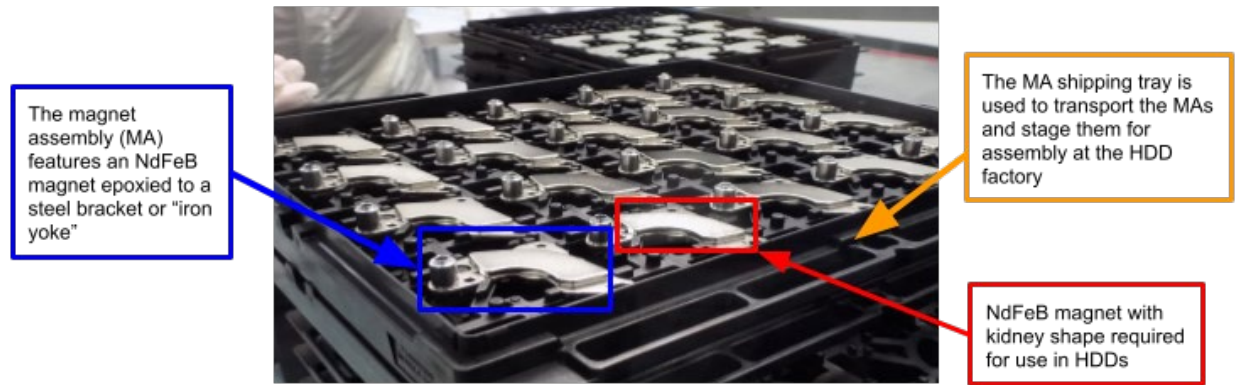


Figure 3.1. Magnet assembly (MA) within a specialized shipping tray. Image used with permission (photo courtesy of Ikenna Ike).

3.2.2.1 *Business As Usual (BAU) System*

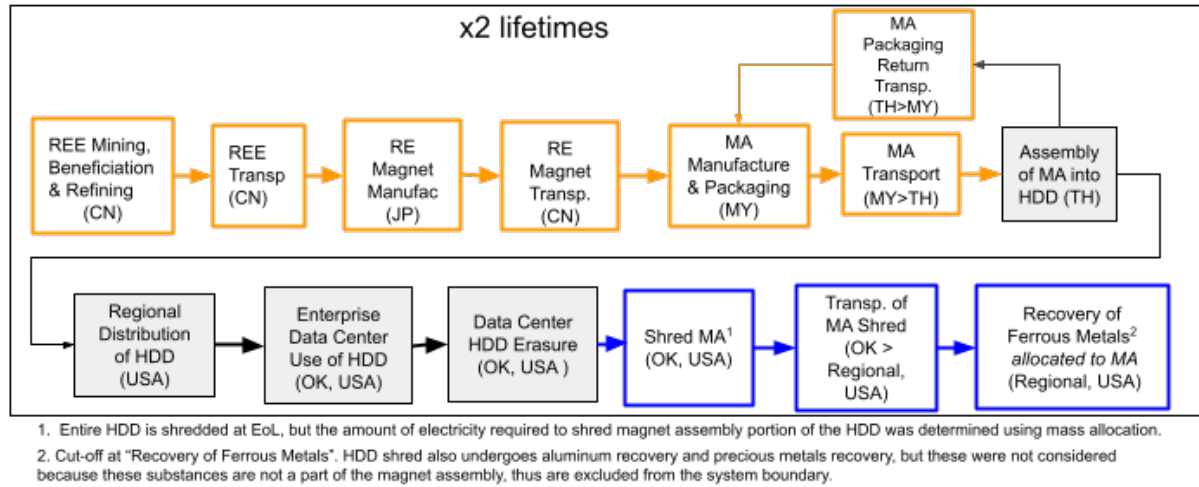
The life cycle of the BAU magnet includes the extraction, refining and transport of virgin materials, manufacturing of RE magnets, manufacturing and assembly of the MA, transportation of the MA to the assembly facility for HDD production, transportation of the HDD to the DC for use, HDD data erasure, HDD shred (including the magnet), and ferrous metals recovery. Figure 2a is a general schematic of the MA lifecycle and serves as the BAU (i.e. baseline scenario) for our comparative assessment. Boxes in gray were excluded from the system boundary in our comparative assessment because they are assumed to be equal in the BAU and R&R systems.

3.2.2.2 *Magnet Assembly Recovery & Reuse (R&R) System*

Figure 2b represents the process flow diagram for the MA recovery & reuse (R&R) pathway to be compared with the BAU shown in Figure 2. The processes that are unique to R&R include the EoL recovery and reuse processes introduced by the new, circular recovery system which consist of HDD disassembly, MA extraction and packaging in a cleanroom environment, transport to the HDD assembly facility, and cleaning for placement into a new HDD. For this comparative LCA, we elaborate only processes that are unique to each system and exclude the common processes of HDD production, transport from the HDD manufacturer to the user, or use phase of the product from our system boundary. Use phase performance is considered to be the same between a new and recovered MA, which has been validated through quality control testing - no difference was observed in HDD's power consumption when using new MAs vs. recovered MAs. We consider

only one additional useful lifetime of the MA and assume shred and ferrous metals recovery at the end of the second life of the MA. As noted in Section 3.1.4, the R&R system is expected to have a very high yield (~100%), although other yield scenarios are presented in the SI.

a)



b)

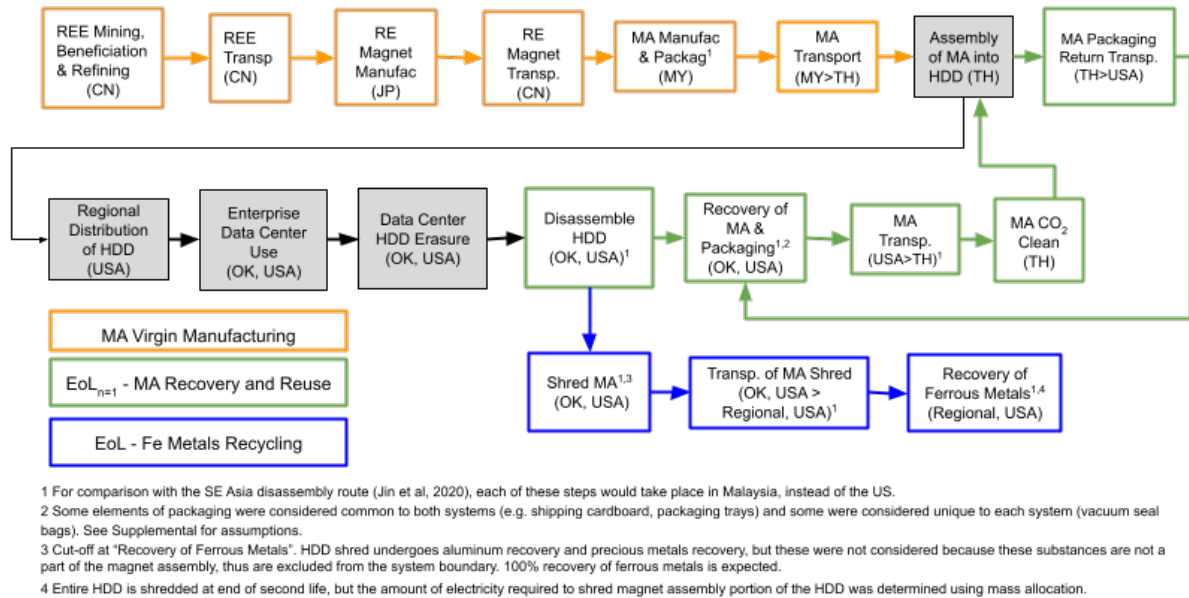


Figure 3.2. Fig (a) is the Business As Usual (BAU) process, depicting MA virgin manufacturing processes and EOL treatments for two sets of MAs. Fig (b) depicts the life cycle diagram for the MA R&R system with one-time reuse of one MA set. Boxes in green represent the new R&R processes and boxes in orange represent virgin manufacturing processes. Boxes shaded in gray represent those processes that are common to both the BAU and R&R systems, which are excluded from our system boundary for the comparative assessment. Boxes in blue depict EoL recycling processes that occur at the end of first life for BAU and second life for R&R. CN=China, JP=Japan, MY=Malaysia, TH=Thailand, OK=Oklahoma, USA.

As recovered MAs are directly substituted for virgin MAs within the same product system without loss of quality/function/lifetime, a full credit was given to the R&R system for the avoided burden of MA virgin production, (Allacker et al, 2017). Such a credit incentivizes the R&R system for RE magnets reuse, whose value is currently almost entirely lost due to shredding and mixed scrap recovery.

Eq 3.1 represents the life cycle impacts of production of one set of MAs under BAU assumptions. Eq 3.2 shows the net life cycle impact (including credits for avoided burden) of an MA set for the R&R system, under a 1-time reuse scenario. These equations are used to calculate the comparative results shown in Figure 3.5.

$$EF_{MA,BAU} = E_{V,MA} + E_{EoL,Fe\ recycling} - E_{V,Fe\ scrap} \quad (3.1)$$

$$EF_{MA,R\&R} = E_{V,MA} + E_{EoL,R\&R} + E_{EoL,Fe\ recycling} - (E_{V,MA} - E_{EoL,Fe\ recycling} + E_{V,Fe\ scrap}) \quad (3.2)$$

where:

$EF_{MA,BAU}$ = environmental footprint from production and EoL treatment of one MA set in the BAU system

$EF_{MA,R\&R}$ = one life cycle equivalent impacts of an MA set modeled via avoided burden approach for the R&R system

$E_{V,MA}$ = environmental footprint from production of a virgin MA set

$E_{EoL,R\&R}$ = environmental footprint from the MA value recovery process (e.g., collection, disassembly, transportation and remanufacturing).

$E_{EoL,Fe\ recycling}$ = environmental footprint from shredding and transportation of iron scrap.

$E_{V,Fe\ scrap}$ = environmental credit from the iron scrap generated at EOL of MAs (i.e., the displaced acquisition impact of iron scrap).

3.2.3 Life Cycle Inventory

3.2.3.1 Description of Pilot MA Recovery & Reuse System

The MA R&R pilot study was conducted over 6 weeks (42 days) in a DC in Oklahoma (OK), USA. During this time 6,100 units of HDDs were disassembled, each containing a set of magnet assemblies with two RE magnets (MA_{upper} + MA_{lower}). The MAs were manually removed in a cleanroom (CR) environment and then packaged and sealed. The process required 2.5 full-time equivalent (FTE) operators which results in processing approximately 25 units (i.e. HDDs) per hour. The MAs were transported from OK to the HDD manufacturing facility in Thailand. It is worth noting that over 80% of global HDDs are manufactured in Thailand (AEC+ Business Advisory, 2019), so the current logistics assumption is valid for a variety of HDDs. The MAs were visually inspected, cleaned, and placed into the production line for newly manufactured enterprise HDDs, and eventually deployed back into DCs. Data on material use, electricity use, and transport logistics were collected throughout the pilot project. Figure 3 shows a detailed process flow diagram depicting the resource inputs and associated unit process (UP) data for the R&R system inventory.

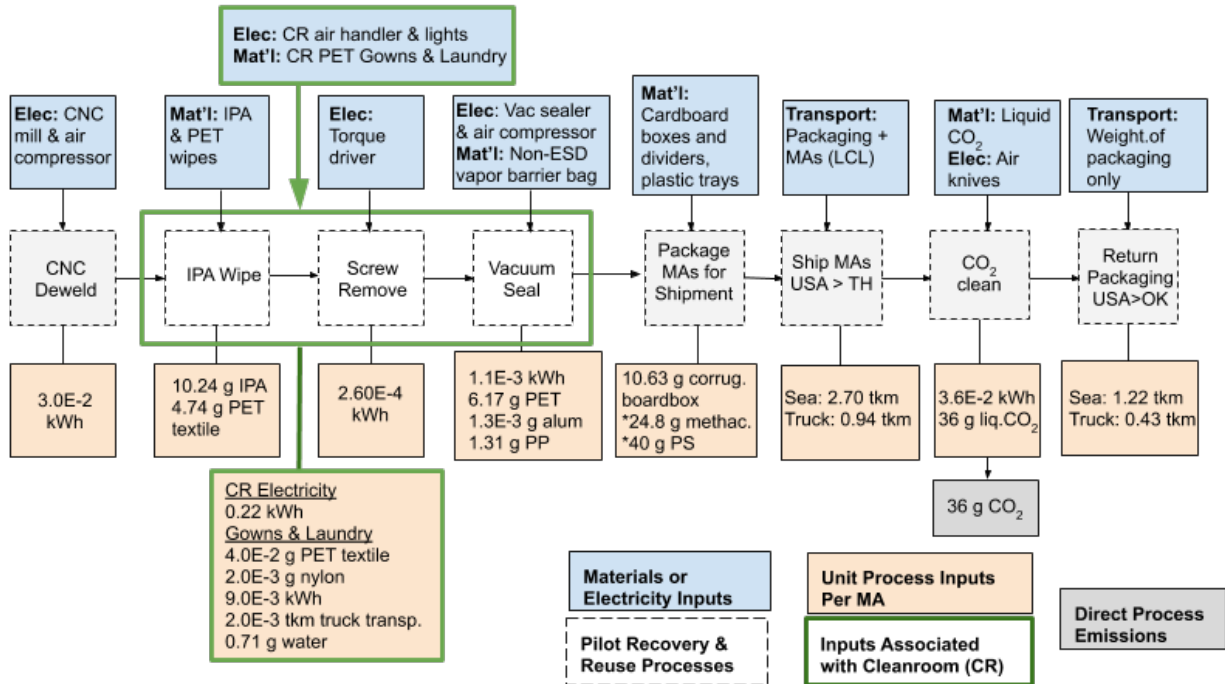


Figure 3.3. Material and energy inputs, direct emissions, and associated unit process data for the MA recovery process of the MA set from one HDD (Model Number ST16000NM003G). IPA= isopropyl alcohol, PET= polyethylene terephthalate, CNC= computer numerical controlled, methac. = methacrylate, PS= polystyrene, Non-ESD = non-electrostatic discharge, PP = polypropylene. Material and electricity inputs associated with operation of the cleanroom (CR) are highlighted separately in the green boxes.

3.2.3.2 Data Collection

3.2.3.2.1 Electricity Use

3.2.3.2.1.1 Tools

Power draw by each of the tools used in the recovery process was measured using a Kill-A-Watt® P4400 voltage meter (P3 International, 2020). Total electricity consumption was calculated using power use data combined with measurements of active and standby operating time for each piece of equipment. The MA recovery process was operated 8 hours per day, 5 days a week, over the span of the 6-week pilot. Electricity use for the CO₂ cleaning process at the HDD manufacturing facility was estimated by the HDD manufacturer.

The following equation shows how tool power consumption data was used to estimate electricity use per MA set (i.e. the functional unit). The specific data on electricity use per process is available in Figure 3 and the SI.

$$\text{Elec Use per MA (kWh)} = (TPU_{active} [kW] \times Time_{active}[sec] + TPU_{standby} [kW] \times Time_{standby}[sec]) / 3600 \frac{sec}{hr} \quad (3.3)$$

Where:

TPU_{active} or Tool Power Use_{active}: measured power draw by the tool while in active use mode (kW)

$Time_{active}$: measured time the tool was in active use per set of MAs (sec).

$TPU_{standby}$ or Tool Power Use_{standby}: measured power draw by the tool during downtime between active uses (kW).

$$Time_{standby}: \left(\frac{\text{Total time the tool was powered on during study (240 hrs} \times 3600 \frac{sec}{hr})}{\# \text{ of MA sets processed during study}} \right) - TPU_{active}$$

3.2.3.2.1.2 Cleanroom (CR)

The MAs must be removed in a CR environment to reduce the likelihood of particle contamination during the recovery process. The CR setup for this pilot's manual DC recovery system consisted of one modular ISO 7 (Class 10,000) and one modular ISO 6 (Class 1000) rated CRs, each occupying a 64 square foot area for a total of 128 sq. ft (1024 ft³). A modular cleanroom is one that is entirely self-contained: the air handler, lights, and structure can be assembled onsite and sized for the needs of the project.

Each of the CR air handlers was operated 24 hours a day, 7 days a week (24/7) for the duration of the 6-week pilot because the CR must be operated continuously to maintain its certificate of compliance for contamination control. CR lights were assumed to be operated during working hours: 8 hours a day for 30 days. The power draw of the CR air handler was measured using a voltmeter and had comparable efficiency (i.e., 0.67 kWh/ft³) to CRs of similar ratings (i.e., 0.63 kWh/ft³) (Mathew & Sartor, 2009). See the SI for a detailed description of CR specs and inventory data. The modular CRs were used only for the pilot recovery process, thus the associated power draw was attributed entirely to the MA recovery process and normalized to the functional unit.

The scenario analysis in Section 3.3.3 explores options for maximizing the process throughput relative to the CR footprint.

3.2.3.2.2 Material Use

Material inputs for the pilot were either directly measured or estimated based on material specification sheets provided by the HDD manufacturer. The major materials used in the recovery process were 1) the polyethylene terephthalate (PET) wipes and isopropyl alcohol (IPA) used to manually clean the drives during disassembly, 2) the vacuum seal bags used to package the trays containing the recovered MAs and maintain cleanliness during shipping, 3) cardboard packaging materials used to ship the MAs, and 4) liquid CO₂ to clean the recovered MAs before assembly into HDDs. The cardboard packaging for shipment is identical between R&R and BAU and was not included in the comparative assessment. However, the contribution analysis for the R&R system incorporated all material impacts (including packaging) from the R&R process to assess for any material use hotspots.

PET wipes and IPA are used to wipe down each HDD before and during disassembly in order to minimize the amount of particulate contamination associated with the disassembly processes. A unit process for PET fabric wipes was constructed using datasets provided by van der Velden et al. (2013) for the electricity, materials, and fuel required for PET fabric processing (e.g. spinning, knitting, washing, drying). If multiple values were available for a process, an average was used.

3.2.3.2.3 Transportation

The MAs are shipped via ocean and truck transport from the DC in Oklahoma to the HDD manufacturer in Thailand. Data was provided by the enterprise HDD end user on likely shipping routes for the MA. Mileage for ocean transport was estimated using an online tool for calculation of distances between seaports (sea-distances.org, 2020), and for truck transport using Google Maps (Google maps, n.d.). The weight of both the packaging and the MAs were included in the comparative assessment for transportation.

3.2.3.2.4 Direct Emissions

The only direct emissions that are unique to the MA recovery process were from the CO₂ cleaning process (assumed all CO₂ inputs were converted to CO₂ emissions) and the CR gown laundering process from Vozzolo et al. (2018).

Detailed assumptions, calculations, and associated unit process data for each of the R&R processes can be found in Tables S1, S3, and S8.

3.2.3.3 Business As Usual (BAU) Processes

The BAU process for HDD MA production consists of mining and refining of RE metals in China, the production of NdFeB (RE) magnets in Japan, and manufacturing of the MAs in Malaysia. The MAs are then shipped to the HDD assembly facility in Thailand and placed into the HDD along the manufacturer's assembly line. The HDDs are distributed to end users (e.g. a hyperscale or enterprise DC) where the HDD is used for 3-5 years. After the useful lifespan has ended, the HDD is shredded, and the HDD shred is sent to a regional metal recycler where the ferrous portions of the MA are recovered as well as other base metals and precious metals from the remainder of the HDD. During this process, RE metals are not recovered and become trace contaminants in the mixed iron scrap.

Because the MA manufacturer was not directly involved in this study, several assumptions were made about the MA manufacturing processes. MA manufacturing includes the process of manufacturing the steel bracket and adhering the NdFeB magnets to the assembly using epoxy. The materials consumption data were drawn from bill of materials provided by the HDD manufacturer, and MA manufacturing process was modeled by the unit process of "Metal working, average for chromium steel product manufacturing {GLO}| market for | APOS, U", similar to prior studies (Jin et al., 2020).

Table 3.2. Summary of distinctive processes and associated data collection for major materials and energy inputs for the R&R and BAU systems. The table follows the process order outlined in the resource flow diagram (Figure 3). Refer to Table S1 and S2 for documentation of all processes used in the study.

Processes that require material or energy inputs	Description of Process	Data Collected or Estimated	Data Source	Ecoinvent Unit Process	Amount (Unit)
Recovery & Reuse Process					
CNC Deweld	HDD is placed inside a CNC mill to deweld (i.e. break the HDD perimeter seal) between the cover plate and rest of HDD.	Power draw (W) in active and standby use modes by CNC mill and air compressor, Measurement of active time to deweld (sec), and standby time (calculated)	Direct measurement of pilot process using voltmeter and stopwatch	Electricity, medium voltage {SPP} market for APOS, U	2.98E-02 (kWh)
IPA Wipe	Manual process to wipe the surfaces of the HDD with a specialty made PET wipe that is wetted with isopropyl alcohol (IPA). This cleaning process reduces particulate matter contamination during subsequent recovery processes.	Amount and specifications of PET wipes and gallons of IPA used during the study	Direct measurement of IPA use, estimated use of PET wipes over course of pilot	Isopropanol {RoW} market for isopropanol APOS, U	1.02E-02 (kg)
				PET textile production (custom UP using data from van der Velden et al (2013).	4.13E-03 (kg)
Cleanroom Air Handler & Lights	The MAs must be removed in a CR environment to reduce particle contamination. The air handler for the CR was in operation 24/7 during the pilot study. Cleanroom lights were powered on during working hours. The prep room was ISO 7 (Class 10,000) certified and the disassembly room was ISO 6 (Class 1,000) certified.	ISO 7 (Class 10,000) & ISO 6 (Class 1000) CR. Total power use was measured (W) and allocated to each room based on the number of air handlers and lights required to power each room. The number of air handlers required to maintain a cleanliness standard is related to the size of the room and the number of air exchanges required.	Specs of cleanroom provided by datacenter; Direct measurement of power draw using voltmeter	Electricity, medium voltage {SPP} market for APOS, U	2.18E-01 (kWh)

Table 3.2 continued

Transport from DC to HDD Manufacturer	Ocean and truck transport from OK, USA > Los Angeles, CA > Singapore > Thailand	Calculated t*km using ocean and truck transport distances and total weight of pallet + packaging + MAs t*km = weight of shipment (tons) * distance shipped (km)	Google Logistics team provided locations, distances estimated using GoogleMaps, measured weight of pallet	Transport, transoceanic freight ship/OCE U	2.7E+00 (t*km)
				Transport, freight, lorry, unspecified {RoW} market for transport, freight, lorry, unspecified APOS, U	9.39E-01 (t*km)
CO ₂ Clean	Process of cleaning the recovered MAs before placement into a new HDD. This technology uses 'air knives,' or pressurized CO ₂ , to clean the MAs in their trays.	Data was provided for electricity consumption and CO ₂ consumption on a per MA basis. CO ₂ emissions from the process were assumed to equal CO ₂ inputs	Data on electricity and CO ₂ use from HDD manufacturer	Carbon dioxide, liquid {RoW} market for APOS, U	3.60E-02 (kg)
				Electricity, medium voltage {TH} market for APOS, U	3.60E-02 (kWh)
Return Transport from Manufacturer to DC	Because the trays used to ship the MA are specially made, empty trays must be returned to the datacenter for future packaging.	The weight of the return packaging was used to determine transport impacts. This includes all packaging but excludes the weight of the MAs	Calculated by using the manufacturer's packaging configuration and subtracting the weight of MAs	Transport, transoceanic freight ship/OCE U	1.22E+00 (t*km)
				Transport, freight, lorry, unspecified {RoW} market for transport, freight, lorry, unspecified APOS, U	4.25E-01 (t*km)

Table 3.2 continued

BAU Processes					
RE Metals	Mining and refining processes required to process basnasite/monazite ore into individual RE oxides and then RE metals for high-tech applications	HDD Bill of Materials (BoM) used to determine Nd and Pr amounts in final product, assuming yield loss factor of 1.26 to derive REO weights (only used for transport)	Used Arshi et al (2018) impact data for 1 kg of Nd and Pr metals and scaled to RE metals in Evans drive	Transport, freight, lorry, unspecified {RoW} market for transport, freight, lorry, unspecified APOS, U	4.22E-03 (t*km)
				Transport, aircraft, freight, intercontinental/RER U	3.71E-02 (t*km)
				Impacts from producing 1 kg of Nd metal and 1kg of Pr metal are directly derived from Arshi et al (2018)	Included in magnet
NdFeB magnets	The process to combine RE metals with iron, boron, nickel coating and adhesives to create the magnet. This process also includes grinding and slicing of the magnet to get appropriate shape for HDD	Used HDD BoM to adjust unit process data from Jin et al (2020). Used magnet average yield loss factor of 1.7	Jin et al, 2018, 2020 (updated)	Modified from Jin et al, see SI Table S9 for full unit process inputs.	

Table 3.2 continued

Magnet Assembly	The process to create the steel assembly and adhere the RE magnets	Used HDD BoM for weight of steel and epoxy	Ecoinvent stainless steel process	Epoxy resin, liquid {RoW} market for epoxy resin, liquid APOS, U	3.00E-06 (kg)
				Steel, chromium steel 18/8 {GLO} market for APOS, U	7.26E-02 (kg)
				Solvent, organic {GLO} market for Alloc Def, U	1.17E-04 (kg)
				Metal working, average for chromium steel product manufacturing {RoW} processing APOS, U	1.04E-01 (kg)
				Transport, freight, lorry, unspecified {RoW} market for transport, freight, lorry, unspecified APOS, U	1.42E-01 (t*km)
				Transport, freight, lorry, unspecified {RoW} market for transport, freight, lorry, unspecified APOS, U	1.17E-01 (t*km)

3.2.4 Unit Process Data & Impact Assessment Methods

Ecoinvent v.3 database was primarily used to model the unit processes (UPs) associated with the BAU and R&R systems. Several of the most important UPs are described in Table 3.2 and the remaining UP data are available in the supplemental information. Environmental impacts from Nd and Pr production were directly quoted from Arshi et al (2018), a study which also employed the Ecoinvent database v.3.

Environmental impacts were characterized using the US EPA TRACI v.2.1 impact assessment methodology framework (Tool for Reduction and Assessment of Chemicals and Other Environmental Impacts) (Bare, 2011). TRACI was chosen because of its compatibility with prior LCAs on RE metals and magnets production (Arshi et al., 2018; Jin et al., 2018; Jin et al., 2020).

3.2.5 Life Cycle Interpretation

3.2.5.1 *Renewable Energy Purchasing*

Electricity impacts associated with the datacenter MA recovery process (most notably, CR electricity use) is the largest contributor to GHG impacts from the R&R process, thus a scenario of using renewable energy purchasing was explored to see its impact on GHG emissions. The Oklahoma DC matches 100% of their annual electricity consumption with renewable energy purchases, which takes the form of a power purchase agreement (PPA) (Google, 2013). To understand the effect of this renewable energy matching on the LCA results, each of the electricity-using processes at the Oklahoma DC were modeled with the typical grid mix for the Southwest Power Pool (i.e. coal, gas and wind) as well as with the energy mix provided by the PPA. Under this PPA, in 2019, electricity consumption at the Oklahoma DC was matched 96% by carbon-free energy (CFE) on an hourly basis, with the remaining 4% supplied by fossil fuels (i.e. carbon-based energy) (Google, 2020). This ratio of CFE to CBE was represented by the following unit processes: “Electricity, high voltage {SPP}| electricity production, wind, 1-3MW turbine, onshore | APOS, U”) and “Electricity, medium voltage {SPP}| market for | APOS, U”. Infrastructure processes were included for all electricity generation types, as is recommended when comparing traditional and renewable electricity generation (Hauschild, 2018). Only processes occurring within the OK DC were modeled with the carbon-free energy mix.

3.2.5.2 Automated MA Recovery

An important step towards optimizing and scaling the MA circular recovery process is a transition from manual disassembly to an automated process. To measure the potential effects of automation on environmental impacts, scenarios were modelled using assumptions about a semi-automatic and automatic process for MA recovery and compared to data from the baseline (i.e. manual) process.

The “semi-automatic” process requires an operator to place the drive into the CNC machine to deweld the HDD cover seal. The automated portion of the “semi- automated” process includes the use of a semi-automatic harvester instead of manual processes for screw removal, MA retrieval, and placement into MA trays. The semi-automated process has a buffer of 1 HDD and requires 1 FTE operator to feed the machine every HDD cycle (process requires 2 FTEs total). Semi-automation requires an additional 272 sq. ft of CR space and an addition of a 5000 W harvester and yields an estimated recovery of 10 units per hour (UPH).

The “full automation” tool partially replaces manual steps required for the CNC deweld and fully automates the screw removal, MA harvest, and placement into MA trays. The “full automation” machine also removes and separates many subassemblies such as the read/write head stack assembly (HSA), media discs, desiccant packets/filters, aluminum cast enclosure. The separated material/part is then ready for general recycling of raw material. This requires an automation line which draws an estimated 10,000 W of power and requires an additional 368 sq ft of CR space. The automation line can process an estimated 60 UPH with an input buffer of 100 HDDs and requires 1 FTE operator. A summary of comparative CR specs is available in Table S5.

3.2.5.2.1 Electricity & Material Use for Automated MA Recovery Scenario

Due to the size of the automation tools, the semi and fully automated recovery process occupies a much larger CR footprint than the manual process. The estimated CR footprint for a fully automated recovery setup was 192 square feet of ISO 7 (i.e., 3 times larger than the manual process for HDD preparation and storage) and 304 square feet of ISO 6 (i.e., about 2.5 times larger than manual process for disassembly and packaging). CR power draw is assumed to scale linearly with

the size of the cleanroom; thus, measured power draw from the manual recovery system was used to quantify the estimated power needs for the larger CR footprint.

Material inputs are unlikely to be largely affected by automation because packaging and shipping configurations are unchanged. There is a potential that fewer operators would be needed, reducing demand for CR gowns and laundry. There is also a potential that less PET wipes and IPA will be needed to clean the drive before disassembly, but this is not well understood at this time. As such, material inputs were assumed to remain constant per MA as a conservative assumption.

3.2.6 Data Limitations & Uncertainty Analysis

3.2.6.1 Scaling Assumptions

An effort was made, where possible, to estimate how the R&R process would scale. For example, transport logistics and packaging were assumed for a scaled process because of extensive internal documentation and similarity to existing BAU processes. Where these scaling extrapolations could not be easily made, data from the pilot-scale were used to be conservative. For example, the pilot process consumed 0.5 PET wipes per functional unit. The consumption of PET wipes may be improved for a permanent process, but because the amount of this improvement is not well understood, pilot estimates were used to be conservative. Another example is how scaling could impact total process throughput. The scenario analysis described in Section 3.3.3 was conducted to explore improvements to process throughput using assumptions such as 24/7 manual disassembly or various levels of automation. One of the biggest impacts of process throughput improvement would be on cleanroom utilization per functional unit.

3.2.6.2 Monte Carlo Uncertainty Analysis

The material losses encountered during the RE magnet manufacturing process have a substantial impact on the total environmental impacts of the BAU process (see Section 3.1.1). The machining process which is used to slice and grind the magnet block into the characteristic kidney shape required for HDDs, as well as out of spec magnets, can lead to losses at the manufacturers and magnet fabricators. Total yield losses have been reported with a great variance in the literature (ranging from 6-73%) for magnet applications, in general, and the specific losses for HDD magnets

have not been available. These yield losses increase the material and energy inputs required for RE magnet production and waste for the following magnet inputs: Nd metal, Pr metal, Fe (iron pellet) and Fe sludge, boron carbide, and electricity. Jin et al. (2020) assumed an average yield loss of ~40% after communication with a magnet manufacturer. This study also utilizes 40% as the baseline loss but conducted Monte Carlo Uncertainty Analysis (MCUA) simulation to address the large uncertainty for this estimate.

Monte Carlo analysis is used to characterize uncertainty by running repeated analyses using random numbers generated from a range of input values which are represented by a probability distribution (Robert & Casella, 2004). A triangular distribution was chosen as the appropriate MCUA probability distribution function for magnet material loss because we have a minimum (6%), maximum (73%), and mode (most likely value based on professional judgement, 40%) (Ross & Cheah, 2019). Monte Carlo simulation was conducted on the yield loss values using 1,000 model runs. Results of this analysis were converted to a multiplier to ascertain the additional amount of material or electricity inputs required to manufacture two NdFeB (RE) magnets for the Evans HDD. This was multiplied by the associated global warming impacts for each unit process input and visualized using boxplots. The individual process inputs required under various yield scenarios and their effect on global warming impacts are summarized in Table S13.

3.3 Results & Discussion

3.3.1 Life Cycle Impact Assessment (LCIA)

3.3.1.1 Comparative Analysis: MA Recovery & Reuse vs BAU

Direct reuse of MAs in new HDDs is estimated to result in an 86% reduction in greenhouse gas (GHG) emissions per MA when compared to BAU (Fig. 3.4). Specifically, global warming impact from the MA recovery and reuse process results in 0.60 kg of CO₂-eq and that from virgin MA production results in 4.30 kg of CO₂-eq. Figure 3.4 also depicts the impacts of shipping the whole HDD to Malaysia for disassembly and reuse of the MA. This scenario used assumptions from Jin et al. (2020) which were updated with specs from the newer HDD model and disassembly process data from the U.S. DC recovery pilot. Although the impacts from this scenario show similar

reductions in GHGs (3.61 vs 3.70 kg CO₂-eq), there are notable disadvantages associated with this option, namely the transboundary movement of e-waste and data security concerns.

The large disparity in GHG emissions between the BAU and R&R system is mainly due to foregoing the environmental impacts associated with virgin production of RE magnets (Fig 3.5). Specifically, mining and refining of RE-containing ore into Neodymium (Nd) and Praseodymium (Pr) metals accounts for 67% of the GHG emissions attributed to the BAU scenario and from 33-87% of impacts across the remaining impact categories of TRACI, such as acidification and eutrophication (Fig 3.6).

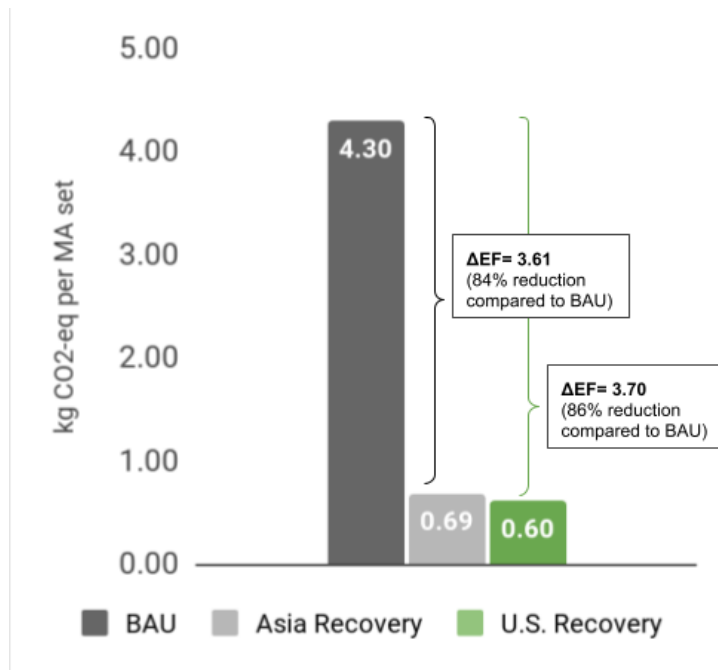


Figure 3.4. Comparison of GHG impacts in kg CO₂-eq for one life cycle of an MA set, Business As Usual (dark gray; modeled with Eq. 1), Asia MA Recovery (light gray; modeled with Eq. 4, using sea transportation of an entire HDD to Asia and disassembly for MAs), and U.S. MA Recovery (light green; modeled with Eq. 2, using the US domestic disassembly of an HDD and shipping only MAs to Asia). The net GHG benefits (or the reduced GHG impacts via R&R) are represented by ΔEF.

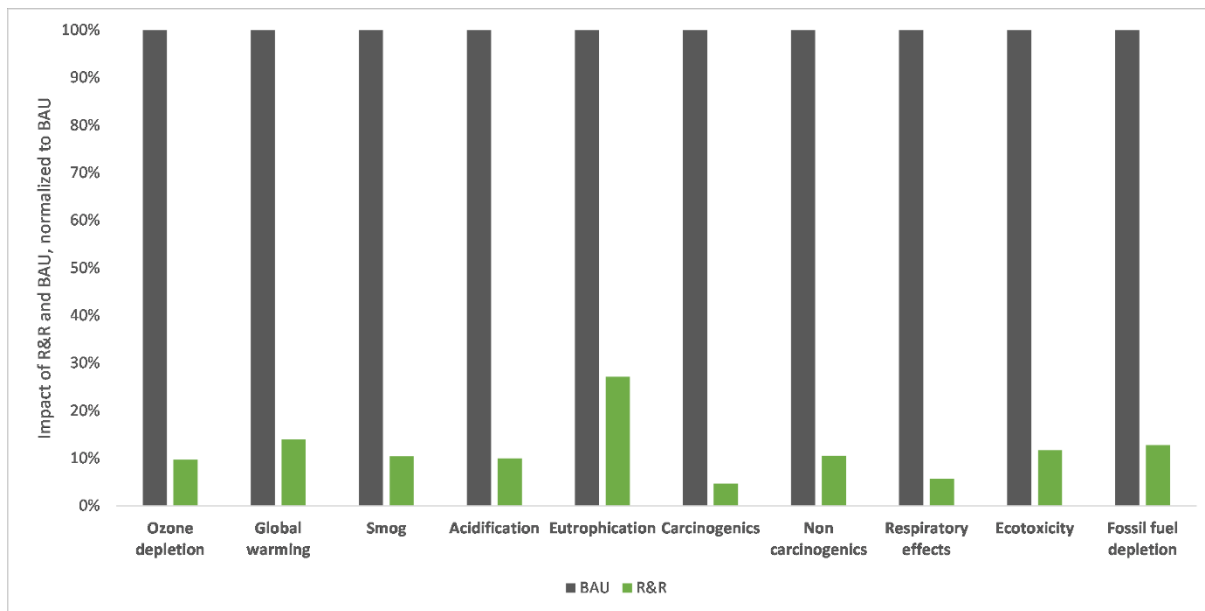


Figure 3.5. The difference in environmental impacts between BAU and R&R, with BAU considered the base case.

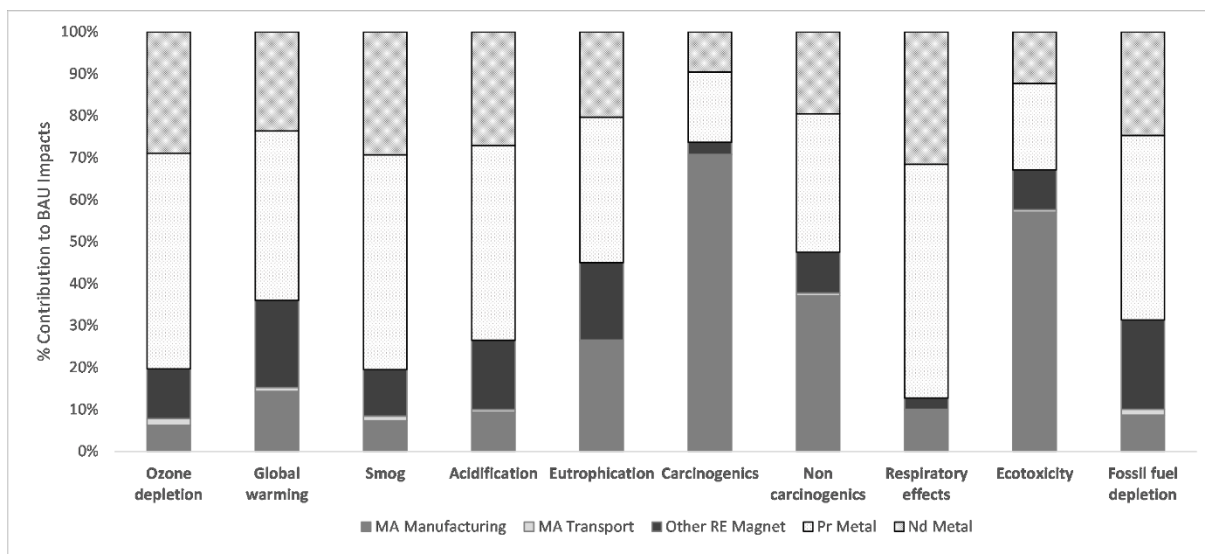


Figure 3.6. Contribution of upstream RE magnet processing impacts and MA manufacturing and transport to the BAU scenario. Nd and Pr Metals, shown here with patterned bars, includes the mining, refining, separation, and transport of RE metals to the magnet manufacturer. This includes yield losses of RE metals inputs during magnet processing. “Other RE Magnet” includes the iron, nickel coating, electricity, and other process chemicals required to manufacture a sintered NdFeB magnet (including yield losses of input materials). MA manufacturing includes raw materials and forming of the steel bracket and the process and materials required to adhere the NdFeB magnet to the bracket. MA transport includes the transport of the MA to the HDD manufacturer and return transport of the MA trays. EoL is not depicted due to its minor contribution to BAU impacts (0.25%).

3.3.1.2 Contribution Analysis: MA Recovery & Reuse (R&R)

The purpose of an in-depth contribution analysis is to optimize the newly created circular process to minimize environmental impact and/or acknowledge tradeoffs required to balance economic and environmental sustainability. Figure 7 details the contribution by each unit operation in the R&R system and indicates that transportation and cleanroom energy were environmental hotspots in this system. Transport of the MAs and their associated packaging from the US to Thailand, and the return trip of just packaging from Thailand back to the US DC was inevitable due to the current supply chain structure that focuses on HDD assembly in Thailand and the specialized nature of the packaging trays (i.e. trays are used to stage the MAs for placement into the HDD assembly line). It is worth noting that this project already reduced the transportation impact by setting up a disassembly line in the US to enable transporting only MAs overseas (see Fig. 3.4). Electricity use for the recovery process is dominated by the CR air handler in the data center (Fig 3.7). As mentioned above, the CR air handler must run 24/7 to maintain its cleanliness certification, although the recovery of drives only occurs for one 8-hr shift per day. Therefore, improving CR utilization by adding more shifts, increasing throughput by process automation, or extensive adoption of renewable energy could be explored to reduce the environmental impact per MA of the R&R system.

The use of cleaning wipes in the disassembly process is the dominant material impact (50% of all material impacts are due to the PET wipes), highlighting the importance of optimizing cleaning wipes consumption or exploring alternative cleaning materials. While global warming impacts are split nearly evenly among the transport, materials and electricity, eutrophication, carcinogenic, non-carcinogenic, respiratory, and ecotoxicity impacts are dominated by electricity impacts from the OK datacenter which utilizes the SPP Electricity Grid Mix (as implemented in Ecoinvent 3.0), comprised of 49% coal, 19% natural gas, 19% wind, 7% nuclear, and ~6% other. Transport is the predominant impact driver with regards to ozone depletion, smog, and acidification impact categories from the use of diesel fuel and heavy fuel oil for truck and ship transport, respectively.

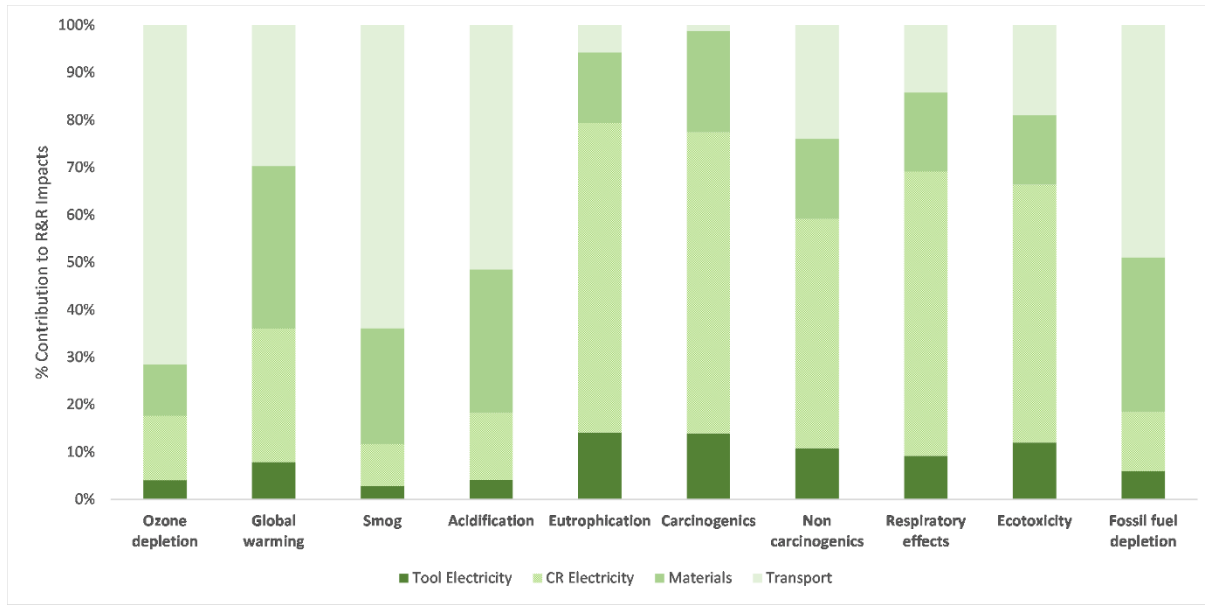


Figure 3.7. Summarized unit operation contribution to each of the TRACI impact categories for the R&R system. Tool Electricity includes electricity for dewelding, screw removal, and vacuum sealing during the disassembly and recovery process. CR Electricity includes the CR air handler and lights. Materials includes the PET wipes, isopropyl alcohol, vacuum seal bags, CR gowns, MA packaging, and CO2 required to clean the MAs. Transport includes the transport from the datacenter to the HDD manufacturer and return transport of the MA trays to the datacenter.

3.3.2 Data Center Renewable Energy Purchasing

The LCIA indicates a 97% reduction in electricity-related global warming impacts attributable to the DC (Figure 3.8a). This corresponds to a 30% reduction in the R&R system global warming impacts when compared to R&R modeled with Grid Electricity (Figure 3.8b).

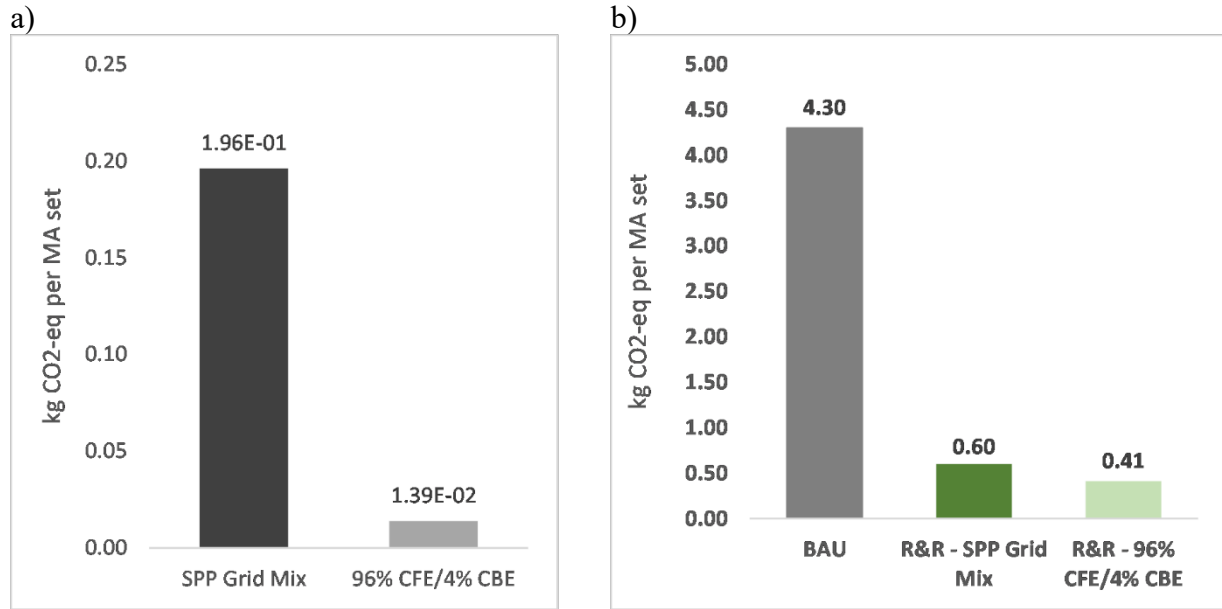


Figure 3.8. Figure (a) depicts the global warming impacts (in kg CO₂-eq) due to electricity supplied from SPP Grid Mix vs the DC grid mix which is comprised of 96% CFE and 4% CBE. Figure (b) displays the overall system impacts of BAU, R&R with SPP grid mix, and R&R with 96/4 mix.

3.3.3 Scenario Analysis – Automated MA Recovery

Global warming impact for each of the DC disassembly scenarios - manual, semi-automated, and fully automated - are depicted in Figure 3.9. Automation requires an increase in electricity consumption due to an expanded CR footprint required to accommodate automation tools but leads to a higher throughput disassembly process. For example, doubling the CR space for full automation could result in an estimated 2.4 times more MAs processed per hour (i.e. ~60 units per hour [UPH] vs 25 UPH). Changes in material impacts are expected to be negligible and transport impacts will remain the same for all three scenarios.

The largest impact driver for automation is the increased electricity required by the expansion of the CR footprint. The CR must operate 24/7, even though MAs are only recovered during one 8 hr-shift, 5 days a week (8/5). Automation maximizes the potential throughput that could be achieved for the recovery process but is limited by the current assumption of operating only one shift per day. Fig 3.9 depicts the results of a theoretical exercise assuming a fully optimized automated process (operating 24/7). If drive disassembly could be operated continuously, the efficiency gains would nearly offset increased CR electricity use. Continuous operation over the

study period (42 days) would lead to an estimated recovery of 60,480 MAs using the full automation process.

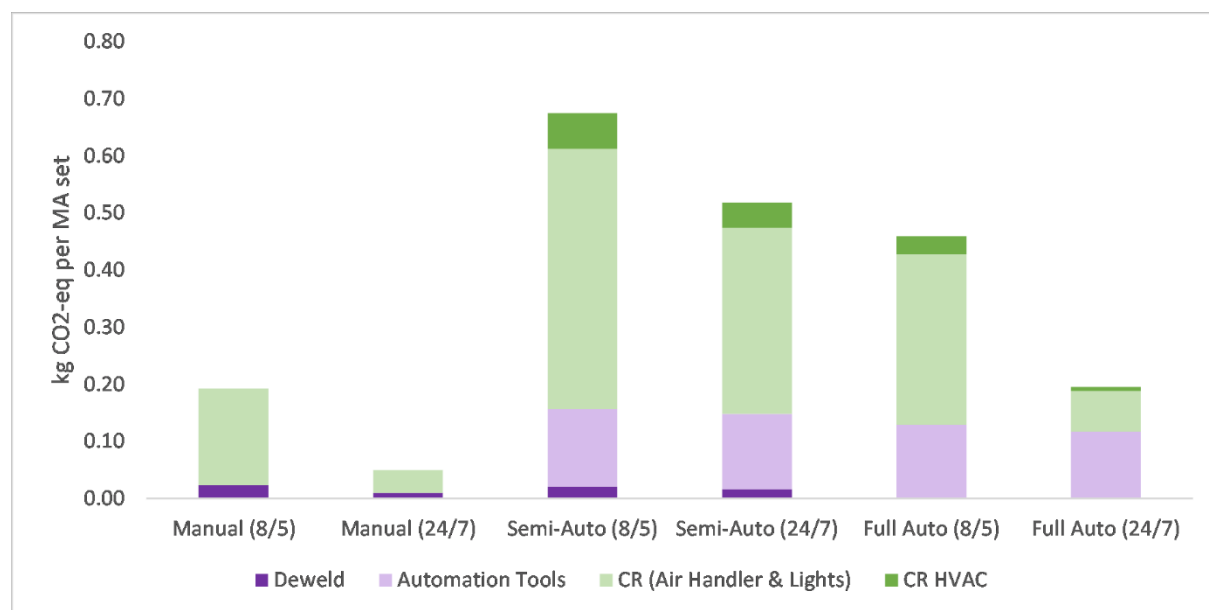


Figure 3.9. Global warming demand of DC recovery steps in kg CO₂-eq per set of MAs under manual, semi-automated, and fully automated operating scenarios under two assumptions: 1) an underutilized CR operating an 8-hr shift, 5 days a week (8/5), and (2) a fully utilized CR operating 24 hours a day, 7 days a week (24/7). This *Processes such as screw removal and vacuum seal are not depicted due to minor impact contribution. For the automation scenarios the deweld process is included as part of the category “automation tools”, instead of being considered as a separate process step.

3.3.4 Uncertainty Analysis

Current baseline assumptions about magnet yield loss result in a total of 3.41 kg CO₂-eq impacts for Nd, Pr, Fe, Fe sludge, boron carbide, and electricity, whereas the mean of the MC analysis is 3.57 (3.51-3.62 95% CI, min=2.19, max=7.08) (Fig 3.10). The implications of this analysis suggest that the CO₂ impacts attributed to the BAU system, which are highly sensitive to Nd and Pr metal inputs, may be mischaracterized in the current baseline analysis due to uncertainty in the published values for yield loss. Given the scant data available to construct the probability distribution, future work should attempt to ascertain these values directly from measuring the material losses by an HDD NdFeB magnet manufacturer because of the distinctive shape required for HDD magnets.

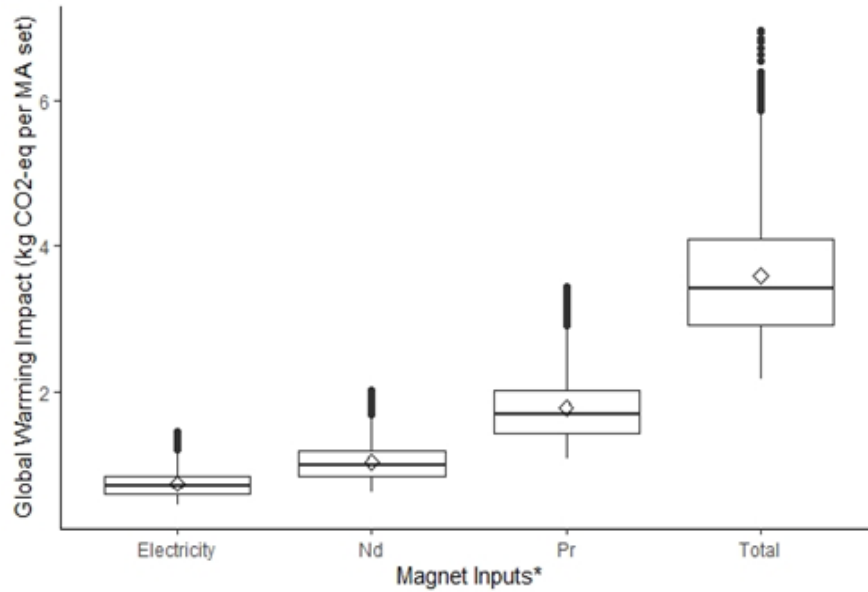


Figure 3.10. Boxplots representing the distribution of global warming impacts associated with each of the RE magnet inputs affected by yield loss. In this plot the diamond is the mean, the bar is the median, the lower and upper hinges represent the 25th-75th percentile, and the whiskers extend to the minimum and maximum. *Fe, Fe sludge, and Boron carbide are not depicted separately in the graph due to their relatively small impact contribution but are included in the Total plot.

3.4 Conclusions

This study examined the environmental impacts of a circular recovery process piloted by two major HDD stakeholders for the reuse of a high value subassembly. The magnet assembly was recovered from an enterprise helium HDD which is expected to serve as flagship technology in DCs for the next decade. This required a close collaboration between an enterprise HDD end user and HDD manufacturer to create a certified manufacturing process within a datacenter (DC) and coordinate movement of materials. LCA is used to substantiate expected environmental benefits, and as such, validate the next step of expanding the piloted recovery process into a permanent large-scale circular model. LCA results indicate that the circular processes for magnet assembly (MA) recovery initiated by this pilot will result in significant environmental benefits when compared to BAU.

Based on this study, we recommend establishing colocated disassembly facilities with product end users (e.g., DCs) to increase the environmental benefits of value recovery. For the case of

HDDs, additional benefits of collocation include enhanced data security, avoiding transboundary shipment of wastes, and better process and quality control. In addition, we recommend adopting renewable energy and implementing efficient processes in value recovery to maximize the environmental benefits. For MA recovery, cleanroom electricity was a significant impact driver, which can be mitigated through use/purchase of renewable energy and automating the disassembly process to enable 24/7 utilization of the cleanrooms, which may be difficult to achieve by a manual process.

A limitation to reuse of MAs is the functional requirement that an MA be reused within the same HDD platform or model family. Because HDD technology progresses rapidly, and MA design similarly must support progression of those platforms, opportunities for reuse of MAs are currently limited. However, MAs should be a priority for 'design-for reuse': in addition to the performance stability and reliability of these assemblies, the yield on recovery of the MA is expected to be nearly 100% if recovered through a qualified process. Design requirements of the MA must be expanded in the future to identify opportunities for commonality between platforms and extending potential MA reuse. Fortunately, an emerging focus on environmental impacts of REs and their supply criticality can be used to drive design goals.

There are approximately 22 million HDDs available for some level of component or material recovery (i.e. cannot be reused) in North American DCs each year (Handwerker et al., 2017). If this MA recovery model were expanded to all 22 million HDDs and if MAs could be successfully recovered and reused interchangeably, approximately 660 mTons of NdFeB magnets would be recovered, which could meet 20% of the average global HDD NdFeB magnet demand per year (Schulze & Buchert, 2016). This would also result in 78,540 Metric Tons of CO₂-eq. global warming impact reduction per year. However, this would require industry coordination and a shift in how MAs are designed; thus, other promising recovery strategies for magnet-to-magnet and REE extraction technologies must be pursued in parallel.

Other high-value components, such as the printed circuit board assembly (PCBA), should also be explored for recovery in DCs, given that they contain some of the most environmentally impactful components (i.e. integrated circuits) and are economically valuable. An automated disassembly

process could be designed to co-recover MAs, PCBAs, and other components of value, and if coupled with a thoughtful design-for-reuse strategy for key components, would enable recovery and reuse of multiple HDD components in the future.

In light of the COVID-19 pandemic and its associated disruption to worldwide supply chains (Linton & Vakil, 2020;), companies are exploring options for increasing the resiliency of their supply chain (Howells, 2020;), which is crucial with regard to critical materials (U.S. DOE, 2011; Vinoski, 2020). The circular business model assessed by this study describes a pathway for domestic sourcing of high-grade rare earth metals, which could help offset supply chain risk associated with Chinese REEs and associated NdFeB magnets. Going forward, supply chain resiliency may be a key factor in the case for circularity; however, as circular business models are increasingly being implemented, there is an ongoing need to validate assumptions about environmental sustainability using mature analysis methods such as LCA.

3.5 References

- AEC+ Business Advisory. (21 February 2019). Thailand's HDD Industry Outlook 2019 https://kasikornbank.com/international-business/en/Thailand/IndustryBusiness/Pages/201902_Thailand_HDD_outlook2019.aspx
- Ahmadi, L., Yip, A., Fowler, M., Young, S. B., & Fraser, R. A. (2014). Environmental feasibility of re-use of electric vehicle batteries. *Sustainable Energy Technologies and Assessments*, 6, 64-74.
- Arshi, P. S., Vahidi, E., & Zhao, F. (2018). Behind the scenes of clean energy: the environmental footprint of rare earth products. *ACS Sustainable Chemistry & Engineering*, 6(3), 3311-3320. DOI: <https://doi.org/10.1021/acssuschemeng.7b03484>
- Bailey, G., Joyce, P. J., Schrijvers, D., Schulze, R., Sylvestre, A. M., Sprecher, B., ... & Van Acker, K. (2020). Review and new life cycle assessment for rare earth production from bastnäsite, ion adsorption clays and lateritic monazite. *Resources, Conservation and Recycling*, 155, 104675.
- Baldé, C. P., Forti, V., Gray, V., Kuehr, R., & Stegmann, P. (2017). The Global E-waste Monitor—2017, United Nations University (UNU), International Telecommunication Union (ITU) & International Solid Waste Association (ISWA), Bonn/Geneva/Vienna. *ISBN Electronic Version*, 978-92. Available at: https://collections.unu.edu/eserv/UNU:6341/Global-E-waste_Monitor_2017__electronic_single_pages_.pdf

Barba-Gutiérrez, Y., Adenso-Díaz, B., Hopp, M., 2008. An analysis of some environmental consequences of European electrical and electronic waste regulation. *Resour. Conserv. Recycl.* 52, 481–495. DOI: <https://doi.org/10.1016/j.resconrec.2007.06.002>

Beaulieu, L. (2015). *Circular economy: A critical literature review of concepts*. Centre interuniversitaire de recherche sur le cycle de vie des produits, procédés et services. Available at http://www.ciraig.org/pdf/CIRAIG_CircularEconomyPressRelease_Nov2015.pdf

Blengini, G. A., Mathieux, F., Mancini, L., Nyberg, M., & Viegas, H. M. (2019). Recovery of critical and other raw materials from mining waste and landfills. *Publications Office of the European Union, Luxembourg*.

Buechler, D. T., Zyaykina, N. N., Spencer, C. A., Lawson, E., Ploss, N. M., & Hua, I. (2020). Comprehensive elemental analysis of consumer electronic devices: Rare earth, precious, and critical elements. *Waste Management*, 103, 67-75. DOI: <https://doi.org/10.1016/j.wasman.2019.12.014>

Bobba, S., Mathieux, F., Ardente, F., Blengini, G. A., Cusenza, M. A., Podias, A., & Pfrang, A. (2018). Life Cycle Assessment of repurposed electric vehicle batteries: an adapted method based on modelling energy flows. *Journal of Energy Storage*, 19, 213-225.

CEDaCI, 2020. Circular Economy for the Data Centre Industry. Available at <https://www.cedaci.org/>

Elia, V., Gnoni, M. G., & Tornese, F. (2017). Measuring circular economy strategies through index methods: A critical analysis. *Journal of Cleaner Production*, 142, 2741-2751. DOI: <https://doi.org/10.1016/j.jclepro.2016.10.196>

Ellen Macarthur Foundation. 2018. *Circular Consumer Electronics: An Initial Exploration* Available at: <https://www.ellenmacarthurfoundation.org/assets/downloads/Circular-Consumer-Electronics-FV.pdf>

European Commission. (2019). CORRESPONDENTS' GUIDELINES No 1: Shipments of Waste Electrical and Electronic Equipment (WEEE) and of used Electrical and Electronic Equipment (EEE) suspected to be WEEE. Available at https://ec.europa.eu/environment/waste/shipments/pdf/correspondence_guidelines_1.pdf base1 weee

European Commission. (2015). Communication from the Commission to the European Parliament, the Council, the European Economic and Social Committee and the Committee of the Regions. Available at: https://www.ab.gov.tr/files/000files/2015/11/strateji_belgesi_turkey_related_parts.pdf

European Commission. (2018). Report on critical raw materials and the circular economy. *Comm. Staff Work. Doc.* Available at: <https://op.europa.eu/en/publication-detail/-/publication/d1be1b43-e18f-11e8-b690-01aa75ed71a1/language-en/format-PDF>

Frost, K., Jin, H., Olson, W., Schaffer, M., Spencer, G., & Handwerker, C. (2020). The use of decision support tools to accelerate the development of circular economic business models for hard disk drives and rare-earth magnets. *MRS Energy & Sustainability*, 7. DOI: <https://doi.org/10.1557/mre.2020.21>

Gibbs, B. C. 2019. Critical chemical commodities. *Nature Chemistry*, 11, 99-101. DOI: <https://doi.org/10.1038/s41557-018-0205-6>

Google (n.d.). Discover our data center locations. Retrieved September 5, 2020 from <https://www.google.com/about/datacenters/locations/>

Google. (2013, September). *Google's Green PPAs: What, How and Why*. Available at <https://static.googleusercontent.com/media/www.google.com/en/us/green/pdfs/renewable-energy.pdf>

Google. (2020, September). *24/7 by 2030: Realizing a Carbon-free Future*. Available at <https://www.gstatic.com/gumdrop/sustainability/247-carbon-free-energy.pdf>

Google maps (n.d.). [Google Maps directions]. Retrieved December 4, 2019 from [google.com/maps](https://www.google.com/maps)

Handwerker C.A. and Olson W. (2019). *Value Recovery from Used Electronics Project. iNEMI Final Project Report Phase 2*, August 2019. Available at: <https://www.inemi.org/value-recovery-2-final-report>

Haupt, M., & Hellweg, S. (2019). Measuring the environmental sustainability of a circular economy. *Environmental and Sustainability Indicators*, 1, 100005. DOI: <https://doi.org/10.1016/j.indic.2019.100005>

Handwerker C.A., Olson W., and Rifer W. (February, 2017). Value Recovery from Used Electronics. iNEMI Final Project Report – Phase 1. Available at: https://community.inemi.org/value_recovery.

International Electronics Manufacturing Initiative (2020). Value recovery from used electronics, Phase 2. Available at: https://community.inemi.org/value_recovery_2 (accessed September 3, 2020).

Işildar, A., Rene, E. R., van Hullebusch, E. D., & Lens, P. N. (2018). Electronic waste as a secondary source of critical metals: Management and recovery technologies. *Resources, Conservation and Recycling*, 135, 296-312.

Jin, H., Afiuny, P., Dove, S., Furlan, G., Zakotnik, M., Yih, Y., Sutherland, J.W., 2018. Life cycle assessment of neodymium-iron-boron magnet-to-magnet recycling for electric vehicle motors. *Environ. Sci. Technol* 52. DOI: <https://doi.org/10.1021/acs.est.7b05442>.

Jin H., Frost K., Sousa I., Ghaderi H., Bevan A., Zakotnik M., and Handwerker C. (2020). Life cycle assessment of emerging technologies on value recovery from hard disk drives. *Resour. Conserv. Recycl.* 157, 104781 DOI: <https://doi.org/10.1016/j.resconrec.2020.104781>.

King, Alexander. *When Agendas Align: Critical Materials and Green Electronics*. United States. <https://doi.org/10.1109/EGG.2016.7829825>

Lee, J.C. and Wen, Z. (2016). Rare earths from mines to metals: comparing environmental impacts from China's main production pathways. *J. Ind. Ecol.* DOI: <https://doi.org/10.1111/jiec.12491>

Linton, T. and Vakil, B. (2020, March 5). *Coronavirus Is Proving We Need More Resilient Supply Chains*. Harvard Business Review. Available at <https://hbr.org/2020/03/coronavirus-is-proving-that-we-need-more-resilient-supply-chains>

Lund, S., Manyika, J., Woetzel, J., Barriball, E., Krishnan, M., Alicke, K., Birshan, M., George, K., Smit, S., Swan, D. & Hutzler, K. (2020). *Risk, resilience, and rebalancing in global value chains*. McKinsey Global Institute. Available at: <https://www.mckinsey.com/~media/McKinsey/Business%20Functions/Operations/Our%20Insights/Risk%20resilience%20and%20rebalancing%20in%20global%20value%20chains/Risk-resilience-and-rebalancing-in-global-value-chains-full-report-vH.pdf>

Mathew, P., Sartor, D., & Tschudi, W. (2009). *Self-benchmarking Guide for Cleanrooms: Metrics, Benchmarks, Actions*. United States. DOI: <https://doi.org/10.2172/983249>

Nguyen, R.T., Diaz, L.A., Imholte, D.D., Lister, T.E., 2017. Economic assessment for recycling critical metals from hard disk drives using a comprehensive recovery process. *JOM* 69, 1546–1552. DOI: <https://doi.org/10.1007/s11837-017-2399-2>.

P3 International. P4400 Kill-A-Watt Operation Manual. Rev 0214. Available at http://www.p3international.com/manuals/p4400_manual.pdf

Peiró, L. T., Girón, A. C., & i Durany, X. G. (2020). Examining the feasibility of the urban mining of hard disk drives. *Journal of Cleaner Production*, 248, 119216. DOI: <https://doi.org/10.1016/j.jclepro.2019.119216>

Perez-Gallardo, J. R., Azzaro-Pantel, C., & Astier, S. (2018). A multi-objective framework for assessment of recycling strategies for photovoltaic modules based on life cycle assessment. *Waste and Biomass Valorization*, 9(1), 147-159.

Rehberger, M., & Hiete, M. (2020). Allocation of Environmental Impacts in Circular and Cascade Use of Resources-Incentive-Driven Allocation as a Prerequisite for Cascade Persistence. *Sustainability*, 12(11), 4366.

Responsible Business Alliance. (2019). RBA Compass Awards 2019: Case Studies on Leadership, Innovation, and Implementation. Available at <http://www.responsiblebusiness.org/media/docs/RBACompassAwardsCaseStudies2019.pdf>

Richa, K., Babbitt, C. W., Nenadic, N. G., & Gaustad, G. (2017). Environmental trade-offs across cascading lithium-ion battery life cycles. *The International Journal of Life Cycle Assessment*, 22(1), 66-81.

Schulz, K. J., DeYoung, J. H., Seal, R. R., & Bradley, D. C. (Eds.). (2018). *Critical Mineral Resources of the United States: Economic and Environmental Geology and Prospects for Future Supply*. Geological Survey.

Schulze, R., & Buchert, M. (2016). Estimates of global REE recycling potentials from NdFeB magnet material. *Resources, Conservation and Recycling*, 113, 12-27. DOI: <https://doi.org/10.1016/j.resconrec.2016.05.004>

Sea-distances.org. (2020). Online tool for calculation distances between sea ports. Retrieved January 12, 2020 from sea-distances.org

Seagate (2016). Makara Enterprise HDD LCA Summary. Available at <https://www.seagate.com/files/www-content/global-citizenship/en-us/docs/seagate-makara-enterprise-hdd-lca-summary-2016-07-29.pdf>

Söderman, M. L., & André, H. (2019). Effects of circular measures on scarce metals in complex products—Case studies of electrical and electronic equipment. *Resources, Conservation and Recycling*, 151, 104464. DOI: <https://doi.org/10.1016/j.resconrec.2019.104464>

Sprecher, B., Xiao, Y., Walton, A., Speight, J., Harris, R., Kleijn, R., Visser, G., Kramer, G.J., 2014. Life cycle inventory of the production of rare earths and the subsequent production of NdFeB rare earth permanent magnets. *Environ. Sci. Technol.* 48, 3951–3958. DOI: <https://doi.org/10.1021/es404596q>.

Staub, C. (2019, May 2). *Rare earth magnet recovery feeds new hard drives*. E-Scrap News. <https://resource-recycling.com/e-scrap/2019/05/02/rare-earth-magnet-recovery-feeds-new-hard-drives/>

Synergy Research Group. (2020, July 7). *Hyperscale Data Center Count Reaches 541 in Mid-2020; Another 176 in the Pipeline*. Available at <https://www.srgresearch.com/articles/hyperscale-data-center-count-reaches-541-mid-2020-another-176-pipeline>

Tunsu, C., Menard, Y., Eriksen, D. Ø., Ekberg, C., & Petranikova, M. (2019). Recovery of critical materials from mine tailings: a comparative study of the solvent extraction of rare earths using acidic, solvating and mixed extractant systems. *Journal of Cleaner Production*, 218, 425-437.

United Nations Framework Convention on Climate Change. (n.d.). *The Paris Agreement*. <https://unfccc.int/process-and-meetings/the-paris-agreement/the-paris-agreement>

U.S. Chamber of Commerce Foundation. (2015). *Achieving a Circular Economy: How the Private Sector is Reimagining the Future of Business*. Washington, DC. Available at: <https://www.uschamberfoundation.org/sites/default/files/Circular%20Economy%20Best%20Practices.pdf>

Vahidi, E., Navarro, J., Zhao, F., 2016. An initial life cycle assessment of rare earth oxides production from ion-adsorption clays. *Resour. Conserv. Recycl.* 113, 1–11. DOI: <https://doi.org/10.1016/j.resconrec.2016.05.006>.

van der Velden, N.M., Patel, M.K. & Vogtländer, J.G. (2014). LCA benchmarking study on textiles made of cotton, polyester, nylon, acryl, or elastane. *Int J Life Cycle Assess* 19, 331–356. DOI: <https://doi.org/10.1007/s11367-013-0626-9>

Vinoski, J. (2020, April 7). *The U.S. Needs China For Rare Earth Minerals? Not For Long, Thanks To This Mountain*. Forbes. Available at <https://www.forbes.com/sites/jimvinoski/2020/04/07/the-us-needs-china-for-rare-earth-minerals-not-for-long-thanks-to-this-mountain/#18c7f58c28b9>

Vozzola, E., Overcash, M., & Griffing, E. (2018). Life Cycle Assessment of Reusable and Disposable Cleanroom Coveralls. *PDA journal of pharmaceutical science and technology*, 72(3), 236–248. DOI: <https://doi.org/10.5731/pdajpst.2017.007864>

Walker, S., Coleman, N., Hodgson, P., Collins, N., & Brimacombe, L. (2018). Evaluating the environmental dimension of material efficiency strategies relating to the circular economy. *Sustainability*, 10(3), 666. DOI: <https://doi.org/10.3390/su10030666>.

Woolven, J. (2021, January 18). *A new measure of business success: Why data and measurement are key to a circular economy transition*. Circulate. <https://medium.com/circulatenews/a-new-measure-of-business-success-9e53b7aafafa>

World Economic Forum. (2014). *Towards the Circular Economy: Accelerating the scale-up across global supply chains*. Geneva, Switzerland. Available at http://www3.weforum.org/docs/WEF_ENV_TowardsCircularEconomy_Report_2014.pdf

3.6 Appendix. Chapter 3 Supporting Information

Supporting tables in Excel spreadsheet format for this chapter can be found at the reference below.

Frost, K. D.; Hua, I. (2021), "Supporting Information for *Environmental Impacts of a Circular Recovery Process for Hard Disk Drive Rare Earth Magnets*". (DOI: [10.4231/PF9S-PG56](https://doi.org/10.4231/PF9S-PG56)).

4. A REGIONALIZED CHEMICAL FOOTPRINT METHOD FOR HARD DISK DRIVE RARE EARTH MAGNETS

4.1 Introduction

4.1.1 Environmental Impacts of Rare Earth Elements

Rare earth elements are vital to the production of many electronic products including hard disk drives (HDDs), electric vehicles, wind turbines, and LEDs. The HDD industry is a major consumer of rare earth (RE) permanent magnets and thus, there has been great interest in quantifying the environmental impacts of HDD RE magnet production (Arshi et al, 2018; Jin, et al, 2018; Sprecher et al, 2014).

Light rare earth elements (LREEs) such as neodymium and praseodymium, are now the dominant RE metals found in HDD magnets. REEs, although crustally abundant, are only found in minable concentrations in limited areas, and China (58%), the United States (U.S.) (27%), Myanmar (13%), and Australia (7%) are the only countries currently mining notable amounts of REEs (Gambogi, 2021). A majority of the world's LREEs are mined from the monazite/bastnasite deposits within the Bayan Obo mining region of China. Beneficiation and further processing to RE oxides and metals occurs nearby in Baotou, located 150 km south of the Bayan Obo mine (Fig 4.1). This region in Inner Mongolia currently accounts for 60% of allocated Chinese LREE production (Hu, 2020) and the associated environmental and social impacts from RE extraction and processing in this area have been well-publicized (Bontron, 2012).

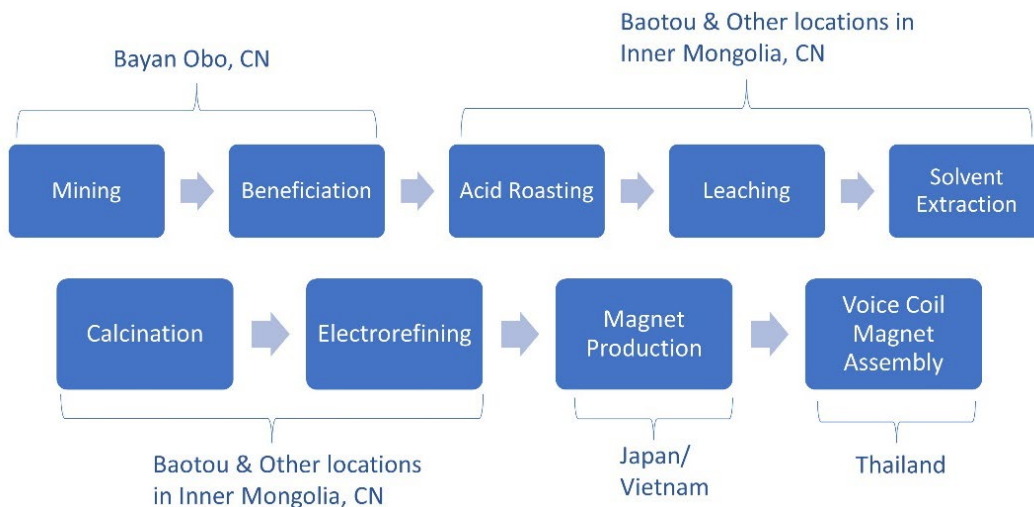


Figure 4.1. Process flow diagram for HDD RE magnets with locations assumed for this study (Bailey et al, 2020; Frost et al, 2021).

4.1.2 Human and Ecotoxicity of Rare Earth Mining and Processing

Previous LCA work has characterized the human and ecotoxicity impacts from Chinese RE production processes, which is primarily attributed to rare earth oxide (REO) solvent extraction (Bailey et al, 2020). Using LCA data to quantify the chemical toxicity of products and processes is well-established and relies on the toxicity characterization factors from the USEtox database, a UNEP-SETAC consensus model which includes fate, exposure, and effect parameters for hundreds of substances (Fantke et al., 2017).

In addition to toxicity impacts modeled through LCA, direct measurements of waterbodies draining the Bayan Obo RE mining and processing sites indicate that toxic levels of heavy metals (e.g. Cr, Cd, and Pb) are accumulating in the environment (Fan et al, 2008; Ma et al, 2016). Many studies also indicate the presence of radiological species such as thorium and uranium, emitted from both natural and anthropogenic sources (FindeiB & Schaffer, 2016). Process emissions of radiological species have been included in RE LCA inventory studies (Lee and Wen, 2016); however, chemotoxicity and radiotoxicity of these nuclides have only been included in one RE LCA study, to date (Bailey et al, 2020), and these did not include ecotoxicity impacts.

4.1.3 LCA & Chemical Footprint

While LCA can quantify the amount and types of emissions relative to a functional unit of product, it does little to describe the highly localized relationships between sources and receiving environments (Bare, 2006; Hauschild & Potting, 2005) or account for the impacts of the total volume of emissions (Kara et al, 2018). Thus, a hybridized approach using LCA to determine life cycle emissions and quantitative risk assessment (QRA) to quantify local or regional ecotoxicity impacts, may be preferred (Garcia et al, 2017).

One promising metric for deeper exploration and communication of toxicity impacts is a chemical footprint (ChF). A chemical footprint has been defined by Sala as “a quantitative measure describing the environmental space needed to dilute chemical pollution due to human activities to a level below a specified boundary condition” (2013). Chemical footprints are a part of the footprint family (i.e. carbon, ecological, water footprints), which have been proposed as a method for assessing perturbation of planetary boundaries (Fang et al, 2015; Posthuma et al 2014; Vanham et al, 2019) and more robust measurements of a growing, global chemical pollution problem (Landrigan et al., 2018).

According to Zijp et al. (2014), the chemical footprint should consider 1) exposure assessment, 2) impact assessment (grounded in traditional risk assessment and LCA principles), 3) boundary conditions (i.e. safe thresholds of pollution defined at local, regional or global scale [Steffen et al., 2015]), and 4) the dilution volume needed to maintain the boundary condition, which is a concept introduced by the European Eco-label scheme (1995) and further developed for water footprinting (Hoekstra, 2011).

The initial application of ChF methods was focused on sector-level, macroscale ecosystem impacts of agricultural and chemical pollutants (Bjorn et al, 2014; Sala et al, 2013; Zijp et al 2014,). However, product-level ChFs have been developed more recently for textile and pharmaceutical products and Li et al (2021) noted these studies primarily use a weighted toxicity approach derived from LCA and USETox. Further advancements for regionalizing product ChFs have been proposed (Makaraova et al, 2018; Wang, 2019), but a clear path forward has yet to be established.

4.1.4 Dilution Volume of Receiving Body

The dilution volume (m^3) of a receiving water body is the volume of surface freshwater available to dilute chemical emissions below an ecological or regulatory threshold and relates chemical emissions to the specific dilution capacity of an aquatic ecosystem (Hoekstra et al, 2011; Bjorn et al, 2014). The emergence of datasets such as HydroATLAS (Linke et al, 2019) makes calculation of an aquatic ecosystem's dilution capacity more reliable than previous studies which relied on coarser granularity databases or estimates for volumes of freshwater bodies (Bjorn et al, 2014). HydroATLAS is a database of “hydro-environmental sub-basin and river reach characteristics at 15 arc-second resolution”, providing consistent calculation of hydrological characteristics and an understanding of up and downstream river reach connectivity’ (Lehner, 2019).

4.1.5 Research Gaps & Aims

Chemical footprint studies, to date, lack standardized hydrological data as a reference point for calculating dilution capacity, a key parameter to assess chemical impact on water bodies. Further, the global fate and transport factors provided as the default within USETox (Kounina et al., 2014; Rosenbaum et al, 2008,) (and therefore LCA software) should be substituted with regionalized fate and exposure factors that have recently become more readily accessible (Verones et al, 2020). Additionally, to the authors knowledge, downscaling of Chinese grid mix emissions to allocate a site-specific chemical emissions profile has not been applied within chemical footprinting.

This study will apply a regionalized, product-level ChF methodology to explore the aquatic freshwater ecotoxicity of the production of HDD RE magnet assemblies. Because most of the global HDD RE magnet extraction, processing, and assembly occurs within a few known regions, a high-resolution, spatially explicit assessment is possible, and should highlight any toxicity hotspots from virgin RE magnet production, and how it relates to existing aquatic ecosystem carrying capacity.

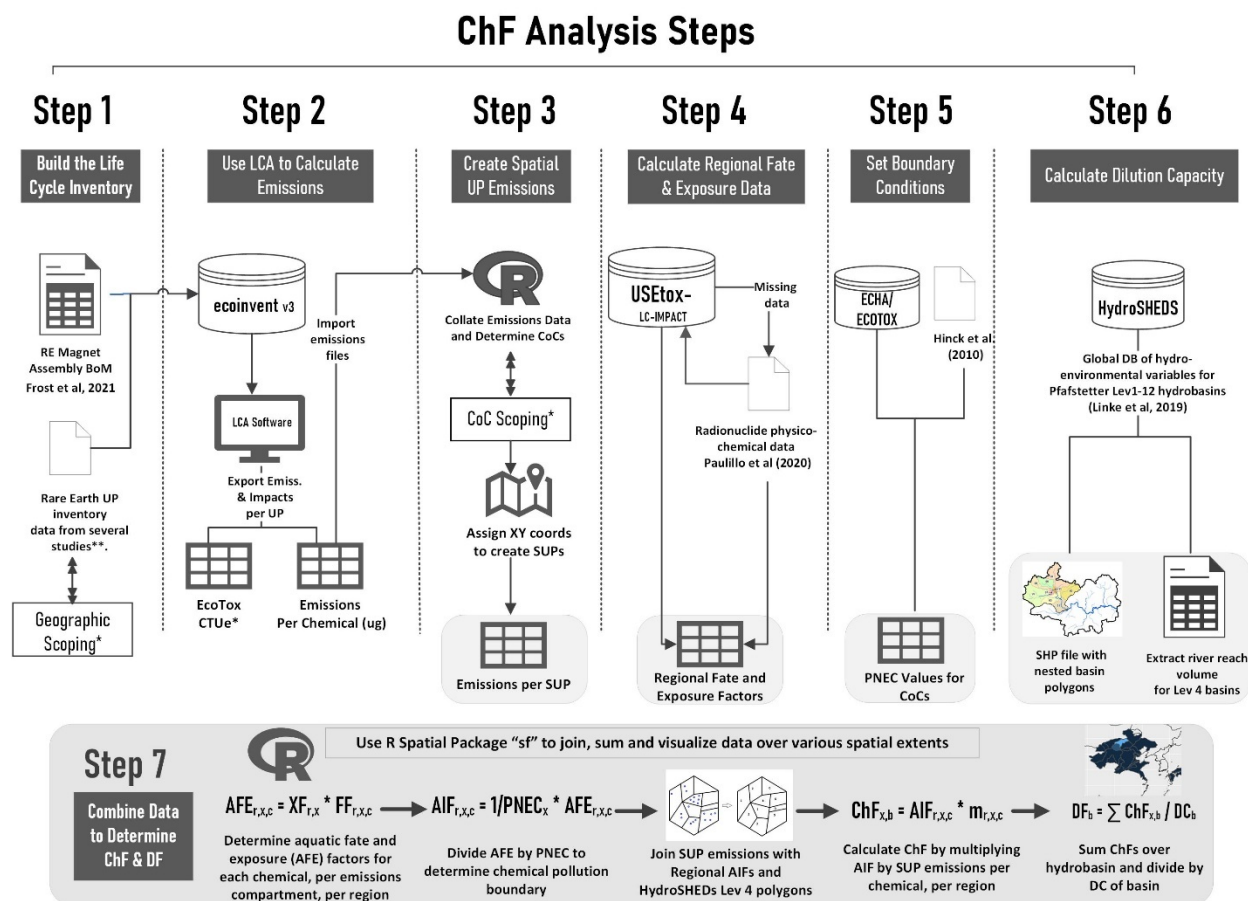
This study also aims to advance regionalized, product-level ChF methods in several ways:

1. High resolution emissions data from a global power plant database (Byers et al, 2019) will be used to downscale electricity grid emissions to a watershed (i.e. hydrobasin) level.

2. Use of regional fate and exposure factors for chemicals of concern (CoCs) from USETox/LC-IMPACT and estimated impacts for radionuclides on aquatic ecosystems using newly calculated factors.
3. Implement state-of-the-art hydrological data for consistent and accurate calculation of dilution volumes per river reach.

4.2 Methods

This study followed the major analysis steps outlined by Zijp et al. (2014) and methodology developed by Bjorn et al. (2014) for combining LCA and USETox data to derive a chemical footprint. Figure 4.2 provides an overview of the major methodological steps used in this study and the data sources and transformations performed.



* Bailey et al (2020), Arshi et al (2018), Jin et al (2020)

**Scoping – There were several scoping steps within the study: geographic scoping (boundary of the receiving body), chemicals of concern (CoCs), and the product system boundary (foreground and background).

Figure 4.2. Summary of the major methodological steps used in this study and the data sources and transformations performed. This methodology can be applied to any manufactured product, by adjusting Step 1 to include the product-specific Bill of Materials and supply chain (i.e. geographic scoping).

4.2.1 Target and Scope

The target product or ‘functional unit’ for this study is a set of RE magnet assemblies (i.e. voice coil magnet assembly) from a 16TB enterprise HDD, described by Frost et al. (2021). The RE magnet assembly examined in this study was considered a reasonable proxy for other HDD magnet assemblies currently in production.

There were several scoping steps within the study, namely geographic scoping (hydrobasin boundary of the receiving body), chemicals of concern (CoCs), and the product system boundary. Each of the scoping steps is described in more detail in Section 4.2.1.1, 4.2.2.2, and 4.2.5.

4.2.1.1 System Boundary & Spatiotemporal Scale

This was a cradle-to-gate LCA; however, transportation impacts between manufacturing locations were not considered. Figure 1 depicts the production processes included in the system. This study assessed emissions to air, soil and water, which would be transferred to freshwater ecosystems (rivers and lakes) but did not consider emissions to seawater.

Emissions were calculated based on annual production volumes of HDDs (and their mass of associated magnet assemblies). This was determined using the 2019 global annual sales data for HDDs where 260,300,000 HDDs (Forbes, 2020) contain approximately 27,000 tons of HDD RE magnet assemblies.

4.2.2 Quantification of Emissions

4.2.2.1 LCA Unit Process Inventory - Step 1

To construct the detailed unit process (UP) data required for a spatially explicit assessment, UP inventory data from Bailey et al. (2020) was used to build the life cycle inventory for the mining, beneficiation, acid roasting, leaching, and solvent extraction processes. Inventory data from Arshi et al. (2018) was used for the conversion of RE oxides to RE metals processing steps, and finally, data from Jin et al. (2020) and Frost et al. (2021) were used to construct processes for NdFeB magnet production and voice coil magnet assembly (VCMA) manufacturing (i.e. final product assembly where the magnet is epoxied into the steel bracket). In total, 95 production processes were used to create the unit process inventory (Step 1 of Figure 2). The ecoinvent v3 database was used to create all inputs and was modeled within Simapro software v 8.5.2 (Pre Consultants, 2018). Table S1 provides the complete life cycle inventory and associated data sources.

4.2.2.2 Emissions Inventory – Step 2

The emissions inventory for each UP, which describes emissions to land, water, and air per substance, were exported from Simapro and compiled in R to summarize emissions per UP (in kg). A screening-level ecotoxicity impact assessment was also used to narrow the emissions inventory to a smaller list of CoCs, for further ChF analysis. The cutoff for inclusion in the CoC list was a 0.01% contribution to total aquatic ecotoxicity (in CTUe), which aligns with the recommendation

from USEtox to include any chemical representing greater than 1/1,000th contribution to toxicity for in-depth analysis (Fantke, 2017). Nineteen chemicals (17 metals and 2 organics) were selected as CoCs and an additional 3 substances, Thorium-232, Uranium-238, and Radium-226, did not have ecotoxicity data in USEtox, but were included as CoCs because of concerns with radioactive emissions from RE mining and processing (Lee and Wen, 2016; Bailey et al 2020; FindeiB & Schaffer, 2016).

4.2.2.3 Assigning Spatial Unit Processes - Step 3

4.2.2.3.1 Manufacturing Materials

Manufacturing locations along the RE magnet life cycle were taken from the literature (Bailey et al, 2020; Frost et al, 2021). Manufacturing occurs in more than one location for some of the UPs and emissions were allocated based on approximate production volumes for each site where locations were known. Each UP was assigned latitude-longitude coordinates and became part of the ‘Spatial Product System’ (Marzullo et al, 2018), referred to herein as a spatial unit process, or SUP. Note: the manufacturing locations described in this study can be considered a theoretical supply chain for RE magnet assemblies based on a combination of known existing supplier locations, but it is not inclusive of all the possible manufacturing locations for this product.

4.2.2.3.1.1 Steel Manufacturing Emissions

One of the major contributors to ecotoxicity impacts from the RE Magnet is from the engineered steel bracket (‘iron yoke’) which houses the RE magnet (Frost, 2021). This is the largest component in the assembly, with a mass of 72.6 g (combined mass of upper and lower yokes), compared to 31.2 g for the RE magnets. Thus, both the engineered steel and stainless steel that comprise the yoke were considered to be a high impact material and further disaggregation of the likely steel supply chain was needed to understand spatial variation of impacts related to its production. The RE magnet is adhered to the yoke in Thailand, but the steel material for the yoke was likely imported, given the low amount of domestic steel production in Thailand, an assumption further justified by the specialty nature of the steel alloy used in these assemblies. The Global Steel Trade Monitor (ITA, 2021) provides import-export data for many of the countries within the global steel exchange markets. The top two trade partners with Thailand are Japan and China. For

Japan, the emissions were spatially allocated at the country-level which aligned with the scale of the hydrobasin (Section 4.2.5.2) and for China, steel production impacts were allocated to the major steel exporting provinces (Worldsteel, 2020). The steel spatial allocation process is fully documented in Appendix C.

4.2.2.3.2 Electricity

4.2.2.3.2.1 Chinese Electricity Emissions

Electricity from the grid is used to supply many of the manufacturing processes in the RE magnet supply chain, so impacts from electricity were allocated to the specific location where power was generated. The Global Power Plant Database's (GPPD) facility-level, annual generation values (Byers et al, 2019) were used to construct the supply mixes for each of the six electricity grids within the Chinese mainland, following grid boundaries described in Frost and Hua (2019). This approach is preferred over provincial or regional grid mix estimates provided by the LCA databases because it incorporates a large and representative amount of up-to-date facility-level production data. However, the GPPD dataset only supplies generalized fuel types (i.e. hydroelectric, solar, wind, natural gas, etc.), so sub-fuel mixes within a fuel type (e.g. Hydroelectric Pumped Storage vs Hydroelectric Run-of-River) were taken from ecoinvent v3 grid mix profiles (Treyer & Bauer, 2016). A custom unit process for each general technology/fuel type was then constructed as a weighted average of emissions based on the contribution of each of these sub-fuel types. Example calculations of the sub-fuel mix are available in Appendix C.

$$FME_{x,f,g} = w_{s,g} * m_{x,s,g} \quad (4.1)$$

where:

FME = Fuel Mix Emissions, where m is the mass of emissions per chemical (x), per sub-fuel type (s), and w is the proportion of electricity produced by the sub-fuel type within a particular electricity grid (g).

4.2.2.3.2.2 Other Countries

Due to less geographic variability in grid mixes within Japan and Vietnam and the geographic scope of the receiving watershed (Figure 4.3), national level grid mixes were considered representative for these countries. The electricity grid in Thailand was excluded from this analysis because of the lack of data on electricity consumption in foreground processes for the VCMA manufacturing step. Grid mixes for Japan and Vietnam were derived from IEA 2019 tables (IEA, 2019) and provide up-to-date data for production capacity by fuel type, per country. Sub-fuel type mixes for Japan and Vietnam from ecoinvent v3 were implemented as described in Section 4.2.2.3.2.1.

4.2.2.3.2.3 Downscaling Grid Emissions to each Power Plant Facility

Emissions per fuel type (e.g. coal, natural gas, hydroelectric) and per country (or per province, in China) were exported from the LCA software and each fuel mix profile was constructed in R using Equation 4.1. The electricity usage for each manufacturing step was allocated to each RE manufacturing SUP to understand how much electricity was used in each location. Each SUP was then associated with an electricity grid and spatially joined to the GPP database where annual generation from individual power plants could be used to downscale the emissions for each fuel mix to the exact facility locations (and basins) associated with each fuel (Eq 4.2).

$$PPE_{x,f,g} = FME_{x,f,g} * w_{i,f,g} \quad (4.2)$$

where:

PPE = Power Plant Emissions, where FME is derived from Eq 4.1 and w is the proportion of total electricity produced by individual power plant (i) of fuel type (f) within grid (g).

4.2.2.4 Summarizing Emissions Per CoC – Step 3 & Step 7

The emissions data for all SUPs, per chemical, can then be summarized over any spatial scale of interest (i.e. Lev 1-12 basins). For the Lev 4 basins used in this study, it was assumed that emissions were limited to the basin where the source was located. This may not always be the case for certain source types (e.g. air emissions from power plants) due to wind speed/direction and complex

atmospheric transport and transformation mechanisms associated with air emissions from tall stacks. However, the geographic scope of the basins used in this analysis ($\sim 1\text{E}+04 \text{ km}^2$) encompasses near field dispersion of emissions ($< 50 \text{ km}$ radius from source) (Perry et al, 2005).

4.2.3 Quantifying Fate and Exposure of CoCs - Step 4

Regional fate and exposure factors are provided in the LC-IMPACT database (Verones et al, 2020), which are an extension of USETox v2.12 factors and have been used to determine regionalized exposure data for each CoC. Impact factors for radiological chemicals are not currently integrated into the USETox database, so fate and transport factors were constructed in USETox using physico-chemical data from Paulillo et al. (2020), with the assumption that TENORMs (technically enhanced naturally occurring radioactive materials) behave similarly to metals with respect to solubility and mobility (MDEQ, 2015).

There were three geographic regions of interest in this study with respect to fate and exposure factors: Eastern China, Japan and the Korean peninsula, and SE Asia (Vietnam, Malaysia and Thailand). Regionalized impacts were sometimes five- to ten-fold larger than the default, global average factors, underscoring the need for more spatial granularity in impact assessment. For example, the fate factor for transport of cadmium (Cd^{2+}) from rural air to freshwater is $1.72\text{E}+02$ and $3.40\text{E}+01 \text{ (d}^{-1}\text{)}$, for China and the global average, respectively. Fate and eco-exposure factors per chemical can be summarized using the following equations, adapted from Rosenbaum et al. (2008).

$$AFE_{r,x,c} = XF_{r,x} * FF_{r,x,c} \quad (4.3)$$

where:

AFE = Aquatic Fate and Exposure in kg/day , where, r is the region of interest, x is the CoC, and c is the environmental compartment (land, air, water) transferring chemicals to freshwater (e.g. continental urban air to freshwater, continental rural air to freshwater).

XF = Regional Eco-exposure Factor derived in LC-Impact (i.e. regionalized USETox) which represents the fraction of chemical dissolved in freshwater (dimensionless) which could impact aquatic freshwater species.

FF = Regional Fate Factor is rate of transfer in (d^{-1}) for the transfer of emissions from air, water, and soil to freshwater.

4.2.4 Chemical Pollution Boundary – Step 5

The chemical pollution boundary or ‘ecotoxicity effect factors’ embedded in USETox are derived using the HC50 (i.e. the concentration at which 50% of the species are exposed above their EC50) and are widely implemented in LCA modeling. However, given the hybridized approach intrinsic to chemical footprinting, there is an opportunity to consider regulatory, risk-assessment based boundaries, such as the NOEC or PNEC. The use of more ‘average’ toxicity factors such as the HC50 versus more sensitive, conservative factors such as the NOEC or PNEC, are heavily debated amongst practitioners of LCA and QRA, with five alternative recommendations from these authors for use in the EU’s Product Environmental Footprint (Saouter et al, 2017).

The boundary chosen for this study was the predicted no effect concentration (PNEC) which is a “policy” or regulatory boundary (Zijp et al, 2014) and is available from the European Chemicals Agency’s (ECHA) database of REACH registration dossiers (ECHA, 2021). A $PNEC_{\text{freshwater}}$ was chosen as the policy boundary because of a) ready access to freshwater hazard information for a large, standardized, database of chemicals and b) calculation of PNECs follows a precautionary principle (Hauschild, 2005) by selecting the most sensitive species among the available ecotoxicity effect data and applying assessment factors to account for uncertainty (Saouter et al, 2017). However, there are drawbacks to using a regulatory boundary such as a PNEC: it does not take into account existing chemical pressures in the receiving waterbody or the specific existing species assemblages and their exposure to a mixture of chemicals (although conservative assessment factors partially account for this uncertainty).

For most of the heavy metals being considered in this study, PNECs are readily available from ECHA or U.S. EPA’s ECOTOX database (EPA, 2021). For radionuclides, PNEC data was obtained from Hinck et al. (2010) and is represented by $\mu\text{Gy/hr}$. Gy or (gray) is a unit of ionizing radiation defined as the absorption of one joule of radiation energy per kilogram of matter. For the radionuclides, Radium-226, Thorium-232, and Uranium-238, each chemical is subject to both

chemotoxicity and radiotoxicity PNECs. The PNEC is used, along with the AFE (Eq 4.2), to derive an Aquatic Impact Factor per region, per chemical, and per compartment.

$$AIF_{r,x,c} = 1/PNEC_x * AFE_{r,x,c} \quad (4.4)$$

where:

AIF = Aquatic Impact Factor, where r is the USETox region, x is the CoC and c is the emissions compartment. AFE is the aquatic fate and exposure calculated in Eq 4.3 and $PNEC_x$ is the predicted no effect concentration for freshwater in $\mu\text{g/L}$ or $\mu\text{Gy/hour}$ for radionuclides.

Using the results of Eq 4.4, one can calculate the chemical footprint per chemical using the annualized mass of emissions per region, per chemical, and per compartment.

$$ChF_{r,x,c} = AIF_{r,x,c} * m_{r,x,c} \quad (4.5)$$

where:

ChF = Chemical footprint in m^3 , where AIF is Aquatic Impact Factor from Equation 4.4, x is the chemical of concern, c is the media compartment (air, water, land), m is mass of emissions, and r is the regional factor from Verones et al. (2020).

4.2.5 Dilution Volume – Step 6

4.2.5.1 Hydrobasins of Interest

To determine the ChF and dilution capacity (DC) of emissions, each SUP must be associated with a receiving body of water. The HydroBASINS dataset is comprised of hydro-environmental variables such as discharge, land cover, temperature, etc. (Linke et al, 2019). Hydrological data, such as natural discharge, are available via integration of two companion datasets: BasinATLAS and RiverATLAS. BasinATLAS provides the “hierarchically nested sub-basins at multiple scales” and RiverATLAS links these to the individual river reaches which drain each basin (Lehner, 2019). Both datasets are available at a highly granular 15 arc-second (~ 500 m) resolution. Sub-basins are delineated using the Pfafstetter system at levels 1-12, which are derived from high-resolution topography data (Linke, 2019), where Level 1 represents continental-scale watersheds and Level

12 is $\sim 1\text{E}+02 \text{ km}^2$. Level 4 hydrobasins ($\sim 1\text{E}+04 \text{ km}^2$) were selected as the geographic scope of interest for this study because it represented a suitable compromise between spatial granularity and a practical geographic scope relative to the emissions sources. Figure 4.3 depicts the Level 4 hydrobasins used in this study, as well as the high-resolution river reach data used to calculate the dilution capacity of the receiving body (Section 4.2.6).

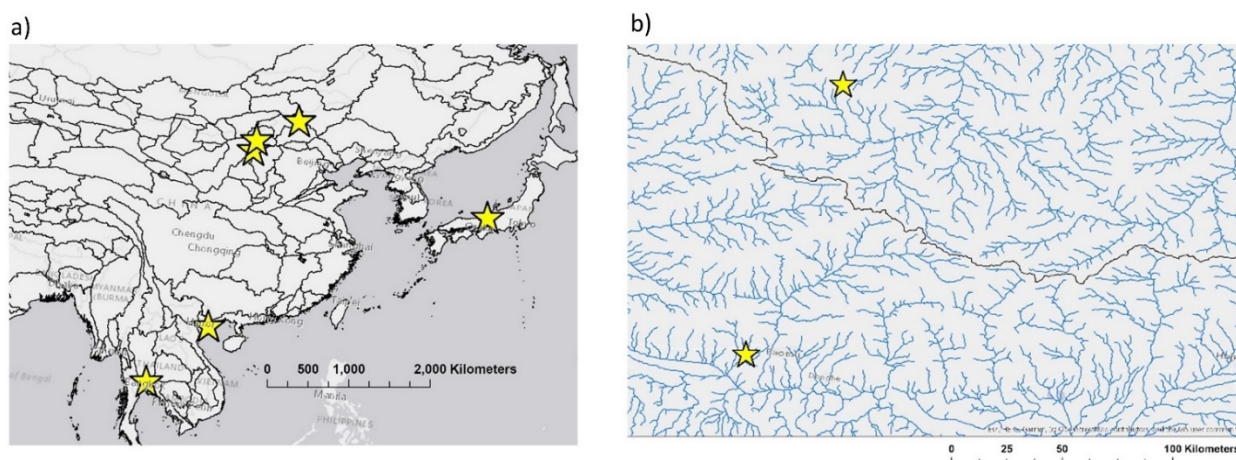


Figure 4.3. Figure a (left) is a map of the Level 4 basins for East Asia available from HydroBASINs with RE manufacturing locations represented as yellow stars. Figure b (right) displays the 15 arc-second resolution river reaches within the Level 4 basin near Bayan Obo (top yellow star) and Baotou (bottom yellow star).

4.2.5.2 Mapping SUP Emissions to Hydrobasins

The latitude-longitude coordinates assigned to each SUP were used to spatially join emissions with the corresponding Level 4 HydroBASIN dataset, using the “sf” library in R (Pebesma, 2018). Level 4 was chosen as the scale for this study; however, results could be aggregated or disaggregated to suit various hydrobasin levels.

HydroBASINs provides data on the natural discharge in m^3/s of each river reach upstream of a sub-basin pour point (i.e. junction of a stream network) (Lehner, 2019). River reach discharge is calculated in HydroBASINs using the globally integrated water balance model WaterGAP which is downscaled to the 15 arc-second ($\sim 500 \text{ m}$) resolution of the HydroSHEDS river network (Lehner & Grill, 2013). Multiplying discharge by seconds per year gives an annual water volume flowing through the river reach which is available for dilution of annual chemical emissions.

4.2.6 Relating ChF to Local Dilution Capacity – Step 7

A chemical footprint for each CoC can be calculated by multiplying the regional aquatic impact factor (AIF_r) by the emissions of the CoC over a given boundary, for a length of time. The boundary for this study is a Level 4 basin and the emissions occur over one year of production. To relate the chemical footprint to the receiving body's dilution capacity, we must sum the footprints of all chemicals within the basin and divide by the total annual dilution capacity (annual river volume) of the river reach which drains the basin. This results in a dilution factor (DF), which is the amount of the annual volume needed to dilute the CoC to the PNEC. A DF > 1 indicates that the volume required to dilute the CoCs exceeds the capacity of the waterbody and DF < 1 means there is enough freshwater available to dilute the CoC to a safe threshold for aquatic life. This is similar to the process to calculate the grey water footprint, or 'critical load approach', however, this calculation does not take into account the existing natural background concentrations of each chemical (Hoekstra et al, 2011).

$$DF_b = \frac{\sum_x ChF_{b,x}}{DC_b} \quad (4.6)$$

DF = Dilution Factor, where ChF is from Equation 5, summed over the basin of interest (b), for each chemical of concern (x).

4.3 Results & Discussion

4.3.1 Chemical Footprint

The cumulative ChF of all CoC emissions to air, soil, and water across the cradle-to-gate RE magnet manufacturing life cycle was 6.91E+12 m³ of freshwater per year. This impact is associated with an annual production of ~27,000 tons of HDD RE magnet assemblies. To understand impacts relative to manufacturing locations and their associated receiving bodies, ChF emissions were also summarized for each Level 4 basin impacted by primary magnet assembly production (Scope 1) and electricity associated with production (Scope 2).

Primary magnet manufacturing emissions occurred in nine Level 4 basins, with impacts predominating in the basins associated with RE processing (Baotou, China) and VCMA

manufacturing (Pathum Thani, Thailand) (Figure 4.4a). The impact of VCMA is due to steel metalworking processes required to shape the steel yoke that are assumed to happen in Thailand. Figure 4.4b displays the chemical footprints summarized by each major production unit, showing the impacts of the steel metalworking (VCMA) and the various RE separation processes including acid roasting and solvent extraction (depicted in ‘Pr Oxide’, ‘Nd Oxide’, and ‘REE sulfate from acid roasting 50 perc’ in Figure 4.4a).

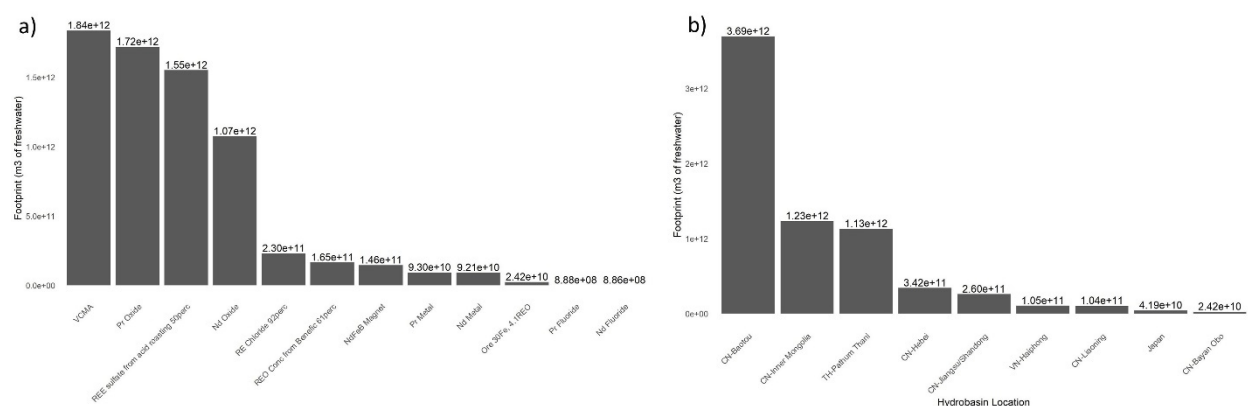


Figure 4.4. Chemical footprint in m3 from Scope 1 magnet manufacturing emissions by basin of interest (a) and by each major production unit (b). The labels for each basin represent a general description of the geographic area (city, province or country) where the manufacturing occurs, based on granularity of location data available.

4.3.2 Dilution Factor (DF)

When comparing the ChF in each hydrobasin to the dilution capacity of its associated freshwater receiving body, the largest impacts were in Thailand, Bayan Obo (Inner Mongolia), and Jiangsu and Shandong provinces in China. The DF is used to reflect the volume of the receiving body and its ability to assimilate chemical emissions. Figure 4.5a depicts the DF required to dilute the annual emissions from magnet processing (Scope 1) to the PNEC for CoCs within the river reach directly draining each watershed. Full results are available in Table S8.

Dilution factors for these watersheds are very high in some cases, with an average DF of 2480 times the available annual dilution volume. This is likely due to the following factors:

- 1) The CoCs in this study are almost exclusively heavy metals, which are highly toxic to aquatic organisms (PNECs $\sim 1\text{E}^{-9}$ g/L), corresponding to a large chemical footprint. In line with LCA & QRA principles, chemical toxicity is considered in an additive manner, which is meant to consider the co-exposure of chemicals with similar modes of action (Saouter et al., 2017), but compounds the conservative uncertainty (i.e. safety) factors that are already applied in PNEC calculations. Several authors have noted the large uncertainty introduced by toxicity parameters (Bjorn et al., 2014; Fantke et al., 2017; Saouter et al., 2017).
- 2) Several of the watersheds in consideration are located in semi-arid to arid climates, which may have very little average annual natural discharge (e.g. $0.4 \text{ m}^3/\text{s}$). As such, these areas likely require different treatment of waste chemicals (e.g. higher dilution of chemicals before emission to waterbodies), and may have contributions to flow from anthropogenic discharge, but this is not taken into consideration by current assumptions.

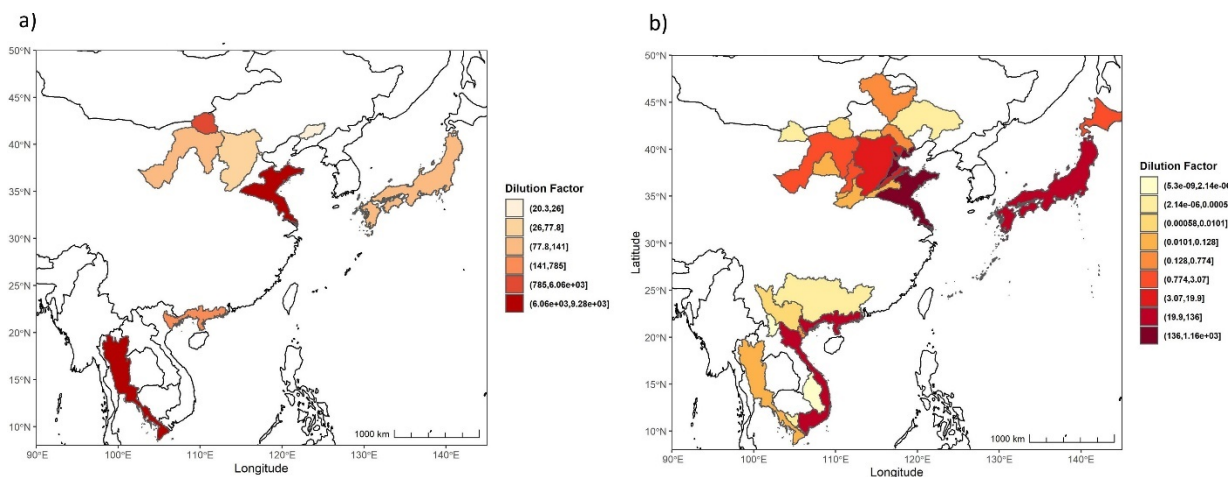


Figure 4.5. Dilution factors of the river reach required to dilute the sum of each of the chemicals of concern to its PNEC for locations associated with RE magnet processing (Scope 1) and process electricity use (Scope 2).

When electricity-related impacts (Scope 2) were also considered, the number of impacted watersheds expanded to 32, due to the large number of watersheds associated with grid-averaged electricity production. Electricity emissions and impacts are generally lower than those associated with materials and more dispersed in China due to the allocation of impacts across several

hydrobasins located within the grid. Figure 4.5b depicts the dilution factor required to dilute the annual emissions from electricity use associated with RE magnet manufacturing (Scope 2) to the PNEC for CoCs within the river reach directly draining each watershed. Full results are available in Table S8.

4.3.3 Chemical Footprint by TENORMs

The total chemical footprint by TENORMs was a minor contributor, when compared to toxicity from heavy metals. This is due to calculations for fate and transport, driven by the extremely low solubility and mobility of these chemicals.

Table 4.1. Radiotoxicity and chemotoxicity footprints of three radionuclides associated with RE mining and processing.

Chemical Substance	Chemotoxicity Footprint (m³)	Radiotoxicity Footprint (m³)
Radium-226	4.04E-14	1.20E-12
Thorium-232	5.99E-22	1.06E-13
Uranium-238	7.52E-19	6.55E-11

However, significant concentrations of these chemicals are present in nearby freshwater bodies due to migration from waste piles and mining/processing tailings ponds, with concentrations of thorium measured at up to 5 mg/L in leaching ponds and 0.1-1 µg/L in remote freshwater sites (Findeiß & Schäffer, 2017). Current LCA emissions and transport modelling data may be an inadequate tool to describe the risk from these TENORMS, especially due to lack of integration of effluent pH and soil-specific mobility concerns (Findeiß & Schäffer, 2017), which are not addressed by generalized TENORM physico-chemical data.

4.3.4 Contribution per CoC

Ecotoxicity impacts were dominated by just a handful of heavy metals associated with RE manufacturing and metalworking. Chromium (VI) was the largest impact driver accounting for 56.1% of the chemical footprint, followed by Cadmium (20.6%) & Nickel (11.3%). Impacts per CoC are somewhat variable over hydrobasins (Figure 4.7), with a different emissions composition

from locations undertaking RE processing (i.e. CN-Baotou) and steel metalworking (i.e. TH-Pathum Thani).

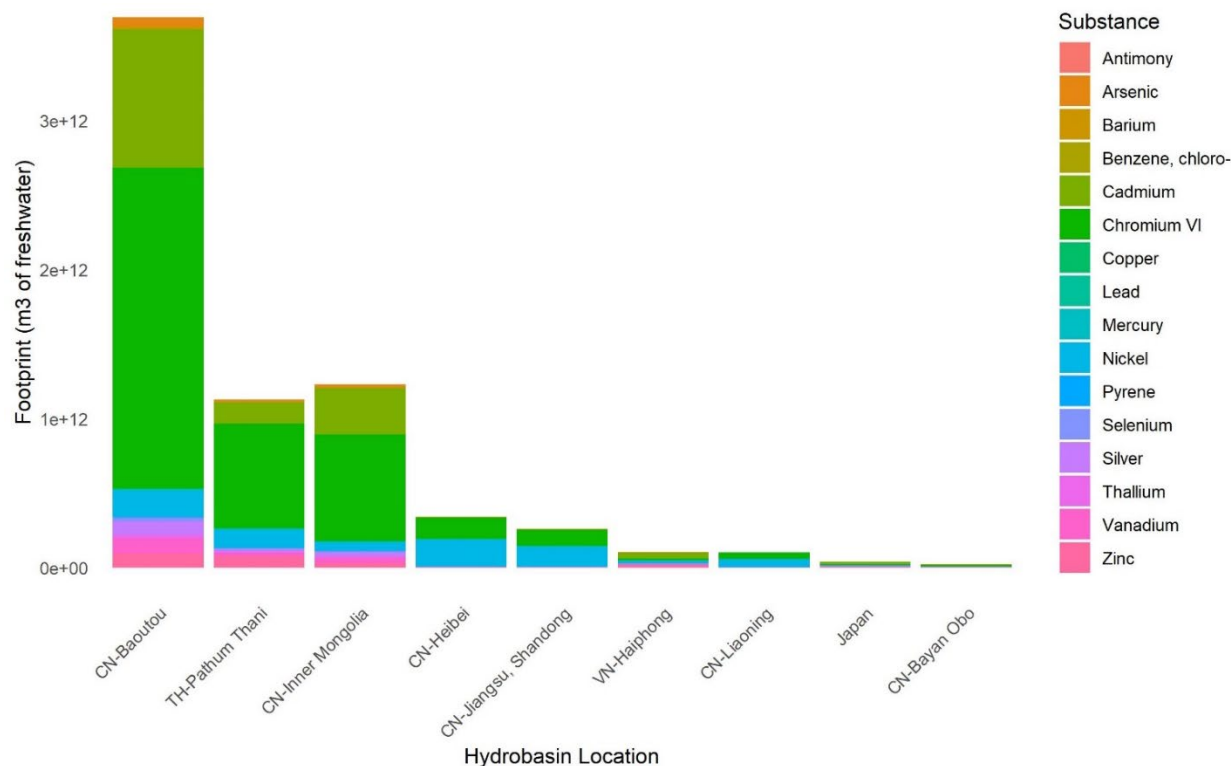


Figure 4.6. Chemical footprint for each hydrobasin, displaying contribution by chemicals of concern (CoCs). This figure excludes CoCs which contribute less than 0.01% of the total footprint.

4.3.5 Predicted vs Sampled Concentrations of CoCs

Predicted emissions from the magnet manufacturing processes and their associated concentration in receiving bodies can be compared to sampling data available for the Yellow River, at locations just downstream of the Baotou processing facilities. For example, concentrations of Cd at these sites ranged from 0.1-4.3 $\mu\text{g/L}$ in water and 0.16-0.53 mg/kg in sediment, respectively (Fan et al., 2008; Ma et al., 2016), compared to modelled concentrations of 6.75 $\mu\text{g/L}$ in water (Table 4.2).

Although these monitored concentrations are within the correct order of magnitude, using LCA data to predict in-stream concentrations may be problematic because: 1) although the goal was to elucidate the impact of HDD magnets, these magnets only comprise a portion of the LREE metals mining and processing in this area, and annual mining and processing quotas may be a better indicator of total burden for the Baotou site, in particular, 2) LCA and USETox modeling relies

on steady-state assumptions of emissions, which does not account for the cumulative contamination from persistent, heavy metals from years of mining, processing, and slag storage in this area and the ongoing exchange between sediment-bound metals and overlying waters, and 3) the natural background levels of heavy metals in water at this location which are not accounted for in the USETox modeling. These issues are true for all LCA-derived emissions and underscores the difficulty of using LCA-derived ChF data to predict concentrations at a particular time and space, rather than as a tool to predict *potential* total ecotoxicity impact.

Table 4.2. Modelled Concentrations vs Selected Monitoring Data from the Yellow River near Baotou, CN Rare Earth Processing Facilities.

Chemical of Concern	Modelled Concentration $\mu\text{g/L}$	Sampled Concentrations		
		Water $\mu\text{g/L}^1$	Sediment ² (mg/kg)	Sediment Background ² (mg/kg)
Chromium (VI)	3.85	N/A	90	41.4-70.2
Cadmium	6.75	0.1-4.3	0.16-0.53	0.1
Nickel	47.2	N/A	15	19.5-36.6
Zinc	74.2	2.8-227	50	58.8-68.5

¹ Fan et al. (2008)

² Ma et al. (2016)

4.4 Conclusions

This study quantified the freshwater ecotoxicity footprint of producing HDD RE magnet assemblies on the waterbodies associated with manufacturing facilities within a theoretical supply chain. Twenty-three chemicals of concern were identified using the unit process emissions data available from the LCA literature. Heavy metals were the dominant drivers of ecotoxicity impact and the three radionuclides of concern were relatively minor by comparison, but may be inadequately represented by non-specific fate and transport factors and an underestimate of emissions.

4.4.1 Beyond LCA

The chemical footprint method gives insights beyond typical LCA by placing emissions and impact within context of the local receiving body (i.e. source-receptor pathway in QRA). This is

important for many products that have known aquatic toxicity concerns and ChFs have been conducted for pesticides, textiles, detergents, and pharmaceuticals, to date. In the case of HDD magnet assemblies, heavy metals toxicity from steel manufacturing and rare earth processing were shown to be impactful, but the main location for rare earth processing (in Baotou, CN) was less impactful than its footprint might suggest due to the high discharge volume of the Yellow River near Baotou processing facilities. By factoring in the dilution capacity of a given receiving body, stakeholders can target the most vulnerable ecosystems with respect to these products, although existing vulnerability due to historic pollution should be considered, as well.

4.4.2 Supply Chain Transparency and SUPs

Compliance with government regulations such as REACH, Restriction of Hazardous Substances (RoHS), and Section 1502 of the Dodd-Frank Act (i.e. conflict minerals) has led to a deepened understanding of chemical use and more transparent supply chains across many sectors of the economy. Given this evolution in ‘responsible sourcing’, it is now possible to pinpoint location-specific impacts of many types of processes and products.

Supply chain data, combined with robust, existing LCA inventory databases can help create spatially explicit, process-based emission inventories for use in chemical footprints and other location-specific impact methods. However, given the complexity of creating a spatial unit process inventory, careful scoping based on geography and processes (or chemicals) of concern is required to make the study feasible. This makes it important for stakeholders to use tools such as screening-level LCA to target processes that are likely driving impact in their supply chain and then pursue information about location-specific emissions, where available. The allocation of emissions by location is crucial to how ecotoxicity hotspots are identified, so this spatial inventory process is one of the most important steps with respect to quantifying the chemical footprint of a particular product and its supply chain.

4.4.3 Tools to Enable Chemical Footprinting

To reduce the analytical burden of conducting chemical footprints generally, we recommend the development of a GIS-based tool which can link regional USETox fate and exposure factors, their

associated PNECs, and global HydroBASINs data including discharge volumes for river reaches at various spatial scales. This compiled information, when coupled with location-specific emissions (from LCA or directly from suppliers) should provide the inputs to calculate a robust, location-specific, chemical footprint.

For this study, electricity impacts were relatively small when compared to direct material impacts, however there are many processes or products (e.g. semiconductor fabrication) where emissions from electricity will play a dominant role in the chemical footprint. The methods developed here to downscale grid-level chemical emissions to individual power plants based on production data from the GPPD should be further developed for other countries and grids of concern.

4.4.4 Potential of HydroBASINs for Use in Footprinting

This standardized, high-resolution dataset contains many additional variables that could support more robust chemical footprinting (or other footprinting) methods. The dataset is rich with environmental and developmental variables which are available at the hydrobasin level. We encourage further exploration of this dataset for use in footprinting, and variables of interest include: a) human development and human footprint indices which could be used as a proxy of existing watershed pollution, in the absence of monitoring data, b) soils (e.g. carbon content) and geology data (for better understanding of site-specific chemical fate and transport mechanisms), c) lake and reservoir volumes (for calculating dilution capacity within these types of waterbodies), d) groundwater table depth (for estimating potential chemical migration and/or dilution with groundwater), and e) freshwater ecoregions (for understanding specific species assemblages and how they may be vulnerable to pollution). Incorporation of these datasets may help to fill existing gaps in chemical footprinting methodology in a standardized manner.

4.4.5 Linking with Science-Based Targets

Ongoing work and future development of local and regionalized planetary boundaries for environmental impact categories, including chemical toxicity (Bjorn et al, 2020), should help organizations to develop science-based targets for toxicity reduction in their products or processes. A standardized, spatially explicit chemical footprinting methodology may play a vital role in

quantifying an organization's impact and their contribution to, or exceedance of local or regional planetary boundaries. To this end, this work aims to further develop and standardize the methodology, but there are still areas for improvement with regard to modeling variability in specific source-receptor interactions, accounting for existing chemical pressures in a waterbody, and linking with robust, aquatic biodiversity data.

4.5 References

Arshi, P. S., Vahidi, E., & Zhao, F. (2018). Behind the scenes of clean energy: the environmental footprint of rare earth products. *ACS Sustainable Chemistry & Engineering*, 6(3), 3311-3320. DOI: <https://doi.org/10.1021/acssuschemeng.7b03484>

Bailey, G., Joyce, P. J., Schrijvers, D., Schulze, R., Sylvestre, A. M., Sprecher, B., ... & Van Acker, K. (2020). Review and new life cycle assessment for rare earth production from bastnäsite, ion adsorption clays and lateritic monazite. *Resources, Conservation and Recycling*, 155, 104675.

Bare, J. C. (2006). Risk assessment and life-cycle impact assessment (LCIA) for human health cancerous and noncancerous emissions: integrated and complementary with consistency within the USEPA. *Human and ecological risk assessment*, 12(3), 493-509.

Bare, J., (2011). TRACI 2.0: The Tool for the Reduction and Assessment of Chemical and Other Environmental Impacts 2.0. *Clean Technologies and Environmental Policy*, 13, (5) 687-696. <https://doi.org/10.1007/s10098-010-0338-9>.

Bjørn, A. Diamond, M., Birkved, M. and Hauschild, M.Z. (2014). Chemical footprint method for improved communication of freshwater ecotoxicity impacts in the context of ecological limits *ES&T*. <https://pubs.acs.org/doi/abs/10.1021/es503797d>

Bjørn, A., Sim, S., King, H., Patouillard, L., Margni, M., Hauschild, M. Z., & Ryberg, M. (2020). Life cycle assessment applying planetary and regional boundaries to the process level: a model case study. *The International Journal of Life Cycle Assessment*, 25(11), 2241-2254.

Bontron, C. (Aug 7, 2012). Rare-earth mining in China comes at a heavy cost for local villages. *The Guardian*. Available at <https://www.theguardian.com/environment/2012/aug/07/china-rare-earth-village-pollution>

Boulay, A.-M., Bare, J., Benini, L., Berger, M., Lathuillière, M. J., Manzardo, A., . . . Pfister, S. (2017). The WULCA consensus characterization model for water scarcity footprints: assessing impacts of water consumption based on available water remaining (AWARE). *The International Journal of Life Cycle Assessment*. doi: <https://doi.org/10.1007/s11367-017-1333-8>

Byers, L., Friedrich, J., Hennig, R., Kressig, A., Li, X., Valeri, L. M., & McCormick, C. (2018). A global database of power plants. Washington, DC: World Resources Institute. Available online at www.wri.org/publication/global-database-power-plants.

- Coughlin, T. (2019, February). 2018 Hard Disk Drive Results. *Forbes*. Retrieved from <https://www.forbes.com/sites/tomcoughlin/2019/02/04/2018-hard-disk-drive-results/#3c1f8df745a7>
- ECHA. (2021). ECHA Registered Substances. Retrieved from <https://echa.europa.eu/fr/information-on-chemicals/registered-substances> (accessed February 2021).
- EPA. (2021). ECOTOX Knowledgebase. Retrieved from <https://cfpub.epa.gov/ecotox/search.cfm> (accessed July 2021).
- Fan, Q., He, J., Xue, H., Lü, C., Sun, Y., Shen, L., ... & Bai, S. (2008). Heavy metal pollution in the Baotou section of the Yellow River, China. *Chemical Speciation & Bioavailability*, 20(2), 65-76.
- Fang, K., & Heijungs, R. (2014). There Is Still Room for a Footprint Family without a Life Cycle Approach—Comment on “Towards an Integrated Family of Footprint Indicators”. *Journal of Industrial Ecology*, 18(1), 71-72.
- Fantke, P. (Ed.), Bijster, M., Guignard, C., Hauschild, M., Huijbregts, M., Joliet, O., Kounina, A., Magaud, V., Margni, M., McKone, T.E., Posthuma, L., Rosenbaum, R.K., van de Meent, D., van Zelm, R., (2017). USEtox® 2.0 Documentation (Version 1), Retrieved from <http://usetox.org>.
- Findeiß, M., & Schäffer, A. (2017). Fate and environmental impact of thorium residues during rare earth processing. *Journal of Sustainable Metallurgy*, 3(1), 179-189.
- Frost, K., Sousa, I., Larson, J., Jin, H., & Hua, I. (2021). Environmental impacts of a circular recovery process for hard disk drive rare earth magnets. *Resources, Conservation and Recycling*, 173, 105694.
- Gambogi, J. (2021, Jan). Rare Earths. U.S. Geological Survey, Mineral Commodity Summaries. <https://pubs.usgs.gov/periodicals/mcs2021/mcs2021-rare-earths.pdf>
- de García, S. O., García-Encina, P. A., & Irusta-Mata, R. (2017). The potential ecotoxicological impact of pharmaceutical and personal care products on humans and freshwater, based on USEtox™ characterization factors. A Spanish case study of toxicity impact scores. *Science of the total environment*, 609, 429-445.
- Hauschild, M., & Potting, J. (2005). Spatial differentiation in Life Cycle impact assessment-The EDIP2003 methodology. *Environmental news*, 80, 1-195.

- Hinck, J. E., Linder, G., Finger, S., Little, E., Tillitt, D., & Kuhne, W. (2010). Biological pathways of exposure and ecotoxicity values for uranium and associated radionuclides. *Hydrological, Geological and Biological Site Characterization of Breccia Pipe Uranium Deposits in Northern Arizona*. U. S. Geological Survey, Scientific Investigations Report, 5025.
- Hoekstra, A. Y., Chapagain, A. K., Aldaya, M. M., & Mekonnen, M. M. (2011). *The Water Footprint Assessment Manual: Setting the Global Standard*. Washington D.C.: earthscan.
- Hu, T. (2020, July 16). China's rare earth mining quota for 2020 up 6% YOY. S&P Global Market Intelligence. Available from <https://www.spglobal.com/marketintelligence/en/news-insights/latest-news-headlines/china-s-rare-earth-mining-quota-for-2020-up-6-yoy-59452763>.
- IEA. (2020). Electricity Generation by Source [Table]. Retrieved tables for Japan, Vietnam and Thailand. Retrieved from <https://www.iea.org/fuels-and-technologies/electricity> (accessed 14 March 2021).
- ITA. (2019, March). Steel Imports Report: Thailand. Global Steel Trade Monitor. Available at <https://legacy.trade.gov/steel/archives/index.asp> (accessed 5 August 2021).
- Jin, H., Afiuny, P., Dove, S., Furlan, G., Zakotnik, M., Yih, Y., Sutherland, J.W., 2018. Life cycle assessment of neodymium-iron-boron magnet-to-magnet recycling for electric vehicle motors. *Environ. Sci. Technol* 52. DOI: <https://doi.org/10.1021/acs.est.7b05442>.
- Jin H., Frost K., Sousa I., Ghaderi H., Bevan A., Zakotnik M., and Handwerker C. (2020). Life cycle assessment of emerging technologies on value recovery from hard disk drives. *Resour. Conserv. Recycl.* 157, 104781 DOI: <https://doi.org/10.1016/j.resconrec.2020.104781>.
- Kara, S., Hauschild, M. Z., & Herrmann, C. (2018). Target-driven life cycle engineering: Staying within the planetary boundaries. *Procedia CIRP*, 69, 3-10.
- Kounina, A., Margni, M., Shaked, S., Bulle, C., & Joliet, O. (2014). Spatial analysis of toxic emissions in LCA: A sub-continental nested USEtox model with freshwater archetypes. *Environment international*, 69, 67-89.
- Landrigan, P. J., Fuller, R., Acosta, N. J., Adeyi, O., Arnold, R., Baldé, A. B., ... & Chiles, T. (2018). The Lancet Commission on pollution and health. *The Lancet*, 391(10119), 462-512.
- Lee, J.C. and Wen, Z. (2016). Rare earths from mines to metals: comparing environmental impacts from China's main production pathways. *J. Ind. Ecol.* DOI: <https://doi.org/10.1111/jiec.12491>
- Lehner, B. (2019, Dec). HydroATLAS: A global compendium of hydro-environmental sub-basin and river reach characteristics at 15 arc-second resolution. Technical Documentation Version 1.0. Available at <https://www.hydrosheds.org/page/hydroatlas>

Lehner, B., Grill G. (2013). Global river hydrography and network routing: baseline data and new approaches to study the world's large river systems. *Hydrological Processes*, 27(15), 2171-2186. doi: 10.1002/hyp.9740.

Li, Y., Cheng, Y., Zhou, L., & Yang, Y. (2021). Advances, Norms, and Perspectives in Product Chemical Footprint Research. *International Journal of Environmental Research and Public Health*, 18(5), 2728.

Linke, S., Lehner, B., Ouellet Dallaire, C., Ariwi, J., Grill, G., Anand, M., Beames, P., Burchard-Levine, V., Maxwell, S., Moidu, H., Tan, F., Thieme, M. (2019). Global hydro-environmental sub-basin and river reach characteristics at high spatial resolution. *Scientific Data* 6: 283. DOI: 10.1038/s41597-019-0300-6.

Ma, X., Zuo, H., Tian, M., Zhang, L., Meng, J., Zhou, X., ... & Liu, Y. (2016). Assessment of heavy metals contamination in sediments from three adjacent regions of the Yellow River using metal chemical fractions and multivariate analysis techniques. *Chemosphere*, 144, 264-272.

Makarova, A., Shlyakhov, P., & Tarasova, N. (2018). Estimating Chemical Footprint on High-resolution Geospatial Grid. *Procedia CIRP*, 69(1), 469-474.

Marzullo, R. D. C. M., dos Santos Matai, P. H. L., & Morita, D. M. (2018). New method to calculate water ecotoxicity footprint of products: A contribution to the decision-making process toward sustainability. *Journal of Cleaner Production*, 188, 888-899.

MDEQ. (2015). Michigan TENORM Disposal Advisory Panel White Paper, 2014-2015. 32 pgs. Michigan Department of Environmental Quality. Available at https://www.michigan.gov/documents/deq/deq-RMG-TENORM_Disposal_Advisory_Panel_White_Paper_-_FINAL_481404_7.pdf

Pebesma, E., (2018). Simple Features for R: Standardized Support for Spatial Vector Data. *The R Journal*, 10(1), 439-446, <https://doi.org/10.32614/RJ-2018-009>

Perry, S. G., Cimorelli, A. J., Paine, R. J., Brode, R. W., Weil, J. C., Venkatram, A., ... & Peters, W. D. (2005). AERMOD: A dispersion model for industrial source applications. Part II: Model performance against 17 field study databases. *Journal of applied meteorology*, 44(5), 694-708.

Pre Consultants. (2018). Simapro Version 8.5.2.

Posthuma, L., Bjørn, A., Zijp, M. C., Birkved, M., Diamond, M. L., Hauschild, M. Z., ... & Van de Meent, D. (2014). Chemical footprints: Thin boundaries support environmental quality management. *Environmental Science & Technology*, 48(22), 13025-13026.

R Core Team. (2017). R: A Language and Environment for Statistical Computing (Version 3.4.3 (2017-11-30). Vienna, Austria. Retrieved from <https://www.R-project.org/>

Rosenbaum, R. K., Bachmann, T. M., Gold, L. S., Huijbregts, M. A., Jolliet, O., Juraske, R., ... & Hauschild, M. Z. (2008). USEtox—the UNEP-SETAC toxicity model: recommended characterisation factors for human toxicity and freshwater ecotoxicity in life cycle impact assessment. *The International Journal of Life Cycle Assessment*, 13(7), 532-546.

Sala, S. and Goralczyk, M. 2013. Chemical Footprint: A Methodological Framework for Bridging Life Cycle Assessment and Planetary Boundaries for Chemical Pollution. *Integrated Environmental Assessment and Management*. <https://setac.onlinelibrary.wiley.com/doi/pdf/10.1002/ieam.1471>

Sprecher, B., Xiao, Y., Walton, A., Speight, J., Harris, R., Kleijn, R., Visser, G., Kramer, G.J., 2014. Life cycle inventory of the production of rare earths and the subsequent production of NdFeB rare earth permanent magnets. *Environ. Sci. Technol.* 48, 3951–3958. DOI: <https://doi.org/10.1021/es404596q>.

Steffen, W., Richardson, K., Rockström, J., Cornell, S. E., Fetzer, I., Bennett, E. M., ... & Folke, C. (2015). Planetary boundaries: Guiding human development on a changing planet. *Science*, 347(6223), 1259855.

Treyer, K. & Bauer, C. (2016). Life cycle inventories of electricity generation and power supply in version 3 of the ecoinvent database—part II: electricity markets. *International Journal of Life Cycle Assessment*, 21, 1255-1268. doi: [10.1007/s11367-013-0694-x](https://doi.org/10.1007/s11367-013-0694-x)

Vanham, D., Leip, A., Galli, A., Kastner, T., Bruckner, M., Uwizye, A., ... & Hoekstra, A. Y. (2019). Environmental footprint family to address local to planetary sustainability and deliver on the SDGs. *Science of the Total Environment*, 693, 133642.

Verones, F., Hellweg, S., Antón, A., Azevedo, L. B., Chaudhary, A., Cosme, N., ... & Huijbregts, M. A. (2020). LC-IMPACT: A regionalized life cycle damage assessment method. *Journal of Industrial Ecology*, 24(6), 1201-1219.

Worldsteel. (2020). Chinese mainland steel plants 2020. Worldsteel Association. Available for purchase at <https://www.worldsteel.org/publications/bookshop.html>?

Wang, L.L. (2019). *Methodology for Accounting for the Chemical Footprint of Products Based on Regional Toxic Stress Indices, China*, (Zhejiang, CN CN201811009866.3). Hangzhou Huiliang Intellectual Property Agency Co., Ltd. 33259. Available online: <http://d.wanfangdata.com.cn/patent/CN201811009866.3> (accessed on 12 August 2021).

Zijp, M.C., Posthuma, L. and van de Meent, D. (2014). Definition and Applications of a Versatile Chemical Pollution Footprint Methodology. *Environmental Science & Technology*, 48 (18), 10588–10597. <https://pubs.acs.org/doi/abs/10.1021/es500629f>

4.6 Appendix. Chapter 4 Supporting Information

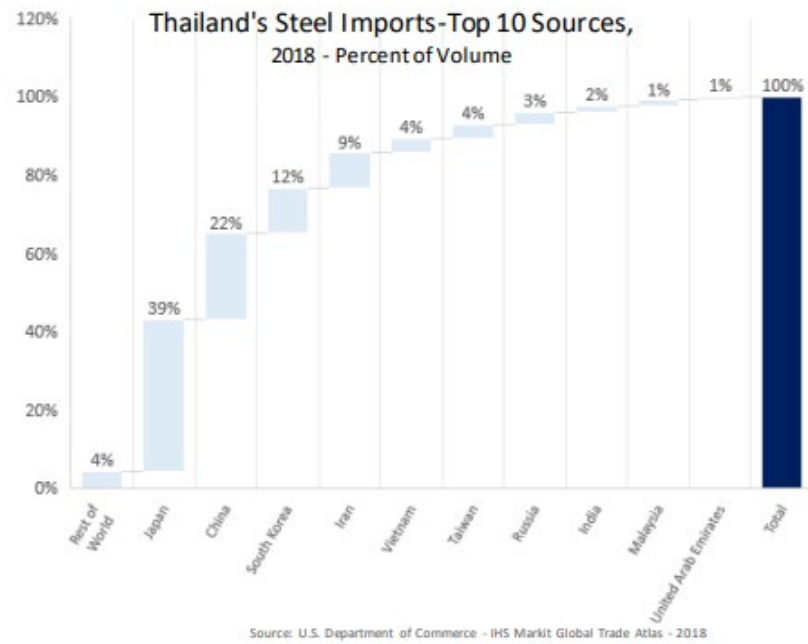
Chapter 4 supplemental tables in Excel spreadsheet format can be accessed using the reference below.

Frost, K. D.; Hua, I. (2022), "Supporting Information for *Application of a Regionalized Chemical Footprint Method to Identify Aquatic Ecotoxicity Hotspots of HDD Rare Earth Magnets*." (DOI: [10.4231/QRYS-CR30](https://doi.org/10.4231/QRYS-CR30)).

1.0 Calculating Emissions from Steel

The engineered steel and stainless steel that comprise the magnet assembly yoke were understood to be a high impact material from LCA (Frost et al, 2021) and further disaggregation of the likely steel supply chain was needed to understand spatial variation of impacts related to its production. The RE magnet is adhered to the yoke in Thailand, but the steel material for the yoke was likely imported, given the low amount of steel production in Thailand, an assumption further justified by the specialty nature of the steel alloy used in these assemblies. The Global Steel Trade Monitor (ITA, 2021) provides import-export data for many of the countries within the global steel exchange markets. The top two trade partners with Thailand are Japan and China. For Japan, the emissions were spatially allocated at the country-level which aligned with the scale of the hydrobasin and for China, steel production impacts were allocated to the major steel exporting provinces of Hebei, Jiangsu, Liaoning, and Shandong which account for 84% of Chinese steel exports. (Worldsteel, 2020). Table S6 provides a list of the Chinese steel allocation factors.

a)



b)

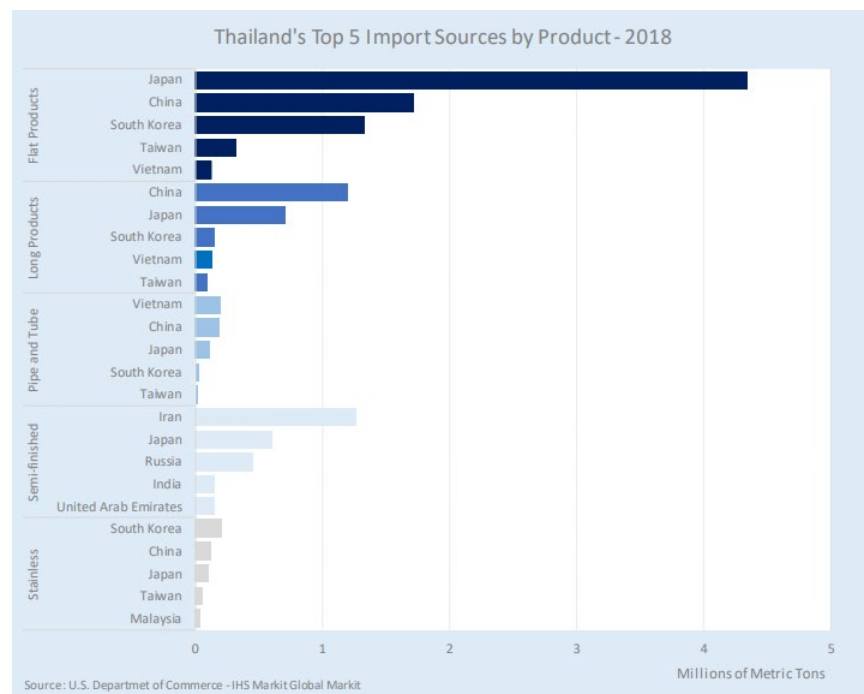


Figure S1. Figure a are the top steel import countries of Thailand. Figure b are Thailand's import sources broken out by products.

2.0 Calculating Emissions from Electricity

2.1 Chinese Electricity Emissions

The Global Power Plant Database's (GPPD) facility-level, annual generation values (Byers et al, 2019) were used to construct the supply mixes for each of the six electricity grids within the Chinese mainland, following grid boundaries described in Frost and Hua (2019). This approach is preferred over provincial or regional grid mix estimates provided by the LCA databases because it incorporates a large and representative amount of up-to-date facility-level production data. However, the GPPD dataset only supplies generalized fuel types (i.e. hydroelectric, solar, wind, natural gas, etc.), so sub-fuel mixes within a fuel type (e.g. hydro pump storage vs hydro run-of-river) were taken from Ecoinvent v3 grid mix profiles (Treyer & Bauer, 2014). A custom unit process for each general technology/fuel type was then constructed as a weighted average of emissions based on the contribution of each of these sub-fuel types.

$$Eq\ 1 \quad FME(x, g) = \sum_{i=1}^n w_{i,g} m_{x,s,g}$$

FME = Fuel Mix Emissions, where m is the mass of emissions per sub-fuel type s , and w is the proportion of electricity produced by the sub-fuel type within a particular electricity grid (g).

An example calculation for the hydroelectric sub-fuel mix profile from the Chinese North Grid is below (full list of weighing factors are available in the accompanying Excel file - Table S2):

$$\begin{aligned} FME_{NorthGrid-Hydro} &= (E_{NorthGrid,Hydro-RoR} * \%_{NorthGrid,Hydro-RoR}) \\ &+ (E_{NorthGrid,Hydro-PumpStorage} * \%_{NorthGrid,Hydro-PumpStorage}) \\ FME_{NorthGrid-Hydro} &= (.0267 * CoC\ Emissions\ of\ Hydro - RoR) \\ &+ (0.973 * CoC\ Emissions\ from\ Hydro - PumpStorage) \end{aligned}$$

The mass of emissions from each chemical associated with the sub-fuel type is available in Table S3. Example calculation for chromium emissions to freshwater is below.

$$FME_{NorthGrid-Hydro} = (0.0267 * 2.71E^{-02} \text{ ug Cr}^{6+}) [Hydro-ROR]$$

$$+ (0.973 * 4.97E^{+03} \text{ ug Cr}^{6+}) [\text{Hydro-Pump Storage}]$$

2.2 Japanese and Vietnamese Electricity Emissions

National level grid mixes were considered representative for Japan and Vietnam, relative to the size of the Lev 4 hydrobasin. The electricity grid in Thailand was excluded from this analysis because of the lack of data on electricity consumption in foreground processes for the VCMA manufacturing step. Grid mixes for Japan & Vietnam were derived from IEA 2019 tables (IEA, 2020) and provide up-to-date data for production capacity by fuel type, per country. Sub-fuel type mixes for Japan and Vietnam from Ecoinvent were implemented as described in Section 1.1.

2.3 Downscaling Grid Emissions to each Power Plant Facility

Emissions per fuel type (e.g. coal, natural gas, hydro) and per country (or province, in case of China) were exported from the LCA software and each fuel mix profile was constructed in R using Equation 1. The electricity usage for each manufacturing step was allocated to each RE manufacturing SUP to understand how much electricity was used in each location. Each SUP was associated with an electricity grid and then spatially joined to the GPP database where annual generation from individual power plants could be used to downscale the emissions for each fuel mix to the exact facility locations (and basins) associated with each fuel (Eq. 2).

Figure S2 depicts the spatial aggregation and disaggregation processes used to 1) construct the Chinese regional grid fuel mix and then 2) allocate the grid emissions mix per fuel type to each facility within the grid.

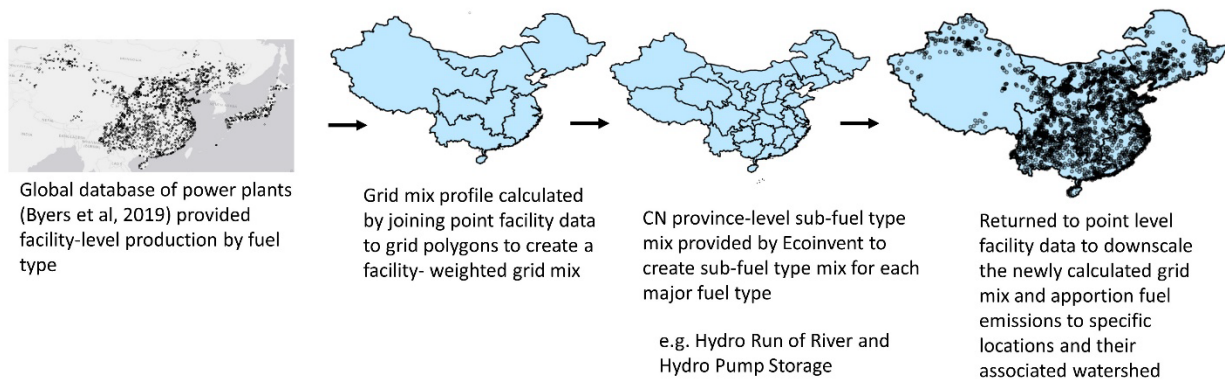


Figure S2. Schematic of the Chinese grid emission calculation and downscaling process.

$$Eq. 2 \quad PPE(f, g) = FME_{x,f,g} * w_{i,g}$$

where:

PPE = Power Plant Emissions, where w_i is the proportion of total electricity produced by individual power plant i of fuel type f within grid g .

Below is an example calculation for how each fuel type in the grid mix was used to downscale emissions to individual power plants for the Chinese North Grid:

$$\begin{aligned} PPE_{CN-NorthGrid} = & (CoC \text{ Emissions of Hydro}) * \text{Proportion of Hydro in the Grid Produced by Facility } i \\ & + (CoC \text{ Emissions of Wind}) * \text{Proportion of Wind in the Grid Produced by Facility } i \\ & + (CoC \text{ Emissions of Nat Gas}) * \text{Prop of Nat Gas in the Grid Produced by Facility } i \\ & + (CoC \text{ Emissions of Coal}) * \text{Prop of Coal in the Grid Produced by Facility } i \\ & + (CoC \text{ Emissions of Nuclear}) * \text{Prop of Nuclear in the Grid Produced by Facility } i \\ & + (CoC \text{ Emissions of Nuclear}) * \text{Prop of Nuclear in the Grid Produced by Facility } i \end{aligned}$$

Tables S4 & S5 provide a list of each of the facilities in CHN-North, Japan and Vietnam and the proportion of electricity produced at each facility for each fuel type. Facility fuel type was used to join the facility data with the fuel emissions profile created in Equation 1.

3.0 Summarizing Emissions Per CoC

3.1 Quantifying Fate, Transport and Exposure of CoCs

There were three geographic regions of interest in this study with respect to the ecotoxicity characterization factors available from Verones et al. (2020) (i.e. LC-IMPACT): Eastern China, Japan & the Korean peninsula, and SE Asia (Vietnam, Malaysia & Thailand). Impact per chemical can be measured by using the following equations, adapted from Rosenbaum et al. (2008).

$$Eq. 3 \quad AFE(r, x, c) = XF_{r,x} * FF_{r,x,c}$$

AFE = Aquatic Fate and Exposure ($\text{kg}_{\text{emit}}/\text{kg}_{\text{comp}} * \text{d}^{-1}$), where, r is the USETox region of interest, x is the CoC, and c is the environmental compartment (land, air, water) transferring chemicals to freshwater (e.g. continental rural air to freshwater)

XF = Regional Eco-exposure Factor (dimensionless) derived in USETox, which represents the fraction of chemical dissolved in freshwater which could impact aquatic freshwater species.

FF = Regional Fate Factor ($\text{kg}_{\text{emit}}/\text{kg}_{\text{comp}}*\text{d}^{-1}$) is the sum of fate factors for the transfer of emissions from air, water, and soil to freshwater.

An example equation using Cr^{6+} emissions to continental rural air (CRA), emissions to continental freshwater (CFW), and emissions to continental natural soil (CNS) in East China is provided below:

$$\begin{aligned}
 AFE_{(\text{East China}, \text{Cr}^{6+}, \text{emissions to air})} &= XF_{\text{East China}, \text{Cr}^{6+}} \\
 &\quad * FF_{\text{East China}, \text{Cr}^{6+}, \text{transport of emissions from CRA to freshwater}} \\
 AFE_{\text{East China}, \text{Cr}^{6+}, \text{emissions to CRA to freshwater}} &= 8.07\text{E-}01 \text{ (unitless)} * 1.60\text{E+}02 \\
 &\quad \text{kg}_{\text{emit}}/\text{kg}_{\text{comp}}*\text{d}^{-1} \\
 &= 129.12 \text{ kg}_{\text{emit}}/\text{kg}_{\text{comp}}*\text{d}^{-1}
 \end{aligned}$$

Table S7 provides a complete list of regional fate and exposure factors used for the CoCs in this study.

3.2 Chemical Pollution Boundary

For most of the heavy metals being considered in this study, PNECs are readily available from the ECHA website. For the radionuclides Radium-226, Thorium-232, and Uranium-238, each chemical is subject to both chemotoxicity ($\mu\text{g/L}$) and radiotoxicity ($\mu\text{Gy/hr}$) PNECs which were obtained from Hinck et al. (2010). The PNEC is used, along with the AFE derived in Equation 3, to calculate an Aquatic Impact Factor per region, per chemical, and per compartment.

$$Eq\ 4 \quad AIF(r, x, c) = 1/PNEC_x * AFE_{r, x, c}$$

where:

AIF = Aquatic Impact Factor, where r is the USETox region, x is the CoC and c is the emissions compartment. AFE is the aquatic fate and exposure calculated in Equation 3 and $PNEC_x$ is the

predicted no effect concentration for freshwater in ug/L or µGy/hr for radioactive species per chemical

An example calculation for Eq 4 below for an AIF of Cr6+ emissions to air in East China:

$$AIF_{(East\ China, Cr6+, emissions\ to\ air)} = 1/PNEC_{Cr6+} * AFE_{East\ China, Cr6+, emissions\ to\ air}$$

$$AIF_{(East\ China, Cr6+, emissions\ to\ air)} = \frac{1}{0.47\ ug/L} * 129.12\ kg_{compartment}^{-1} * d^{-1}$$

Using the results of Eq 5, we can calculate the chemical footprint per chemical using the annualized mass of emissions per region, per chemical, and per compartment.

$$Eq\ 6. \quad ChF(x) = AIF_{r,x,c} * m_{r,x,c}$$

where:

AIF is Aquatic Impact Factor from Equation 5, *x* is the chemical of concern, *c* is the media compartment (air, water, land), *m* is mass of emissions, and *r* is the regional factor from Verones et al. (2020).

An example of Eq 6 below for the ChF of the mass of emissions to continental rural air (CRA), continental freshwater (CFW) and continental natural soil (CNS) of chromium 6+ in East China multiplied by the aquatic impact factor for each compartment.

$$Eq\ 6. \quad ChF_{East\ China, Cr6+} (m^3/yr) =$$

$$(AIF_{E.China, Cr6+, CRA-FW} \left(\frac{kg_{emit}}{kg_{comp}} * d^{-1} * \frac{L}{ug} \right) * \frac{365\ d}{yr} * \left(\frac{1\ m^3}{1000\ L} \right) * m_{E.China, Cr6+, emiss\ to\ air} (kg\ emit) * \frac{1\ e+09\ ug}{1\ kg}) +$$

$$(AIF_{E.China, Cr6+, CFW-FW} \left(\frac{kg_{emit}}{kg_{comp}} * d^{-1} * \frac{L}{ug} \right) * \frac{365\ d}{yr} * \left(\frac{1\ m^3}{1000\ L} \right) * m_{E.China, Cr6+, emiss\ to\ water} (kg\ emit) * \frac{1\ e+09\ ug}{1\ kg}) +$$

$$(AIF_{E.China, Cr6+, CNS-FW} \left(\frac{kg_{emit}}{kg_{comp}} * d^{-1} * \frac{L}{ug} \right) * \frac{365\ d}{yr} * \left(\frac{1\ m^3}{1000\ L} \right) * m_{E.China, Cr6+, emiss\ to\ soil} (kg\ emit) * \frac{1\ e+09\ ug}{1\ kg})$$

3.3 Dilution Volume

3.3.1 Hydrobasins of Interest

To determine the ChF and dilution capacity (DC) of the emissions and exposure data, each SUP and its associated aquatic impact factor must be spatially joined with a hydrobasin (and associated river reaches) using the coordinates for each SUP. The HydroBASINs dataset is comprised of hydro-environmental variables such as discharge, land cover, temperature, etc (Linke et al, 2019). The XY coordinates assigned to each SUP were used to spatially join emissions with the corresponding Level 4 HydroBASIN dataset, using the “sf” library in R using “point in polygon” type joins. Level 4 was chosen as the scale for this study; however, results can be aggregated or disaggregated to suit any geography of interest.

HydroBASINs provides data on the natural discharge in m³/s of each river reach upstream of a sub-basin pour point (i.e. junction of a stream network) (Lehner, 2019). River reach discharge is calculated in HydroBASINs using the globally integrated water balance model WaterGAP which is downscaled to the 15 arc-second (~500 m) resolution of the HydroSHEDS river network (Lehner & Grill, 2013). Multiplying discharge by seconds per year gives an annual water volume flowing through the river reach which is available for dilution of annual chemical emissions.

Below is an example calculation for determining the total annual dilution volume of the reach of the Yellow River which drains the Level 4 Hydrobasin associated with the Baotou, CN RE Processing facilities.

$$\begin{aligned} \text{Eq. 7} \quad \text{Annual DC of River Reach} &= \text{Discharge} \left(\frac{\text{m}^3}{\text{sec}} \right) * 1,233,721,75 \left(\frac{\text{sec}}{\text{yr}} \right) \\ DC_{\text{YellowRiver-HybasID}_{4040548370}} &= 832.769 \left(\frac{\text{m}^3}{\text{sec}} \right) * 1,233,721.75 \left(\frac{\text{sec}}{\text{yr}} \right) \\ &= 1.027\text{E}+09 \left(\frac{\text{m}^3}{\text{yr}} \right) \end{aligned}$$

3.4 Relating ChF to Local Dilution Capacity

To relate the chemical footprint to the receiving body's dilution capacity, we must sum the footprints of all chemicals within the basin and divide by the total annual dilution capacity (river volume) of the river reach which drains the basin.

$$Eq. 7 \quad Dilution Factor_b = \sum ChF_{b,x} / DC_b$$

where:

ChF is from Equation 6, summed over the basin of interest (b) and for each chemical of concern (x).

$$DF_{HYBASID_4040548370} = \frac{ChF_{Cr6+_4040548370} + ChF_{Cd_4040548370} + ChF_{Ni_4040548370} + (...)}{DC_{4040548370}}$$

The full dataset of results per hydrobasin, per CoC, and per production unit is available in Tables S8, S9 and S10, respectively.

References

- Byers, L., Friedrich, J., Hennig, R., Kressig, A., Li, X., Valeri, L. M., & McCormick, C. (2018). A global database of power plants. Washington, DC: World Resources Institute. Available online at www.wri.org/publication/global-database-power-plants.
- Frost, K., & Hua, I. (2019). Quantifying Spatiotemporal Impacts of the Interaction of Water Scarcity and Water Use By the Global Semiconductor Manufacturing Industry. *Water Resources and Industry* 22 (2019): 100115. doi: <https://doi.org/10.1016/j.wri.2019.100115>
- Frost, K., Sousa, I., Larson, J., Jin, H., & Hua, I. (2021). Environmental impacts of a circular recovery process for hard disk drive rare earth magnets. *Resources, Conservation and Recycling*, 173, 105694.
- Hinck, J. E., Linder, G., Finger, S., Little, E., Tillitt, D., & Kuhne, W. (2010). Biological pathways of exposure and ecotoxicity values for uranium and associated radionuclides. *Hydrological, Geological and Biological Site Characterization of Breccia Pipe Uranium Deposits in Northern Arizona*. U. S. Geological Survey, Scientific Investigations Report, 5025.

IEA. (2020). Electricity Generation by Source [Table]. Retrieved tables for Japan, Vietnam and Thailand. Retrieved from <https://www.iea.org/fuels-and-technologies/electricity> (accessed 14 March 2021).

ITA. (2019, March). Steel Imports Report: Thailand. Global Steel Trade Monitor. Available at <https://legacy.trade.gov/steel/archives/index.asp> (accessed 5 August 2021).

Lehner, B. (2019, Dec). HydroATLAS: A global compendium of hydro-environmental sub-basin and river reach characteristics at 15 arc-second resolution. Technical Documentation Version 1.0. Available at <https://www.hydrosheds.org/page/hydroatlas>

Lehner, B., Grill G. (2013). Global river hydrography and network routing: baseline data and new approaches to study the world's large river systems. *Hydrological Processes*, 27(15), 2171-2186. doi: 10.1002/hyp.9740.

Linke, S., Lehner, B., Ouellet Dallaire, C., Ariwi, J., Grill, G., Anand, M., Beames, P., Burchard-Levine, V., Maxwell, S., Moidu, H., Tan, F., Thieme, M. (2019). Global hydro-environmental sub-basin and river reach characteristics at high spatial resolution. *Scientific Data* 6: 283. DOI: 10.1038/s41597-019-0300-6.

Rosenbaum, R. K., Bachmann, T. M., Gold, L. S., Huijbregts, M. A., Jolliet, O., Juraske, R., ... & Hauschild, M. Z. (2008). USEtox—the UNEP-SETAC toxicity model: recommended characterisation factors for human toxicity and freshwater ecotoxicity in life cycle impact assessment. *The International Journal of Life Cycle Assessment*, 13(7), 532-546.

Treyer, K. & Bauer, C. (2016). Life cycle inventories of electricity generation and power supply in version 3 of the ecoinvent database—part II: electricity markets. *International Journal of Life Cycle Assessment*, 21, 1255-1268. doi: [10.1007/s11367-013-0694-x](https://doi.org/10.1007/s11367-013-0694-x)

Verones, F., Hellweg, S., Antón, A., Azevedo, L. B., Chaudhary, A., Cosme, N., ... & Huijbregts, M. A. (2020). LC-IMPACT: A regionalized life cycle damage assessment method. *Journal of Industrial Ecology*, 24(6), 1201-1219.

Worldsteel. (2020). Chinese mainland steel plants 2020. Worldsteel Association. Available for purchase at <https://www.worldsteel.org/publications/bookshop.html?>

5. CONCLUSION

This dissertation explored the spatial variability in impacts from manufacturing of two components that are vital to the technology sector: semiconductors (i.e. chips) that are used to control and process electrical signals and the rare earth (RE) magnet sub assembly within a hard disk drive (HDD), which enables read-write functionality for HDD storage devices, and is a prime candidate for circular economy initiatives. Life cycle assessment was used to quantify the emissions or resource utilization from these components' manufacturing processes, and water and chemical footprint methods were explored to understand impacts on local and regional receiving ecosystems.

In Chapter 2 a modified water footprint approach was used to estimate global water use demand by the semiconductor manufacturing industry. A withdrawals-based water scarcity approach was used as a conservative indicator of freshwater ecological impacts from water deprivation. Although the semiconductor industry is a smaller user of water when compared to primary metals, it is a growing sector and represents a major source of Scope 3 water use within technology companies. Thus, Scope 3 water use impacts from semiconductor manufacturing should be considered as a primary area of concern as these companies work to meet aggressive goals of water positivity and ecosystem protection.

Future work should include benchmarking and validation of the semiconductor water use model presented in Chapter 2 against actual direct and indirect water use from semiconductor fabs. This would increase its usability as a predictive tool for future areas of growth within semiconductor manufacturing. Companies currently publish highly aggregated data (i.e. total from all manufacturing locations), making it difficult to understand impacts of production on a specific watershed. Publication of more granular, location-specific water use data by the semiconductor manufacturing industry would assist in model validation and a more comprehensive understanding of competing water use needs within a watershed. Further, the age of the life cycle assessment data used to estimate water use indicates the possibility that water use impacts are underestimated for newer technology nodes, and where possible, newer fab process water and electricity use measurements should be implemented.

In Chapter 3, a life cycle assessment of an HDD rare earth magnet assembly was undertaken to assess the impact of reusing this component as part of a circular economy. This project served as a real-world case study of a circular economic business model for electronics. LCA was used as a tool to validate assumptions about environmental impact reduction and to assess various scenarios for process implementation. Additionally, impact results across an array of impact indicators (global warming potential, aquatic ecotoxicity, carcinogenicity, etc.) were presented.

In the future, other components of the HDD should be considered for circularity initiatives. This is especially true because retrieving the magnet assembly requires full disassembly of the HDD, enabling separation and sorting of other parts such as the PCBA, motor spindle base, cover, etc. The systems level approach of LCA should continue to be used to assess the environmental impacts of electronics circular economy, to ensure that waste reduction goals advocated by CE are also aligned with other industry or company goals for carbon, water use, and ecosystem protection.

The LCA inventory from Chapter 3 was used to conduct an advanced, regionalized chemical footprint to illuminate aquatic ecotoxicity concerns and potential impacts on regional watersheds within the HDD RE magnet supply chain. The chemical footprint method gives insights beyond typical LCA by placing emissions and impact within context of the local receiving body. By factoring in the dilution capacity of a given receiving body, stakeholders can prioritize the most vulnerable ecosystems with respect to their products.

The use of multi-disciplinary solutions, databases and tools is key to advancing the work of total sustainability. Chapter 4, in particular, shows how standardized toxicology and hydrology datasets can be combined to create an operationalized solution to a complex, chemical footprint method. While there are still several areas to explore and improve, this work aims to bring the method a step closer to a meaningful assessment of a product's, organizations, or sector's impact on local, regional and planetary boundaries.

The ICT sector has a role to play in quantifying and improving environmental impacts from its own supply chain, as well as using technology as an enabler to reduce environmental damage from other sectors. Given the outsized influence and capital wielded by the technology sector, substantial investments in clean power, electricity grid and transport optimization, investments in

R&D for low-carbon materials, and investment in direct reduction technologies such as carbon capture (Varro & Kamiya, 2021) are some of the ways technology companies could contribute to maintaining a safe operating space for humanity.

5.1 Reference

Varro, L. and Kamiya, G. (2021, March 25). 5 ways Big Tech could have big impacts on clean energy transitions. International Energy Agency. Available at <https://www.iea.org/commentaries/5-ways-big-tech-could-have-big-impacts-on-clean-energy-transitions> (accessed 4 November 2021).